Technological Educational Institute of Crete

Educational examples in Structural Acoustics using the Finite Element Method

Nikolaos Tsagarakis

Thesis submitted in partial fulfillment of the requirements
for the Bachelor's Degree in
Music Technology and Acoustics

Supervisor: Dr. Spyros Kouzoupis

Rethymnon, Greece 2014

Preface

This thesis is submitted in partial fulfilment of the requirements for a Greek Bachelor's Degree in music technology and acoustics. It contains work done from April 2012 to June 2014, under the supervision of Dr. Spyros Kouzoupis. The work presented in this thesis was performed solely by the author; most of the text, however, is based on the research of others, and I have done my best to provide references to these sources.

As a student in the school system, and later on in the Technological Educational Institute of Crete, I have always been driven by a need to seek knowledge from a multitude of sources and educators, in order to enhance my academic background and reach my full potential. In this context, I wanted my thesis to serve a wider academic purpose and reach the students and professors of the Department of Music Technology & Acoustics where I have been studying, and hopefully to be of interest for the general music, acoustics, and even physics communities.

The thesis starts with an introduction to vibrations and solids, before moving on to explore more specific vibrating systems, such as strings beams and plates. It then continues by providing an overview of the Finite Element Method and COMSOL Multiphysics® software. In the experimental part of the thesis, a description is given of the testing procedure, and finally a thorough analysis is provided for each of the 8 modeled examples.

Graphs, tables, figures, educational examples and software codes contained in this thesis are available to everyone and may be used for study and research purposes.

Acknowledgements

First and foremost, I would like to express my gratitude to my supervisor, Dr. Spyros Kouzoupis, for his expert guidance and invaluable input, ideas and suggestions throughout the course of this thesis.

I would also like to thank my good friends and fellow students Ara Movsesian, Thanasis Mitakos and Dimitris-Big Thanos, for their understanding, support and good humor, Margie-Boo Mitsou for the paging and overall help, Despina Zenempisi for shooting the experimental procedure picture, and Lydia Linardou for her continuous support and encouragement over the past few years.

Thanks are due to Evgenia Sarantidi, who expertly proof-read this thesis and provided helpful suggestions for improving my attempts at the English language. However, for any errors or inadequacies that may remain in this work, the responsibility is entirely my own.

Finally, special thanks are reserved for my mother, who has always been an indispensable source of moral support and inspiration.

Table of Contents

Theoretical Background

Experimental Part

Examples

List of Figures

List of Tables

Abstract

This thesis presents educational examples mainly on structural acoustics, using theoretical, numerical and experimental methods. Numerical results are obtained through the Finite Element Method in the COMSOL Multiphysics® software environment. A series of static and dynamic problems including strings, beams and plates, in one, two and three dimensions are modeled and solved. Numerical solutions, natural frequencies and mode shapes of the examined systems are also obtained and compared with the analytical results, and in many cases with experimental values.

Περίληψη

Στην παρούσα εργασία γίνεται ανάλυση και παρουσίαση εκπαιδευτικών παραδειγμάτων κυρίως πάνω στη δομική ακουστική, με θεωρητικές, αριθμητικές και πειραματικές μεθόδους. Οι αριθμητικές μέθοδοι υλοποιούνται με την χρήση της Μεθόδου των Πεπερασμένων Στοιχείων μέσω του εμπορικού λογισμικού COMSOL Multiphysics®. Μοντελοποιούνται και λύνονται παραδείγματα στατικών αλλά και δυναμικών προβλημάτων που αφορούν χορδές, ράβδους και πλάκες σε 1, 2 και 3 διαστάσεις. Παρουσιάζονται οι αριθμητικές λύσεις, οι ιδιοσυχνότητες και οι ιδιομορφές που χαρακτηρίζουν τα συστήματα και συγκρίνονται με θεωρητικά αποτελέσματα και σε αρκετές περιπτώσεις με αποτελέσματα μετρήσεων.

Table of Abbreviations

Below follows a list of key abbreviations used in this thesis:

FEM:	Finite Element Method
BC:	Boundary Conditions
MEMS:	Microelectromechanical systems
DC:	Direct current
PDE:	Partial Differential Equations
DFT:	Discrete Fourier Transform

Theoretical Background

1. Vibrations

1.1. Introduction to vibrations

Vibration is the mechanical oscillation of a particle, member, or body from its position of equilibrium. It is the study that relates the motion of physical bodies to the forces acting on them. The basic concepts in the mechanics of vibration are space, time, and mass (or forces). When a body is disturbed from its position, then by the elastic property of the material of the body, it has a tendency to return to its original position.

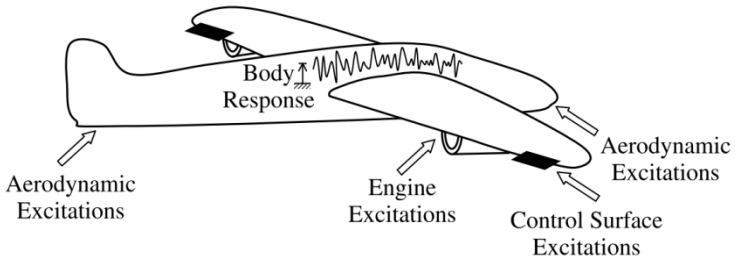

Figure 1.1. In-flight excitations and responses of an aircraft.

1.2. Statics

The study of statics is concerned with two fundamental quantities: length or distance, which requires no explanation, and force. The quantity length can be seen with the eye but with force, the only thing that is ever seen is its effect. We can see a spring being stretched or a rubber ball being squashed but what is seen is only the effect of a force being applied and not the force itself. With a rigid body there is no distortion due to the force and in statics it does not move either. Hence, there is no visual indication of forces being applied.

A force being applied to the human body is detected through the sense of touch or feel. Again, it is not the force itself but its effect which is felt – a person feels the movement of their stomach when going over a humpback bridge in a fast car, or the soles of their feet squashed slightly when standing.

Force cannot be seen or measured directly but must always be imagined. Generally the existence of some force requires little imagination but to imagine all the different forces which exist in a given situation may not be so easy. Furthermore, in order to perform any analysis, the forces must be defined precisely in mathematical terms.

'A force is that quantity which tries to move the object on which it acts.' This qualitative definition will suffice for *statical* problems in which the object does not move, but further consideration will be needed when studying the subject of *dynamics*. If the object does not move, the force must be opposed and balanced by another force. If a person pushes their hand against a wall, they know that they are exerting a force; they also know that the wall would be pushed over if it were not so strong. By saying that the wall is strong it is meant that the wall itself can produce a force to balance the one applied to it.

1.3. Dynamics

In a *dynamics* problem, the applied loadings (and hence the structural response such as deflection, internal forces, and stress) vary with time. Thus, unlike a statics problem, a dynamics problem requires a separate solution at every instant of time. The structure may be considered as subjected to two loadings, namely the *applied load* and the *inertia forces*. The inertia forces are the essential characteristics of a structural dynamics problem.

The magnitude of the inertia forces depends on

i. The rate of loading;
ii. The stiffness of the structure, and
iii. The mass of the structure.

If the loading is applied slowly, the inertia forces are small in relation to the applied loading and may be neglected, and thus the problem can be treated as static. If the loading is rapid, the inertia forces are significant and their effect on the resulting response must be determined by dynamic analysis.

1.4. Wave types

In general, there are many different types of waves; a brief summary of these different wave-types is presented below:

i. Pure longitudinal waves: these wave-types have particle displacements only in the direction of wave propagation and they generally occur in large solid volumes e.g. seismic waves are pure longitudinal waves;

ii. Quasi-longitudinal waves: these wave-types maintain particle displacements which are not purely in the direction of wave propagation - longitudinal waves within the audible frequency range in engineering type structures are quasi-longitudinal;

iii. Transverse plane waves: these wave-types exist in solid bodies because of the presence of shear stresses - the modulus of elasticity, E, is replaced by the shear modulus, G, in the equation for the quasi-longitudinal wave speed;

iv. Torsional waves: these wave-types exist when beams are excited by torsional moments - the wave velocity is identical to that of transverse plane waves;

v. Pure bending waves: these wave-types exist when the bending wavelength is large compared with the dimensions of the structural cross-sectional area;

vi. Flexure waves: the effects of rotary inertia and shear deformation are included in these wave-types;

vii. Rayleigh waves: these wave-types occur at high frequencies and in large, thick structures. They are essentially surface waves with the amplitude decreasing beneath the surface - e.g. ocean waves. Their wave velocities are of the same order as the transverse plane waves.

The subject of wave propagation in solids is a very complex one and special attention will be given only to those waves that are of direct relevance to noise and vibration, and to matters of this study.

2. Solids

2.1. Acting forces on solid structures

The simplest material model consists of the assumption that there exists a linear relation between the stress components σ and the strain components τ at any point of the body. An elastic material is characterized by the property that any deformation imposed by the application of stresses vanishes, if the stresses are removed, whereby the elastic body returns to its original shape. This property applies to any stage of the deformation process, and it is therefore reversible:

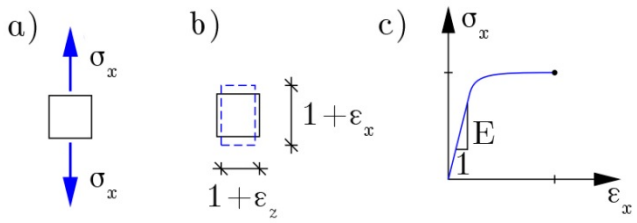

Figure 2.1. a) Normal stress, b) normal strain, c) relationship of stress and strain on a linear isotropic material.

Solids do not only resist changes in volume but also in shape. This resistance to changes in shape comes about because, unlike a liquid or gas, a solid can support tangential stresses on any cutting plane, even with the material at rest. Because these tangential stresses oppose "shearing" displacements parallel to the cutting plane, they are called shear stresses.

It is the shear stresses that make it possible for solids to exist in the shape of rods, plates, shells, etc. It is also because of shear stresses that transverse plane wave motions can occur in solid bodies, where the direction of propagation (x - direction) is perpendicular to the direction of the displacement y.

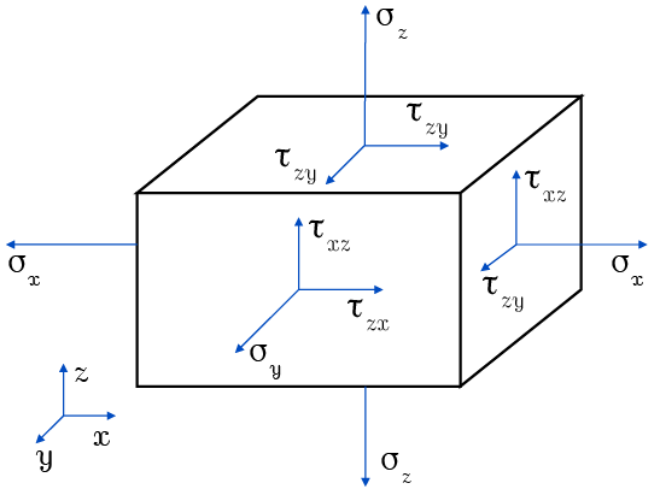

Figure 2.2. Normal stress σ *and shear stress* τ *forces acting on a three-dimensional solid cube.*

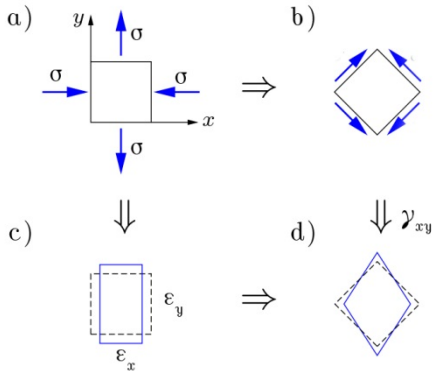

Figure 2.3. The state of stress leads to principal strains $\varepsilon_x, \varepsilon_y, \gamma_{xy}$.

The magnitude of the axial strain ε_x is described by the modulus of elasticity E (also known as the Young modulus), defined such that

$$\varepsilon_x = \frac{\sigma_x}{E}. \tag{2.1}$$

In addition to the axial extension ($x-$axis), it is obvious that there does occur a contraction of the cross-section (y and z axes), therefore the transverse strain (i.e., the strains ε_y or ε_z) may be described by a parameter

$$\varepsilon_y = \varepsilon_z = -\nu\varepsilon_x. \tag{2.2}$$

The constant of proportionality ν is a property of the material and is known as *Poisson's ratio*.

As mentioned above, these shear forces tend to deform solids and cause shear strains; in particular, they cause rectangular elements to become parallelograms. They also cause a "rotation" of the element by the (of course, very small) angle $\gamma_{xy} = \varepsilon_{xy} / 2$. Therefore, transverse waves are also known as "rotational" waves. Figures (2.4) and (2.5) show the effect of shear stress forces upon a two-dimensional and a three-dimensional solid, respectively, which originally was a rectangle with sides dx and dy (and dz in figure (2.5)), and then distorted into a parallelogram.

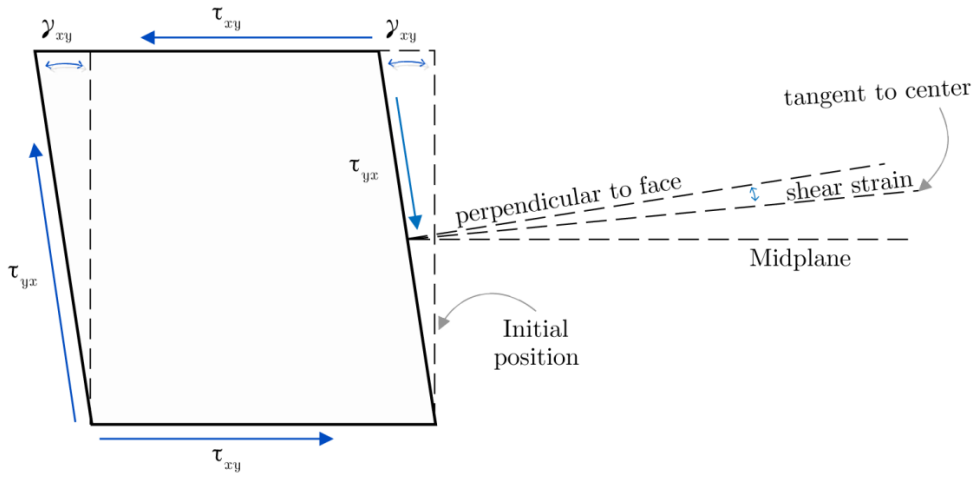

Figure 2.4. Shear stresses and shear strains in a two-dimensional system.

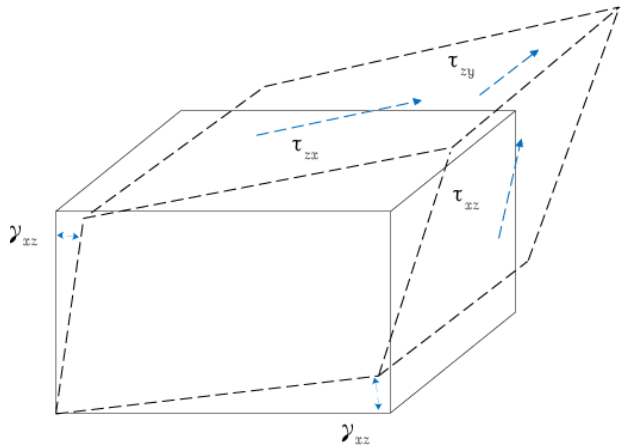

Figure 2.5. Shear stresses and shear strains in a three-dimensional system.

3. Strings

3.1. One-dimensional wave equation

Consider a flexible, taut, string of mass ϱ_L per unit length, stretched under a tension T. Several simplifying assumptions are now made before attempting to describe the vibrational motion of the string. They are:

i. The material is homogeneous and isotropic;
ii. Hooke's law is obeyed;
iii. Energy dissipation (damping) is initially ignored;
iv. The vibrational amplitudes are small - i.e. the motion is linear;
v. There are no shear forces in the string, and no bending moments acting upon it;
vi. The tension applied to the ends is constant and is evenly distributed throughout the string.

For small deflections and slopes, the equation of motion in the transverse direction is obtained from Newton's law:

$$\frac{\partial^2 y}{\partial x^2} = \frac{1}{c^2}\frac{\partial^2 y}{\partial t^2} \tag{3.1}$$

$$c = \sqrt{\frac{T}{\varrho_L}} \tag{3.2}$$

The constant c has units of ms^{-1}; it is the velocity of wave propagation along the string, and it is perpendicular to the particle displacement and velocity.

Equation (3.1) is the one-dimensional wave equation and is essentially the same with the one of longitudinal waves in a mass-spring system; either of these waves could therefore be used to present a system's vibrating modes. However, transverse waves are generally easier to visualize than longitudinal ones.

The wave equation is a second-order, partial differential equation and its most general solution contains two arbitrary independent functions A and B with arguments $(ct - x)$ and $(ct + x)$, respectively - both equations satisfy the wave equation by themselves. Function A represents a travelling wave of constant shape in the positive x -direction and function B represents a travelling wave of constant shape in the negative

x-direction. Both waves travel at the same speed c. The complete general solution of the wave equation is thus:

$$y(x,t) = A(ct - x) + B(ct + x) \tag{3.3}$$

The substitution of Eq. (3.3) into the wave equation (Eq. (3.1)) for any arbitrary functions A and B (e.g. sine or cosine functions, exponential functions, logarithmic functions or linear functions) readily demonstrates that it is indeed a general solution.

However, a string can also be looked upon as a system comprising an infinitely large number of particles. Its displacement response is thus the summation of the response of all the individual particles, each one of which has its own natural frequency and mode of vibration (Fig. (3.1)).

Therefore, instead of wave-type solutions, Eq. (3.1) could also have another solution. By separation of variables, the displacement $y(x,t)$ can now be represented as

$$y(x,t) = H(x) + G(t) \tag{3.4}$$

Substituting Equation (3.4) into Equation (3.1) yields

$$\frac{1}{H(x)}\frac{\partial^2 H(x)}{\partial x^2} = \frac{1}{c^2}\frac{1}{G(t)}\frac{\partial^2 G(t)}{\partial t^2} \tag{3.5}$$

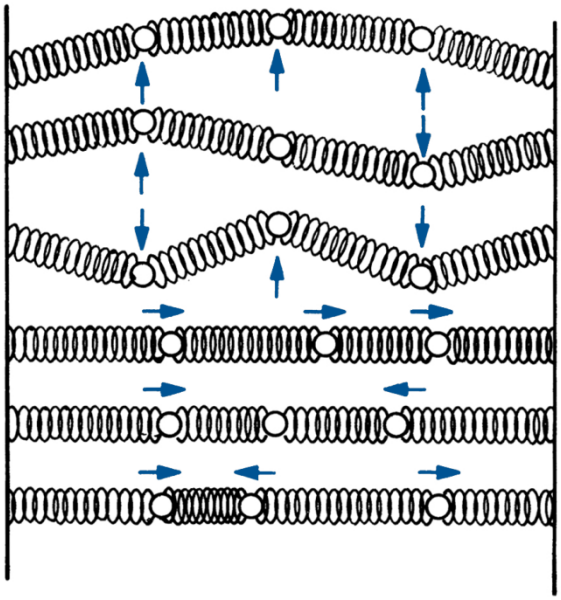

Figure 3.1. Normal modes of a three-mass oscillator.

The left hand side of Equation (3.5) is independent of time and the right hand side is independent of spatial position. For the equation to be valid, both sides have to be equal to a constant which relates to the frequency of the vibration. Let this constant be $-k^2$, where k is the wavenumber (i.e. $k = \omega / c$). Hence,

$$\frac{\partial^2 H(x)}{\partial x^2} + k^2 H(x) = 0, \tag{3.6}$$

and

$$\frac{\partial^2 G(t)}{\partial t^2} + \omega^2 G(t) = 0 \tag{3.7}$$

The solutions to these linear differential equations are:

$$H(x) = A \sin kx + B \cos kx, \tag{3.8}$$

and

$$G(x) = C \sin \omega t + D \cos \omega t. \tag{3.9}$$

The general solution yields from Equations (3.8) and (3.9):

$$y(x, t) = (A \sin kx + B \cos kx)(C \sin \omega t + D \cos \omega t) \tag{3.10}$$

The arbitrary constants A, B, C and D depend upon the boundary and initial conditions.

3.2. String with both ends fixed

Now consider the three possible cases for the boundary conditions at the two ends of a finite string. The two ends could be both fixed, both free, or one fixed and one free. Let the ends be located at $x = 0$ and $x = L$.

When both ends are fixed, the boundary conditions (for all t) are:

At $x = 0$, $y(x, t) = 0$ and at $x = L$, $y(x, t) = 0$ i.e. the displacement is zero (because the end never moves). From Equation (3.10),

for the left end:

$$y(0,t) = 0$$

$$y(0,t) = B(C\sin\omega t + D\cos\omega t) = 0 \Leftrightarrow B = 0 \tag{3.11}$$

Therefore, Eq. (3.10) becomes $y(x,t) = \sin kx(A'\sin\omega t + B'\cos\omega t)$. (3.12)

for the right end:

$$y(L,t) = 0$$

$$y(L,t) = \sin kL\,(A'\sin\omega t + B'\cos\omega t) \Rightarrow \sin kL = 0$$

$$\sin kL = 0\,,\ \text{or}\ \ kL = n\pi \Rightarrow k = \frac{n\pi}{L}\,,\ \text{for}\ \ n = 1,2,3,\text{etc} \tag{3.13}$$

The frequency equation for the fixed-fixed string is thus:

$$k = \frac{\omega}{c} \Leftrightarrow \omega = kc \Leftrightarrow \omega_n = \frac{n\pi}{L}\sqrt{\frac{T}{\varrho_L}} \tag{3.14}$$

A continuous system has an infinite number of natural frequencies. Since the constant $B = 0$, the spatial parameter $H(x)$ (see Eq. 3.8), is now:

$$H_n(x) = \sin k_n x = \sin\frac{n\pi x}{L} \tag{3.15}$$

Equation (3.15) is conceptually very important. It represents the mode shape for the n^{th} mode of vibration of the string. The complete solution for the displacement $y(x,t)$ is thus the sum of all the individual mode shapes:

$$y(x,t) = \sum_{n=1}^{\infty}(C_n\sin\omega_n t + D_n\cos\omega_n t)\sin\frac{n\pi x}{L} \tag{3.16}$$

where constants C_n and D_n are evaluated from the initial conditions.

In the above modal analysis, two important points have emerged. They are: (i) the boundary conditions determine the mode shapes and the natural frequencies of a system, and (ii) the initial conditions determine the contribution of each mode to the total response. The parameters $H(x)$ and $G(t)$ are the basis of the normal mode analysis of more complex continuous systems.

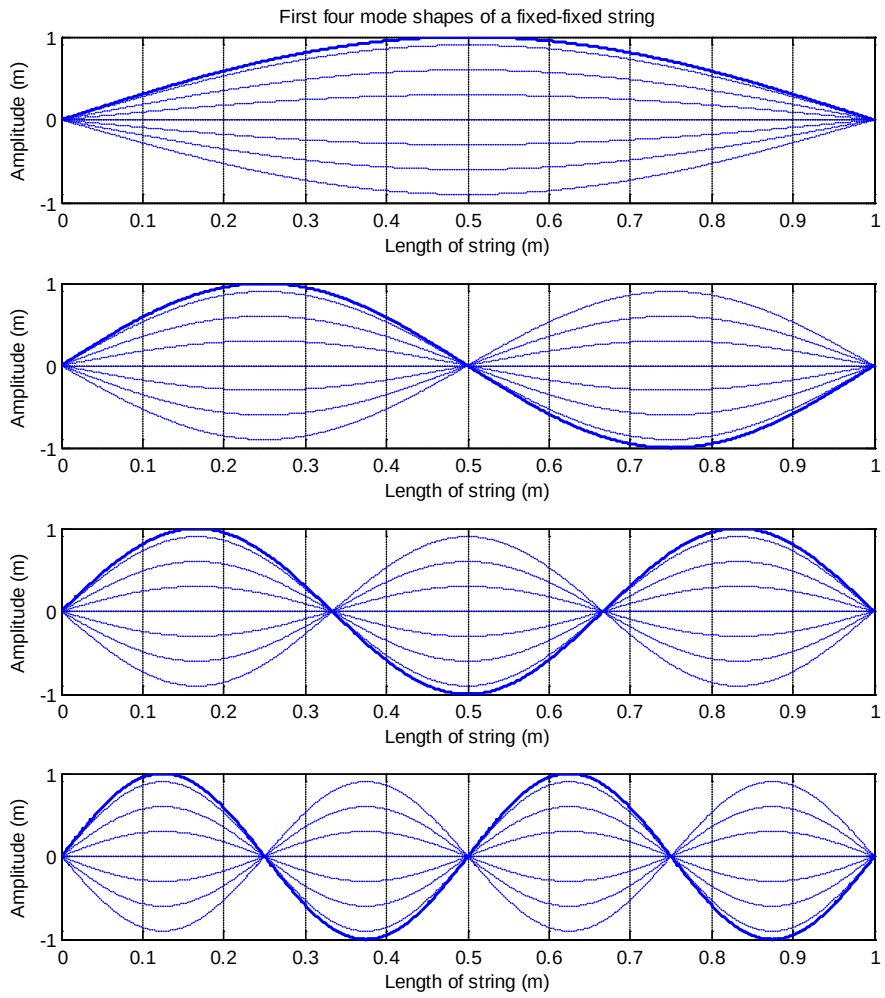

Figure 3.2. Mode shapes for the first four eigenfrequencies of a fixed-fixed string with 1m length.

3.3. String with one fixed and one free end

Let the end located at $x = 0$ be the fixed end and the one at $x = L$ be the free end. In this case, the boundary conditions (for all t) are:

At $x = 0$, $y(x,t) = 0$ and at $x = L$, $\frac{\partial^2 y}{\partial x^2} = 0$ (because the slope must be zero so that there is no transverse force on the massless endpoint).

For the left end:

from Equation (3.11), $B = 0$.

For the right end:

$$\left.\frac{\partial^2 y}{\partial x^2}\right|_{x=L} = 0 \tag{3.17}$$

$$\left.\frac{\partial^2 y}{\partial x^2}\right|_{x=L} = k\cos kL(A'\cos\omega t + B'\sin\omega t) = 0 \Rightarrow \cos kL = 0 \tag{3.18}$$

$$\cos kL = 0\,,\ \text{or}\ \ kL = \frac{(2n-1)\pi}{2} \Rightarrow k = \frac{\left(n-\frac{1}{2}\right)\pi}{L}\,,\ \text{for}\ \ n = 1,2,3,\text{etc} \tag{3.19}$$

The frequency equation for the fixed-free string is thus:

$$\omega_n = \frac{\left(n-\frac{1}{2}\right)\pi}{L}\sqrt{\frac{T}{\varrho_L}}\,, \tag{3.20}$$

And the mode shapes again derive from Equation (3.8):

$$H_n(x) = \sin k_n x = \sin\frac{\left(n\pi-\frac{\pi}{2}\right)x}{L}. \tag{3.21}$$

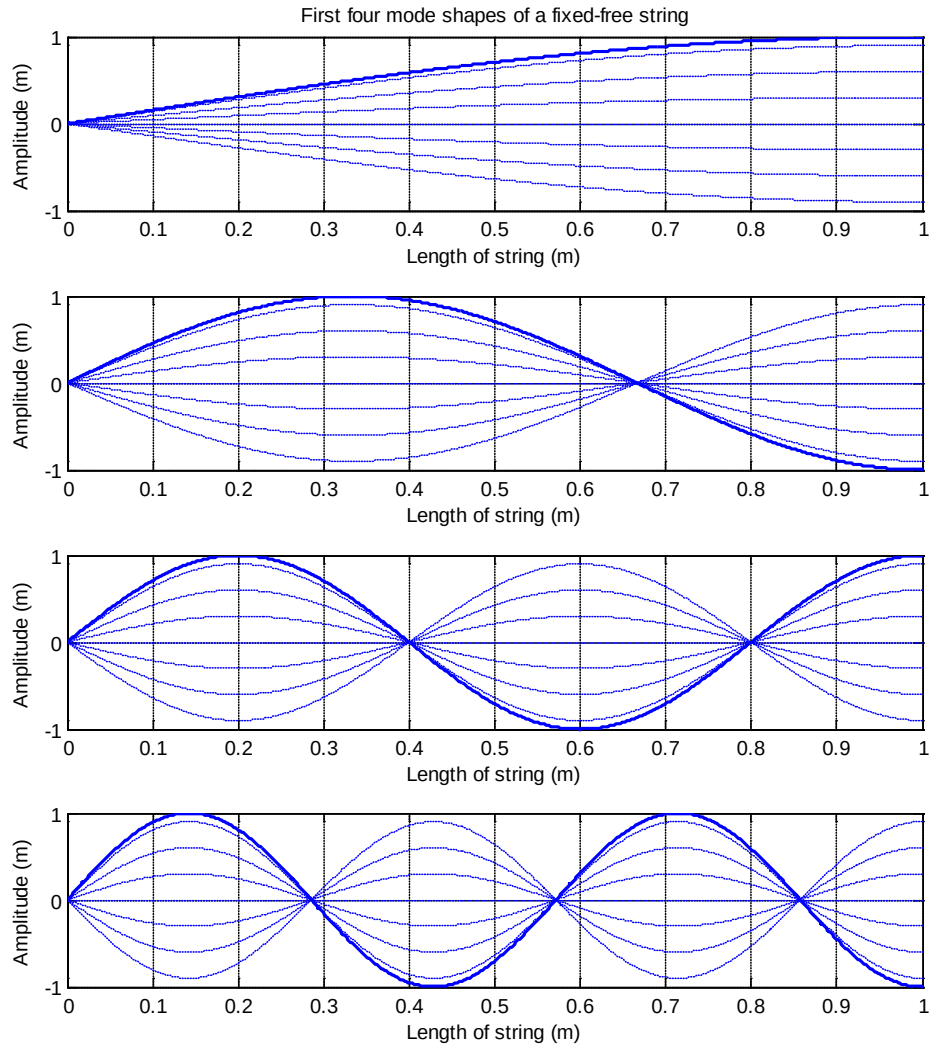

Figure 3.3. Mode shapes for the first four eigenfrequencies of a fixed-free string with 1m length.

3.4. String with both ends free

Boundary conditions (for all t) now are:

$$\text{At } x = 0, \ \frac{\partial^2 y}{\partial x^2} = 0 \text{ and at } x = L, \ \frac{\partial^2 y}{\partial x^2} = 0$$

For the left end:

$$\left.\frac{\partial^2 y}{\partial x^2}\right|_{x=0} = 0,$$

$$\left.\frac{\partial^2 y}{\partial x^2}\right|_{x=0} = A(C\sin\omega t + D\cos\omega t) = 0 \Leftrightarrow A = 0 \tag{3.22}$$

For the right end:

$$\left.\frac{\partial^2 y}{\partial x^2}\right|_{x=L} = 0$$

$$\left.\frac{\partial^2 y}{\partial x^2}\right|_{x=L} = -B\sin kL(C\sin\omega t + D\cos\omega t) = 0 \Rightarrow \sin kL = 0 \tag{3.23}$$

$$\sin kL = 0\,,\ \text{or}\ \ kL = n\pi \Rightarrow k = \frac{n\pi}{L}\,,\ \text{for}\ \ n = 1, 2, 3, \text{etc} \tag{3.24}$$

As a result, the frequency equation for the free-free string is the same as for the string with both ends fixed:

$$\omega_n = \frac{n\pi}{L}\sqrt{\frac{T}{\varrho_L}}\,, \tag{3.25}$$

although the mode shapes differ:

$$H_n(x) = \cos k_n x = \cos\frac{n\pi x}{L} \tag{3.26}$$

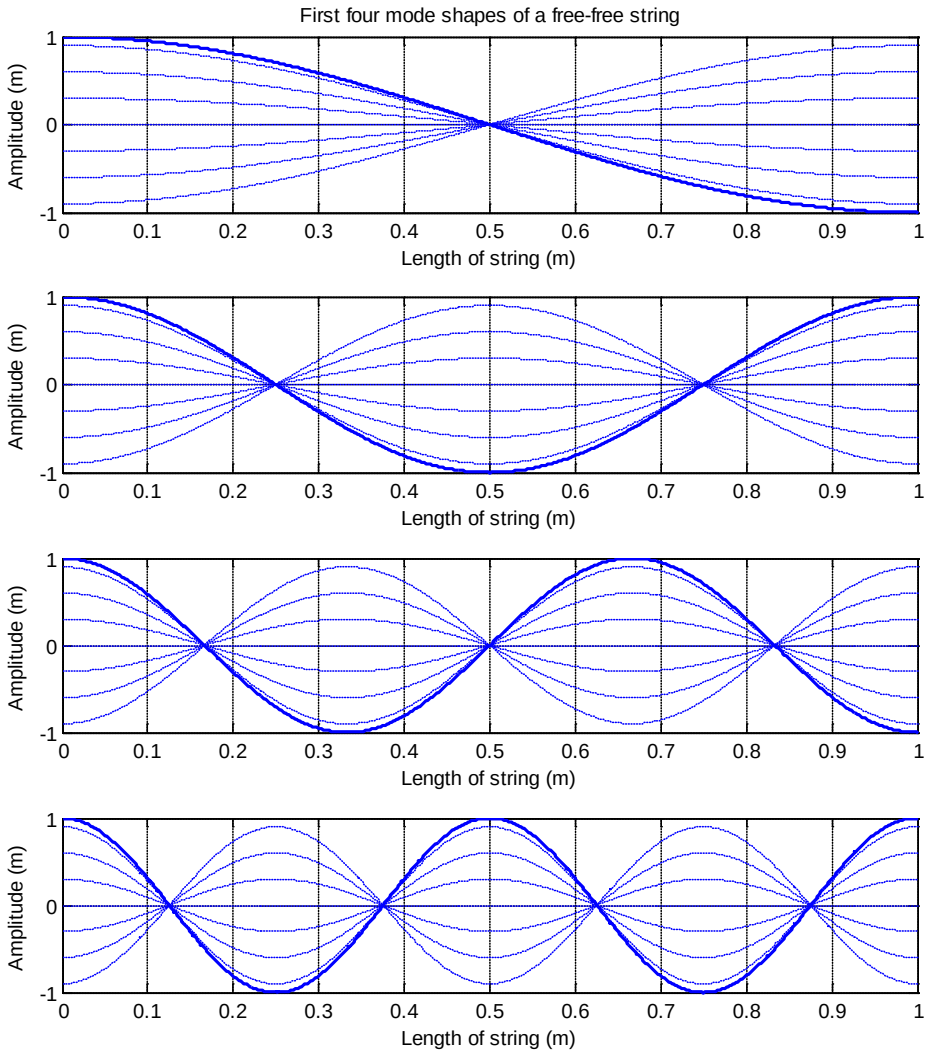

Figure 3.4. Mode shapes for the first four eigenfrequencies of a free-free string with 1m length.

4. Beams

4.1. Forces on beams

The study of the elastic behavior of beams dates back to Galileo, with important contributions by Daniel Bernoulli, Euler, De Saint Venant, and many others. A beam is essentially an elastic solid in which one dimension is prevalent over the others. Often the beam is prismatic (i.e. the cross-sections are all equal), homogeneous (i.e. with constant material characteristics), straight (i.e. its axis is a part of a straight line), and untwisted (i.e. the principal axes of elasticity of all sections are equally directed in space). The unidimensional nature of beams allows simplification of the study: Each cross-section is considered as a rigid body whose thickness in the axial direction is vanishingly small; it has 6 degrees of freedom, three translational and three rotational. The problem is then reduced to a unidimensional problem, in the sense that a single coordinate, namely the axial coordinate, is required.

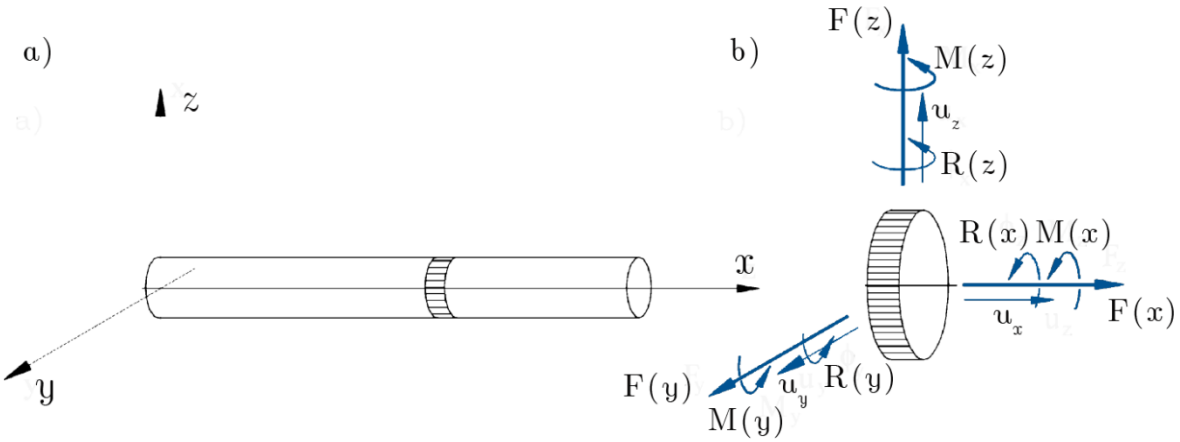

Figure 4.1. Straight beam. (a) Sketch and reference frame; (b) generalized displacements and forces on a generic cross-section.

Setting the x-axis of the reference frame along the axis of the beam (Figure 4.1), the six generalized coordinates of each cross-section are the axial displacement u_x, the lateral displacements u_z and u_y, the torsional rotation $R(x)$ about the x-axis, and the flexural rotations $R(z)$ and $R(y)$ about axes z and y. The generalized forces acting on

each cross-section and corresponding to the 6 degrees of freedom defined earlier are the axial force $F(x)$, shear forces $F(z)$ and $F(y)$, the torsional moment $M(x)$ about the x-axis, and the bending moments $M(z)$ and $M(y)$ about the z-and y-axes.

Table 4.1. Degrees of freedom and generalized forces in a three-dimensional beam.

TYPE OF BEHAVIOR	DEGREES OF FREEDOM	GENERALIZED FORCES
Axial	Displacement u_x	Axial force $F(x)$
Torsional	Rotation $R(x)$	Torsional moment $M(x)$
Flexural (zx-plane)	Displacement u_z Rotation $R(y)$	Shearing force $F(z)$ Bending moment $M(z)$
Flexural (yx-plane)	Displacement u_y Rotation $R(z)$	Shearing force $F(y)$ Bending moment $M(y)$

Because no general approach to the dynamics of an elastic body is feasible, many different models for the study of particular classes of structural elements (beams, plates, shells, etc.) have been developed.

The simplest approach to beams is that often defined as *Euler–Bernoulli beam*, based on the added assumptions that both shear deformation (shear stress) and rotational inertia of the cross-sections are negligible compared with bending deformation and translational inertia, respectively.

These assumptions lead to a good approximation if the beam is very slender, i.e., if the thickness in the y-direction is much smaller than length L.

However, as a beam bends, the various elements rotate through some small angle. The rotary inertia is thus equivalent to an increase in mass and results in a slight lowering of vibrational frequencies, especially the higher ones. As the beam becomes shorter, the effect of shear deformation becomes evident. These forces tend to deform the bar and thus decrease the transverse deflection slightly; therefore, the frequencies of the higher modes are decreased slightly in a thick bar as compared with a thin one.

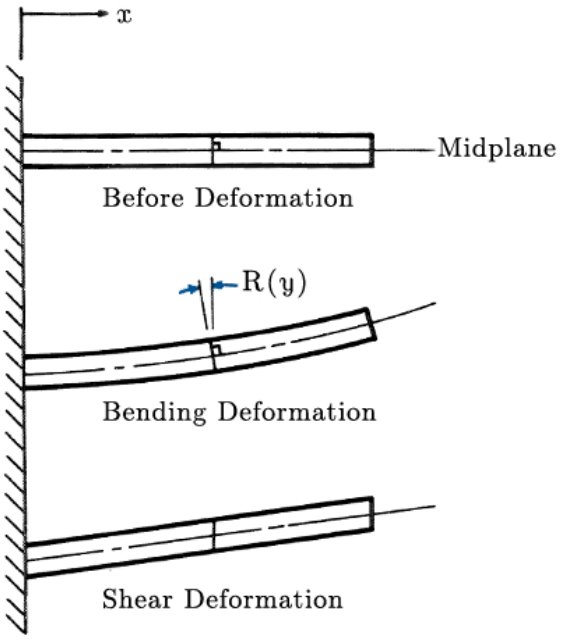

Figure 4.2. State of transverse deformations of a cantilever beam.

Beams modeled including the effects of rotary inertia and shear deformation are called *Timoshenko beams,* and they are preferred in considering thick bars. Figure (4.3) compares the two different beam models.

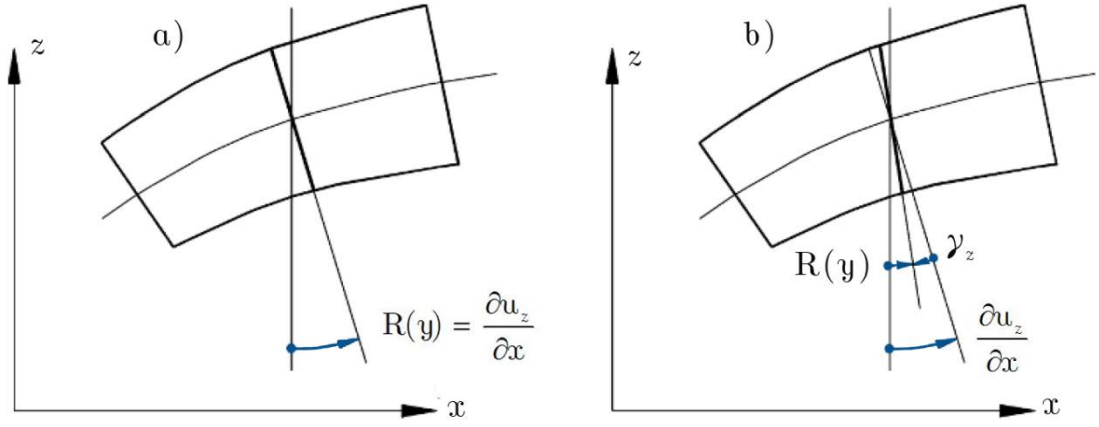

Figure 4.3. Effect of shear deformation on beam bending. (a) Euler-Bernoulli beam; (b) Timoshenko beam.

4.2. Transverse vibrations of beams

From simple beam theory, if bending occurs in the xy-plane, the relevant degrees of freedom are displacement y_x and rotation (slope) $R(x)$. Then the following well-known relationships apply:

$$y = y(x) \tag{4.1}$$

$$\frac{dy}{dx} = R(x) \tag{4.2}$$

$$EI\frac{d^2y}{dx^2} = M(x) \tag{4.3}$$

$$EI\frac{d^3y}{dx^3} = S(x) \tag{4.4}$$

$$EI\frac{d^4y}{dx^4} = W(x) \tag{4.5}$$

where E is the Young's modulus, I is the area moment of inertia of the cross-section about bending axis, y is the displacement normal to the beam centerline at distance x along the beam, $M(x)$ is the bending moment at x, $S(x)$ is the shear force at x, and $W(x)$ is the load per unit length at x.

If there is no applied force or damping, the load distribution $W(x)$ will be the inertia loading due to the mass of the beam:

$$W(x) = -\mu\frac{d^2y}{dt^2} = \varrho A\frac{d^2y}{dt^2}dx \tag{4.6}$$

where μ is the mass of the beam per unit length, constant in this case (ρ is the density of the material and A is the cross-section area), and y is now a function of time, t, as well as of x (the negative sign in Eq. (4.6) is due to D'Alembert's principle).

From Eqs (4.5) and (4.6):

$$EI\frac{d^4y}{dx^4} = \varrho A\frac{d^2y}{dt^2}dx \tag{4.7}$$

is the *Euler beam* equation for bending motion in the transverse direction. It is different from the wave equation for transverse string vibrations and quasi-longitudinal waves in bars, in that it is a fourth-order partial differential equation and the constant ρA is not

the bending wave speed. This is because bending waves are a combination of shear and longitudinal waves.

Due to the assumption that there is no applied force, or damping, only simple harmonic motion is possible, so a solution is considered of the form

$$y(x,t) = y \sin \omega t \tag{4.8}$$

from which

$$\frac{d^2y}{dt^2} = -\omega^2 y \sin \omega t \tag{4.9}$$

where y is a mode shape factor, a function of x only. The maximum loading corresponds to $\sin \omega t = 1$, so for this condition, $\frac{d^2y}{dt^2} = -\omega^2 y$. Substituting this into Eq. (4.7) gives

$$\frac{d^4y}{dx^4} = \frac{\varrho A}{EI}\omega^2 y = \beta^4 y \tag{4.10}$$

where

$$\beta^2 = \frac{\omega}{\sqrt{\frac{EI}{\varrho A}}} = \frac{\omega}{Kc}. \tag{4.11}$$

c is the wave velocity and it is clear that it depends on frequency.

It is also customary to define a constant K called the *radius of gyration* of the cross-section. For a rectangular cross-section, $I = \frac{bh^3}{12}$, where b is the width and h the height of the cross-section (beam's thickness). Since $I = AK^2 = bhK^2$, then $K = h/\sqrt{12}$.

The general solution of Eq. (4.10) for a mode shape (eigenfunction) is a sum of four terms:

$$y(x) = A \sin \beta x + B \cos \beta x + C \sinh \beta x + D \cosh \beta x, \tag{4.12}$$

and the constants A, B, C and D depend upon the boundary conditions.

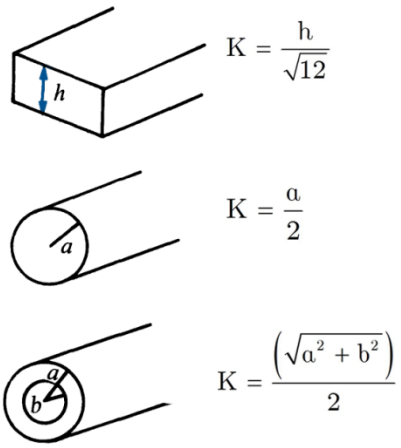

Figure 4.4. Radius of gyration for some simple shapes.

4.3. Boundary conditions

Since the equation of motion is a fourth-order equation, we have four arbitrary constants. We thus need four boundary conditions (two at each end) to determine them.

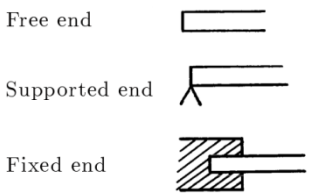

Figure 4.5. Three different end conditions for a beam.

In the cases of study, each end of the beam may be free, clamped or simply supported.

At a free end, displacement and rotations are free, but both the bending moment and the shear force must vanish. This can be expressed by the relationships:

$$EI\frac{d^2y}{dx^2} = 0\,, \qquad EI\frac{d^3y}{dx^3} = 0 \tag{4.13}$$

If, on the contrary, an end is clamped, both the displacement and the rotation vanish. Since the cross-section remains perpendicular to the deflected shape of the beam,

owing to neglecting shear deformation, the rotation of the cross-section is equal to the slope of the inflected shape

$$y = 0, \qquad \frac{dy}{dx} = 0 \tag{4.14}$$

A supported end is free to rotate, and hence the bending moment must vanish, but the displacement is constrained

$$y = 0, \qquad EI\frac{d^2y}{dx^2} = 0. \tag{4.15}$$

As an example, a fixed-free (cantilever) beam, of length L, has the following boundary conditions, where $x = 0$ at the fixed end and $x = L$ at the free end:

$$\text{At } x = 0, y = 0; \qquad \text{at } x = 0, \frac{dy}{dx} = 0 \qquad . \tag{4.16}$$

Substituting these conditions into Equation (4.12), differentiating it as necessary, gives:

$$A = -C \text{ and } B = -D \qquad . \tag{4.17}$$

$$\begin{aligned} C(\sin\beta L + \sinh\beta L) + D(\cos\beta L + \cosh\beta L) &= 0 \\ C(\cos\beta L + \cosh\beta L) + D(\sinh\beta L - \sin\beta L) &= 0 \end{aligned} \tag{4.18}$$

The roots of the simultaneous equations (Eq. (4.18)) are given by the determinant:

$$\begin{vmatrix} (\sin\beta L + \sinh\beta L) & (\cos\beta L + \cosh\beta L) \\ (\cos\beta L + \cosh\beta L) & (\sinh\beta L - \sin\beta L) \end{vmatrix} \tag{4.19}$$

which can be simplified to:

$$1 + \cos\beta L \cosh\beta L) = 0 \tag{4.20}$$

Equation (4.20), the *characteristic equation*, can be solved numerically. The first four roots are:

$$(\beta L)_1 = 1.87510 \quad (\beta L)_2 = 4.69409 \quad (\beta L)_3 = 7.85476 \quad (\beta L)_4 = 10.99554$$

From Eq. (4.11), the natural frequencies, ω_i, are given by:

$$\omega_i = \beta^2 K\sqrt{\frac{E}{\varrho}} \tag{4.21}$$

Table 4.2. Natural Frequencies for uniform Beams in Bending.

END CONDITIONS	CHARACTERISTIC EQUATIONS AND ROOTS $\beta_1 L$	A	B	C	D
Simply-supported (Pinned-pinned)	$\sin\beta_i L = 0$ $\beta_1 L = \pi$ $\beta_2 L = 2\pi$ $\beta_3 L = 3\pi$ $\beta_4 L = 4\pi$	1	0	0	0
Free-free	$\cos\beta_i L \cosh\beta_i L = 1$ $\beta_1 L = 4.73004$ $\beta_2 L = 7.85321$ $\beta_3 L = 10.99561$ $\beta_4 L = 14.13717$	1	$\frac{\sin\beta_i L - \sinh\beta_i L}{\cos\beta_i L - \cos\beta_i L}$	1	$\frac{\sin\beta_i L - \sinh\beta_i L}{\cos\beta_i L - \cos\beta_i L}$
Fixed-fixed	$\cos\beta_i L \cosh\beta_i L = 1$ $\beta_1 L = 4.73004$ $\beta_2 L = 7.85321$ $\beta_3 L = 10.99561$ $\beta_4 L = 14.13717$	1	$-\frac{\sinh\beta_i L - \sin\beta_i L}{\cos\beta_i L - \cosh\beta_i L}$	1	$-\frac{\sinh\beta_i L - \sin\beta_i L}{\cos\beta_i L - \cosh\beta_i L}$
Fixed-free (x is measured from the fixed end)	$\cos\beta_i L \cosh\beta_i L = -1$ $\beta_1 L = 1.87510$ $\beta_2 L = 4.69409$ $\beta_3 L = 7.85475$ $\beta_4 L = 10.99554$	1	$-\frac{\sin\beta_i L + \sinh\beta_i L}{\cos\beta_i L + \cosh\beta_i L}$	-1	$\frac{\sin\beta_i L + \sinh\beta_i L}{\cos\beta_i L + \cosh\beta_i L}$
Fixed-pinned (x is measured from the fixed end)	$\tan\beta_i L - \tanh\beta_i L = 0$ $\beta_1 L = 3.92660$ $\beta_2 L = 7.06858$ $\beta_3 L = 10.21017$ $\beta_4 L = 13.35177$	1	$-\frac{\sin\beta_i L - \sinh\beta_i L}{\cos\beta_i L - \cosh\beta_i L}$	-1	$\frac{\sin\beta_i L - \sinh\beta_i L}{\cos\beta_i L - \cosh\beta_i L}$

Notes: In all cases the natural frequencies, in rad/s, are $\omega_i = \beta_i^2\sqrt{EI/\mu}$, where values of $\beta_1 L$ (where L is the length of the beam, corresponding to the first four non-zero natural frequencies), are given in the second column of the table. The mode shape is given by:

$$y_i = A\sin\beta_i x + B\cos\beta_i x + C\sinh\beta_i x + D\cosh\beta_i x \tag{4.22}$$

where A, B, C and D can be found from the table. The mode shapes are not normalized to any particular amplitude.

The values of the constants A, B, C and D can be found from Equations (4.17) and (4.18), and mode shapes are then given by Equation (4.12). Table (4.2) lists the roots of $\beta_i L$ along with the characteristic equations for several different configurations.

5. Plates

5.1. Short history on plates

The study of plate vibration dates back to the early eighteenth century, with the German physicist, Chladni (1787), who observed nodal patterns for a flat square plate. In his experiments on the vibrating plate, he spread an even distribution of sand which formed regular patterns as the sand accumulated along the nodal lines of zero vertical displacements upon induction of vibration.

In 1877 Lord Rayleigh showed how the addition of "rotatory" (in the language of his day) inertia effects to those of classical translational inertia affected the flexural vibration frequencies of beams. Timoshenko in 1921 showed that the effects of shear deformation, previously disregarded, were equally important. It is well known that both effects serve to decrease the computed frequencies because of increased inertia and flexibility of the system.

5.2. Kirchhoff Plate

According to Kirchhoff theory for vibration, a straight line normal to the midplane remains straight and normal to the midplane in the deformed state (Fig. (5.1)). If the midplane undergoes displacements u_x, u_y, u_z, a point located on the same normal at a distance u_z from the midplane undergoes the displacements

$$w_x = u_x - \frac{\partial u_z}{\partial x} u_0 \tag{5.1}$$

$$w_y = u_y - \frac{\partial u_z}{\partial y} u_0 \tag{5.2}$$

$$w_z = u_z . \tag{5.3}$$

Furthermore, in the classical thin plate theory, no deformation occurs in the midplane of the plate, transverse normal stress is not allowed, and the effect of rotary inertia is negligible.

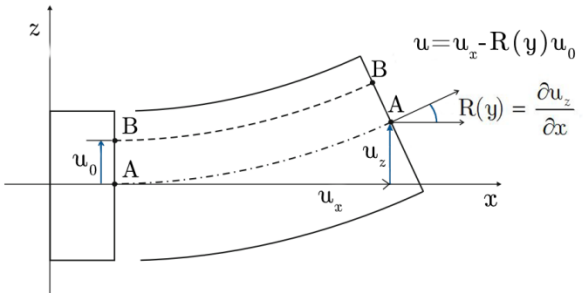

Figure 5.1. Kinematics of a Kirchhoff plate.

5.3. Mindlin Plate

The first assumption of the classical plate theory, i.e., normal to the undeformed middle surface remains normal to the deformed middle surface, tries to neglect the effect of transverse shear deformation. The transverse shear effects as well as the rotatory inertia effect are important when the plate is relatively thick or when higher-mode vibration characteristics are needed. As described in Sections 4.1 & 5.1, the above theory was refined first by Timoshenko (1921) by including the effects of transverse shear and rotatory inertia in beam equations. Accordingly, transverse shear effect was then introduced in the plate equations by Reissner (1945).

Again, both transverse shear effect and rotatory inertia effect were included in the equation of motion of a plate by Mindlin (1951). Thus, the theory of the classical plate equation considering the effect of transverse shear (Hencky (1947) and Reissner (1945)) relaxes the normality condition and the first assumption in the above classical theory will read as: ‘‘normal to the undeformed middle surface remains straight and unstretched in length but not necessarily normal to the deformed middle surface.’’

The above assumption implies a nonzero transverse shear strain giving an error to the formulation. Thereby, Mindlin (1951), as mentioned above, modified the fourth assumption of the classical plate theory too and it reads: ‘‘the effect of rotatory inertia is included,’’ along with the above-modified assumption given by Reissner (1945). The final theory (modified first and fourth assumptions in the classical theory) is known as Mindlin plate theory.

The first-order shear deformation plate theory of Mindlin, however, requires a shear correction factor to compensate for the error due to the assumption of a constant shear strain (and thus constant shear stress) through the plate thickness that violates

the zero shear stress condition at the free surfaces. The correction factors not only depend on material and geometric parameters but also on the loading and boundary conditions.

6. Finite Element Method

6.1. Introduction

The Finite Element Method is a general discretization method for the solution of partial derivative differential equations and it is at present the most common discretization method. Its success is due to the possibility of using it for a wide variety of problems, but above all to the availability of computing machines of ever-increasing power. The method yields usually models with a large number (hundred thousands or millions) of degrees of freedom, but the ODEs so obtained are easily implemented in general-purpose codes for digital computers. It can be used for both time-domain and frequency-domain computations.

The FEM is based on the subdivision of the structure into finite elements where a continuum is divided into a number of relatively small regions called *Elements,* which are interconnected at selected nodes. The deformation within each element is expressed by interpolating polynomials. The coefficients of these polynomials are defined in terms of the element nodal DoF that describe the displacements and slopes of selected nodes on the element. Many different element formulations have been developed, depending on their shape and characteristics: beam elements, shell elements, plate elements, solid elements, and many others. A structure can be built by assembling elements of the same or different types, as dictated by the nature of the problem and by the capabilities of the computer code used.

6.2. Historical Background

The principles of the Finite Element Method were proposed in 1909 by the German mathematician Ritz, and further developed in 1915 by the Russian mathematician Galerkin.

The absence of computers delayed the dissemination and further development of the method, which remained dormant. With the advent of computers, the Finite Element Method was made known and spread among researchers.

The idea of developing the method was born in aerospace from the necessity of finding solutions to the difficult problems encountered in the construction of aircrafts.

In 1941, Hrenikoff introduced the so-called Framework Method, in which a plane elastic medium was represented as a collection of bars and beams.

In 1943, the German mathematician Courant solved the torsion problem using an assemblage of triangular elements and the principle of Minimum Potential Energy, which he named as Rayleigh-Ritz Method. Since computers had not been invented yet, it was impossible to apply Courant's method; it remained forgotten, until computers allowed scientists to re-establish it.

In 1955, Greek J.H. Argyris wrote a paper on 'Energy theorems and structural analysis', introducing the principles of finite elements.

In 1956, the Americans Turner, Clough, Martin and Topp derived the stiffness matrices for beams and other elements.

In 1960, Argyris and Kelsey published their paper, based on the finite element principles.

The term 'Finite Elements' was coined by Professor Clough at the University of California-Berkeley, USA, in a paper he wrote in 1960.

In 1967, Zienkiewicz and Chung wrote the first book on Finite Elements.

Since then, numerous papers and books have been published on the application of the Finite Element Method in Engineering, Fluids, Heat, Acoustics, metal processing, electricity, electromagnetics and other disciplines.

6.3. Mathematical foundation of the Finite Element Method

As the capacity of all computers is finite, continuous problems can only be solved exactly by mathematical manipulation. Here, the available mathematical techniques usually limit the possibilities to oversimplified situations. To overcome the intractability of realistic types of continuum problems, various methods of discretization have from time to time been proposed both by engineers and mathematicians. All involve an approximation which, hopefully, approaches in the limit of the true continuum solution as the number of discrete variables increases.

The discretization of continuous problems has been approached differently by mathematicians and engineers. From a mathematical point of view, the finite element

method is a special form of the well-known Galerkin and Rayleigh-Ritz methods for finding an approximate solution to differential equations. In both methods the governing differential equation first is converted into an equivalent integral form. The Rayleigh-Ritz method employs calculus of variations to define an equivalent variational or energy functional. A function that minimizes this energy functional represents a solution of the governing differential equation. The Galerkin method uses a more direct approach. An approximate solution, with one or more unknown parameters, is chosen. In general, this assumed solution will not satisfy the differential equation. The integral form represents the residual obtained by integrating the error over the solution domain. Employing a criterion adopted to minimize the residual gives equations for finding the unknown parameters.

6.4. Discretization and Elements

As pointed out above, in the FEM, complex structures are replaced by assemblages of simple structural elements known as finite elements and the elements are connected by joints or nodes (Fig. 6.1). This is called the finite element *mesh* and the process of making the mesh is called *mesh generation*.

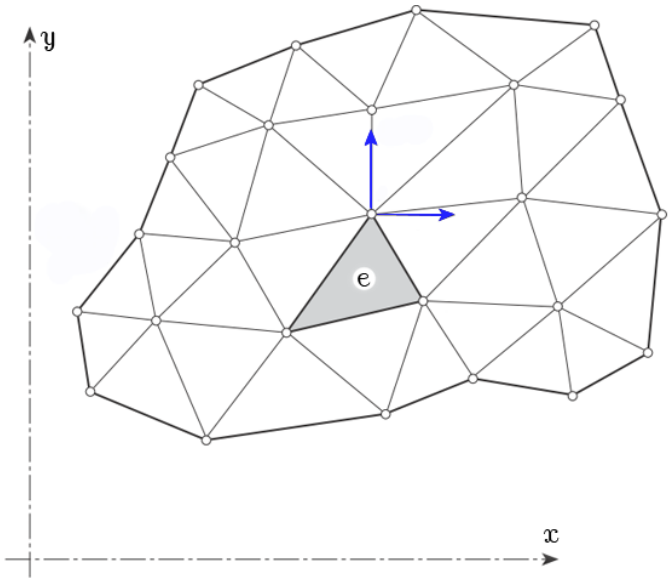

Figure 6.1. A structure region divided into finite elements.

The geometry of an element depends on the type of the governing differential equation. For problems defined by one-dimensional ordinary differential equations, the elements are straight or curved line elements. For problems governed by two-dimensional partial differential equations, the elements are usually of triangular or quadrilateral shape. The element sides may be straight or curved. Elements with curved sides are useful for accurately modeling complex geometries common in applications such as shell structures and automobile bodies. Three-dimensional problems require tetrahedral or solid brick-shaped elements. Typical element shapes for one-, two-, and three-dimensional (lD, 2D, and 3D) problems are shown in Figures (6.2), (6.3) and (6.4). The nodes on the elements are shown as circles.

The simplest two-dimensional continuum element is a triangle and it consists of 3 nodes. These nodes have two displacements each, parallel to the x and y axes, the summation of which gives the number of degrees of freedom for each element. In three dimensions, its equivalent is a tetrahedron, an element with four nodal corners. These nodes have four displacements each, parallel to the axes x, y and z, and similarly each element's number of DoF is arising from the total nodal displacements. In both cases, the system's total DoF is the sum of the DoF for all the elements.

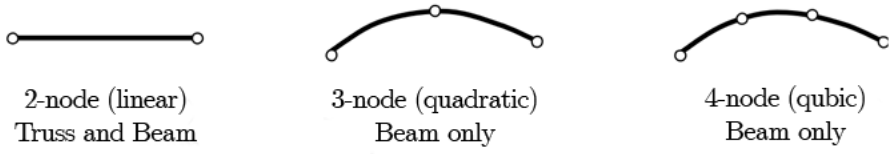

Figure 6.2. Various element shapes for truss and beam elements.

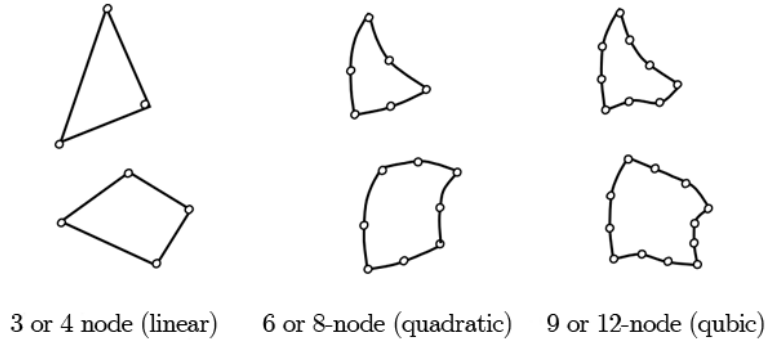

Figure 6.3. Typical plane stress elements.

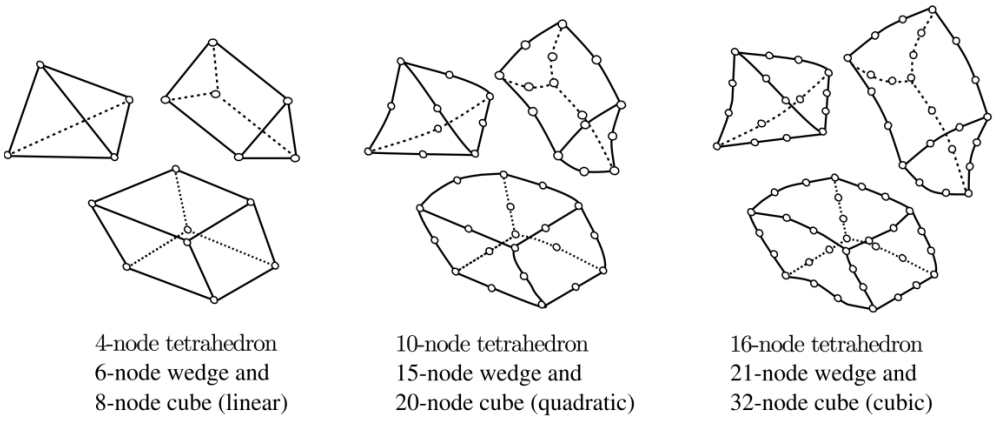

Figure 6.4. Typical 3-D solid elements.

6.5. Direct Approach of the Finite Element Method

The finite element method consists of the following five steps:

i. Discretization of the structure. The first step in the finite element method is to divide the structure or solution region into subdivisions or elements. Hence, the structure is to be modeled with suitable finite elements. The number, type, size, and arrangement of the elements are to be decided;

ii. Element formulation: development of equations for elements and selection of a proper interpolation or displacement model. The description of the behavior of each element generally requires the development of the partial differential equations for the problem and its weak form. Since the displacement solution of a complex structure under any specified load conditions cannot be predicted exactly, we assume some suitable solution within an element to approximate the unknown solution. The assumed solution must be simple from a computational standpoint, but it should satisfy certain convergence requirements. In general, the solution or the interpolation model is taken in the form of a polynomial. However, many times in simple situations, such as systems of springs or trusses, it is possible to describe the behavior of an element directly, without considering a governing partial differential equation or its weak form;

iii. Assembly: obtaining the equations of the entire system from the equations of individual elements, i.e., combining the equations that govern

individual elements to obtain the equations of the system. The element equations are expressed in matrix form;

iv. Solving the equations;

v. Postprocessing: determining quantities of interest, such as stresses and strains, and obtaining visualizations of the response.

The accuracy obtainable from the FEM depends on being able to duplicate the vibration mode shapes. Using only one finite element between structure joints or corners, gives good results for the first lowest mode, because the static deflection curve is a good approximation to the lowest dynamic mode shape. For higher modes, several elements are necessary between structural joints.

7. COMSOL Multiphysics®

7.1. Introduction to COMSOL Multiphysics®

COMSOL Multiphysics® software is a powerful FEM, partial differential equation (PDE) solution engine. It is an interactive environment used to model and solve all kinds of scientific and engineering problems. It can also easily extend conventional models for one type of physics into multiphysics models that solve coupled physics phenomena - and do so simultaneously.

PDEs form the basis for the laws of science and provide the foundation for modeling a wide range of scientific and engineering phenomena. COMSOL can be used in many application areas, including: Acoustics, Bioscience, Chemical reactions, Corrosion and corrosion protection, Diffusion, Electrochemistry, Electromagnetics, Fatigue analysis, Fluid dynamics, Fuel cells and electrochemistry, Geophysics and geomechanics, Heat transfer, Microelectromechanical systems (MEMS), Microfluidics, Microwave engineering, Multibody dynamics, Optics, Particle tracing, Photonics, Plasma physics, Porous media flow, Quantum mechanics, Radio-frequency components, Semiconductor devices, Structural mechanics, Transport phenomena, Wave propagation.

The primary advantage derived from combining computer simulation and first principles analysis is that the modeler can try as many different approaches to the solution of the same problem as needed to get the right result (or at least a result which is approximately right) in the workshop or laboratory before the first device components are fabricated and tested. The modeler can also use the physical device test results to modify the model parameters and arrive at a final solution more rapidly than by simply using the cut-and-try methodology.

When solving the models, COMSOL assembles and solves the problem using a set of advanced numerical analysis tools. The software runs the analysis together with adaptive meshing (if selected) and error control using a variety of numerical solvers. The studies can make use of multiprocessor systems and cluster computing, and batch jobs and parametric sweeps can be run.

7.2. Structural Mechanics Interfaces

7.2.1. Introduction to Structural Mechanics interfaces

Solving PDEs generally means that time must be taken for setting up the underlying equations, material properties, and boundary conditions for a given problem. The software, however, provides a number of physics interfaces that consist of nodes and settings that set up the equations and variables for specific areas of physics.

7.2.2. The Solid Mechanics Interface

The Solid Mechanics interface is intended for general structural analysis of 3D, 2D, or axisymmetric bodies. In 2D, plane stress or plane strain assumptions can be used. The Solid Mechanics interface is based on solving Navier's equations, and results such as displacements, stresses, and strains are computed.

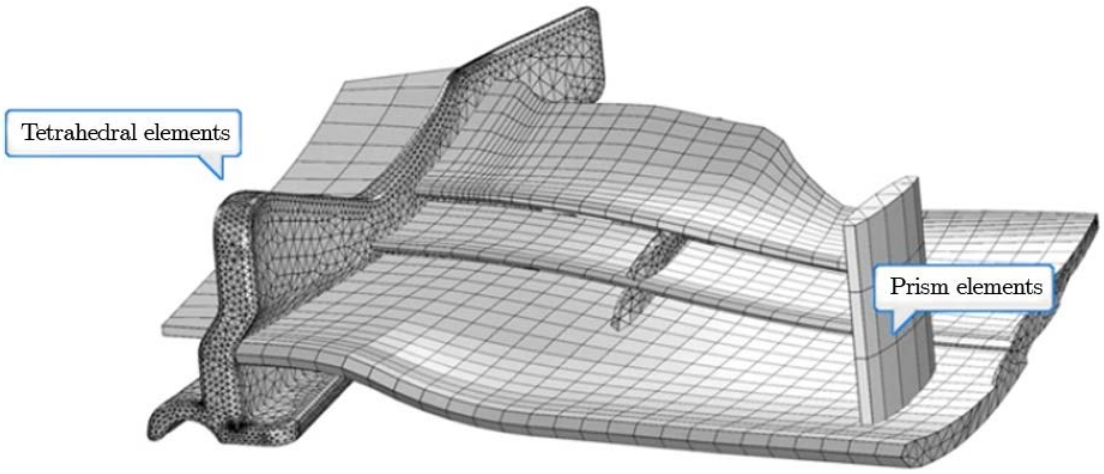

Figure 7.1. Finite element discretization in a Solid Mechanics model

7.2.3. The Truss Interface

The Truss interface is used for modeling slender elements that can only sustain axial forces. It can be used for analyzing truss works where the edges are straight, or for modeling sagging cables like the deformation of a wire exposed to gravity. It is available in 3D and 2D. Geometric nonlinearity can be taken into account. The material is assumed to be linearly elastic.

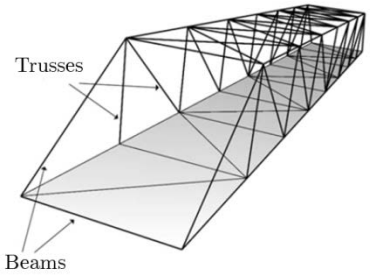

Figure 7.2. Truss and beam structures.

7.2.4. The Beam Interface

The Beam interface is used for modeling slender structural elements, having a significant bending stiffness. The formulation is linear, and beams can be modeled on 2D boundaries and 3D edges.

Two-noded elements with a Hermitian formulation are used and both Euler-Bernoulli and Timoshenko can be solved.

Among the computed results are displacements, rotations, stresses, strains, and section forces. In addition to giving the beam properties explicitly in terms of area, moment of inertia, and so on, several predefined common cross-section types are also available.

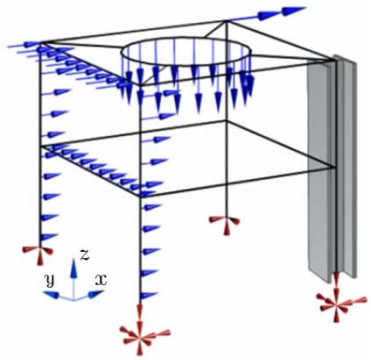

Figure 7.3. Slender structure of beams.

7.2.5. The Membrane Interface

The Membrane is mainly used to model prestressed membranes, but it can also be used to model a thin cladding on a solid. Membranes can be considered as plane stress elements in 3D with a possibility to deform both in the in-plane and out-of-plane directions. The difference between a shell and a membrane is that the membrane does not have any bending stiffness. When a membrane is used by itself, a tensile prestress is necessary in order to avoid singularity because a membrane with no stress or compressive stress has no transverse stiffness.

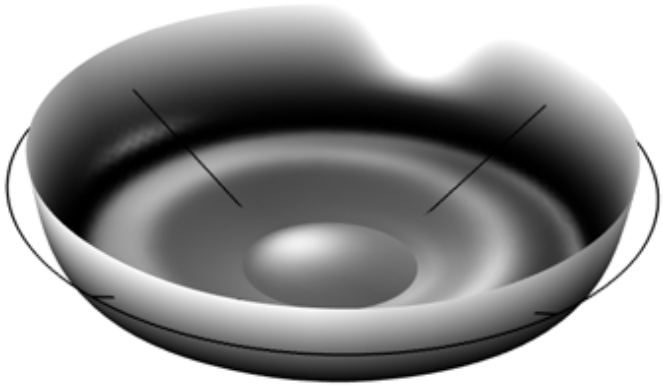

Figure 7.4. Titanium membrane of a loudspeaker.

7.2.6. The Shell and Plate Interface

The Shell interface is intended for the structural analysis of thin-walled structures. The formulation used in the Shell interface is a Mindlin-Reissner type, which – as already mentioned in detail - means that transverse shear deformations are accounted for, and it can therefore be used for rather thick shells as well as thin ones. It is possible to prescribe an offset in a direction normal to a selected surface. The Shell interface also includes other features such as damping, thermal expansion, and initial stresses and strains. The preset studies available are the same as for the Solid Mechanics interface.

The Plate interface is a 2D analogy to the 3D Shell interface. Plates are similar to shells, but act in a single plane and usually only with out-of-plane loads. The

formulation and features for this physics interface are similar to those for the Shell interface.

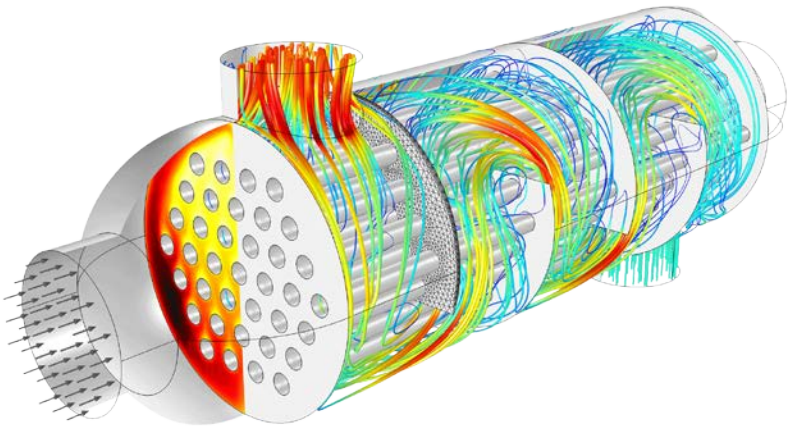

Figure 7.5. Fluid flow around the tubes in a shell-and-tube heat exchanger.

7.3. Available Study Types

7.3.1. Introduction to Study types

The Structural Mechanics Module performs Stationary, Eigenfrequency, Time Dependent, Frequency Domain (frequency response), Linear Buckling, parametric, and quasi-static studies. The different study types require different solvers and equations.

7.3.2. Eigenfrequency Study

An eigenfrequency study solves for the eigenfrequencies and the shape of the eigenmodes. When performing an eigenfrequency analysis, the user can specify whether to look at the mathematically more fundamental eigenvalue, λ, or the eigenfrequency, f, which is more commonly used in a structural mechanics context.

$$f = -\frac{\lambda}{2\pi i} \tag{7.1}$$

If damping is included in the model, an eigenfrequency solution returns the damped eigenvalues. In this case, the eigenfrequencies and mode shapes are complex. A

complex eigenfrequency can be interpreted so that the real part represents the actual frequency, and the imaginary part represents the damping. In a complex mode shape there are phase shifts between different parts of the structure, so that not all points reach the maximum at the same time under free vibration.

Furthermore, it is possible to compute eigenfrequencies for structures which are not fully constrained; this is sometimes referred to as free-free modes. For each possible rigid body mode, there is one eigenvalue which in theory is zero. The number of possible rigid body modes for different geometrical dimensions is shown in the Table 7.1.

Table 7.1. Number of possible rigid body modes in various interfaces.

DIMENSION	NUMBER OF RIGID BODY MODES
3D	6 (3 translations + 3 rotations)
2D axisymmetric	1 (z-direction translation)
2D (solid, beam, truss)	3 (2 translations + 1 rotation)
2D (plate)	3 (1 translation + 2 rotations)

7.3.3. Frequency Domain Study

COMSOL features two frequency analysis studies, Frequency Domain Study and Frequency Domain Modal Study.

The Frequency Domain study is used to compute the response of a linear or linearized model subjected to harmonic excitation for one or several frequencies. For example, in Solid Mechanics, it is used to compute the frequency response of a mechanical structure with respect to particular load distributions and frequencies. In Acoustics and Electromagnetics, it is used to compute the transmission and reflection versus frequency.

A Frequency Domain study accounts for the effects of all eigenmodes that are properly resolved by the mesh and how they couple with the applied loads or excitations. The output of a Frequency Domain study is typically displayed as a transfer function, for example, magnitude or phase of deformation, sound pressure, impedance, or scattering parameters versus frequency.

The actual difference of the first study as compared to the second one is that the former provides a solution based on the harmonic development of the equations (i.e. fixed sinus excitation at the frequency of the sweep range), utilizing the full range of the frequency model. The frequency sweep is achieved with the use of a Parametric Stationary Solver, which is predefined for the linearization of the equations.

On the other hand, Frequency Domain Modal Study uses an Eigenfrequency Analysis to limit the model to a few vibrating modes which the user should predefine and after having first applied Harmonic Perturbation forces, the solver proceeds to find a solution of the reduced model.

7.3.4. Time Dependent Study

A Time Dependent (transient) study solves a time-dependent problem where loads and constraints can vary in time. Time dependent studies can be performed using either a direct or a modal method.

7.3.5. Stationary Study

The Stationary study is used when field variables do not change over time. For example, in electromagnetics, it is used to compute static electric or magnetic fields, as well as direct currents. In heat transfer, it is used to compute the temperature field at thermal equilibrium. In solid mechanics, it is used to compute deformations, stresses, and strains at static equilibrium. In fluid flow it is used to compute the steady flow and pressure fields. In chemical species transport, it is used to compute steady-state chemical composition in steady flows. In chemical reactions, it is used to compute the chemical composition at equilibrium of a reacting system.

It is also possible to compute several solutions, such as the number of load cases, or to track the nonlinear response to a slowly varying load. A Stationary study node corresponds to a Stationary Solver (the default) or a parametric solver, and it is used to solve a stationary problem. There is also an option to run a Stationary Study with an Auxiliary sweep, with or without a continuation parameter. When a continuation parameter is selected, the continuation algorithm is run, which assumes that the sought solution is continuous in these parameters. If no continuation parameter is given, a plain sweep is performed where a solution is sought for each value of the parameters. In both cases a Stationary Solver node plus a Parametric attribute is used. The parametric solver is the algorithm that is run when a Parametric attribute node is active under a Stationary Solver.

7.3.6. Linear Buckling Study

A linear buckling study includes the stiffening effects from stresses coming from nonlinear strain terms. The two stiffnesses from stresses and material define an eigenvalue problem where the eigenvalue is a load factor that, when multiplied with the actual load, gives the critical load - the value of a given load that causes the structure to become unstable - in a linear context. The linear buckling study step uses the Eigenvalue Solver. Another way to calculate the critical load is to include large deformation effects and increase the load until the load has reached its critical value. Linear buckling is available in the Solid Mechanics, Shell, Plate, and Truss interfaces.

7.3.7. Prestressed Analysis: Eigenfrequency and Frequency Domain Study types

The Prestressed Analysis Eigenfrequency and Frequency Domain study types make it possible to compute the eigenfrequencies and the response to harmonic loads that are affected by a static preload. These studies involve two study steps for the solver (a Stationary study step plus an Eigenfrequency or Frequency Domain study step). However, the user needs to add a new study to the model to get access to such combined study types, and they cannot be added directly as new study steps to the existing study (solver sequence).

7.4. Stress and Strain in Structural Mechanics Interfaces

In the initial stages of deformation, many materials exhibit a linear relationship between stress and strain. Furthermore, an accepted assumption is that most materials have the same stiffness properties in all directions, thus the material is set to be linear elastic as well as isotropic.

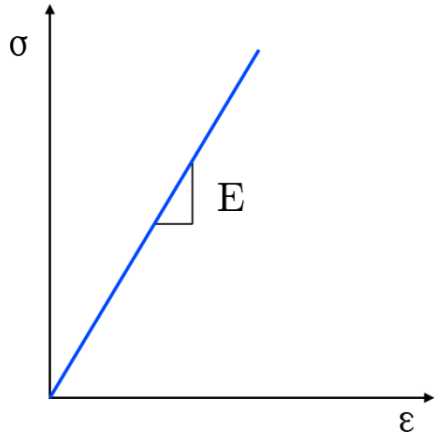

Figure 7.6. Relation between stress and strain in an isotropic material.

However, many materials exhibit some type of anisotropic behavior. A fully anisotropic elastic material requires 21 parameters to specify their elastic behavior:

$$\begin{bmatrix} \sigma_x \\ \sigma_y \\ \sigma_z \\ \tau_{xy} \\ \tau_{yz} \\ \tau_{zx} \end{bmatrix} = \begin{bmatrix} D_{11} & D_{12} & D_{13} & D_{14} & D_{15} & D_{16} \\ & D_{22} & D_{23} & D_{24} & D_{25} & D_{26} \\ & & D_{33} & D_{34} & D_{35} & D_{36} \\ & & & D_{44} & D_{44} & D_{45} \\ & & & & D_{54} & D_{55} \\ & & & & & D_{65} \end{bmatrix} = \begin{bmatrix} \varepsilon_x \\ \varepsilon_y \\ \varepsilon_z \\ \gamma_{xy} \\ \gamma_{yz} \\ \gamma_{zx} \end{bmatrix} \tag{7.2}$$

Experimental Part

8. Experimental Frequency Response of a Cantilever Beam

8.1. Introduction

In this Chapter, the subject of study is the frequency response of a clamped-free steel bar, as resulting from an impulse excitation. More specifically, the bar is excited by an impact hammer, and special attention is given to its first natural frequencies, which in Section (12.4) are compared with theoretical and numerical solutions.

8.2. Experimental Procedure

8.2.1. Geometry

The beam is clamped at such position as to be exactly 0.5m in length (Fig. 8.3). The width and height are 0.035m and 0.0035m respectively.

8.2.2. Experimental Equipment and Configuration

The list below enumerates the equipment used for the testing procedure, and Figure (8.1) gives a perspective view on the setup configuration. Furthermore, Figure (8.2) indicates where from the input and output signals begin, exactly after the impact excitation.

i. Desktop PC (*Intel(R), Pentium(R)* D Processor, CPU 3.40 GHz, 2.00 GB of RAM, Operation System *Windows XP*);
ii. Amplifier and signal conditioner, *PCB PIEZOTRONICS*$^{INC.}$ Model 482A16;
iii. Force Transducer/Impact Hammer, *Brüel & Kjær* Type 8203;
iv. PCI Data acquisition card, *MEASUREMENT COMPUTING* DaqBoard/3000 Series ;
v. Acquisition card hardware interface, *MEASUREMENT COMPUTING* DBK215 16-Connector BNC;
vi. Accelerometer *PCB PIEZOTRONICS*$^{INC.}$ Model 352B10;
vii. *DaqView*$^{®}$ software application for data logging and analysis;

viii. *MATLAB*® software application, Version R2013a, for postprocess analysis.

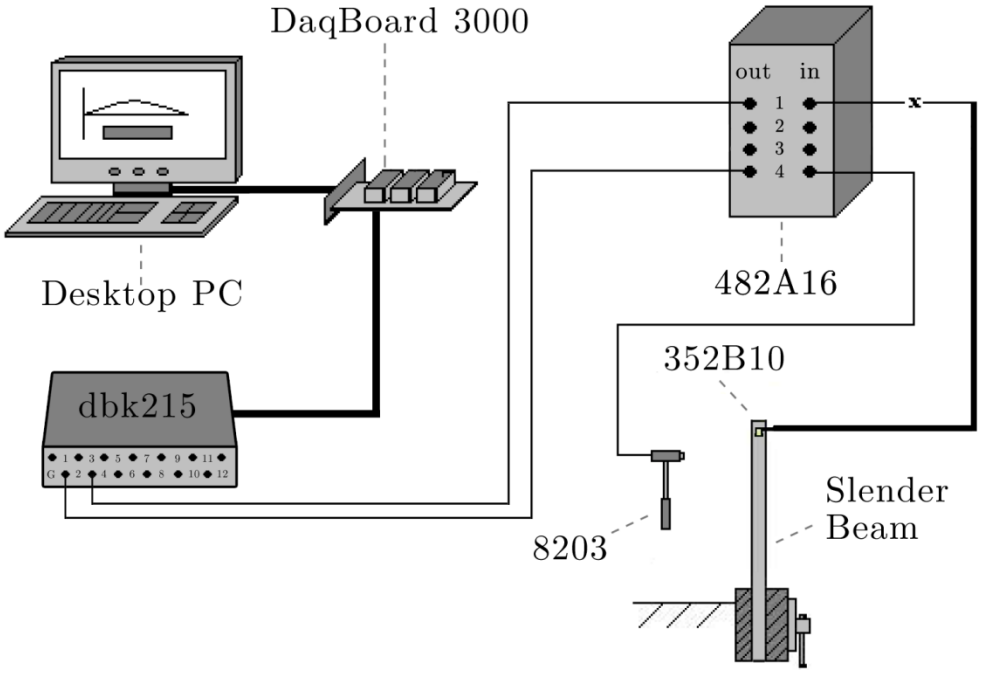

Figure 8.1. Testing setup.

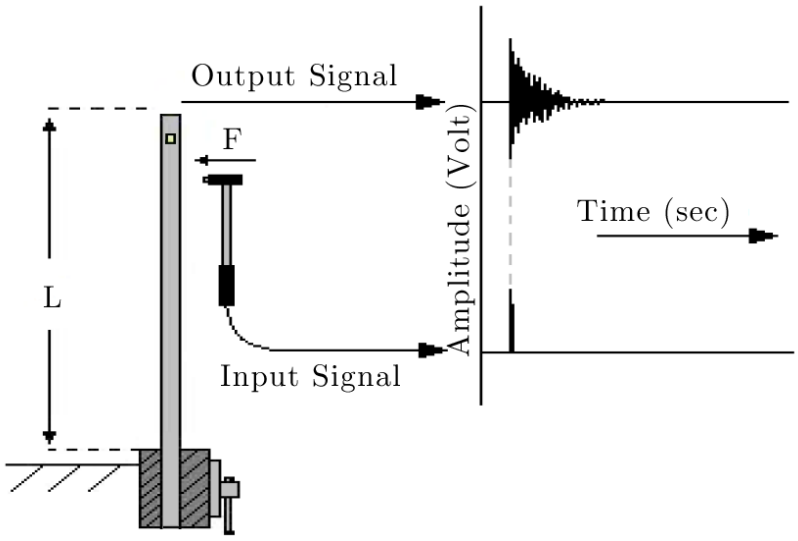

Figure 8.2. Visualization of the testing process.

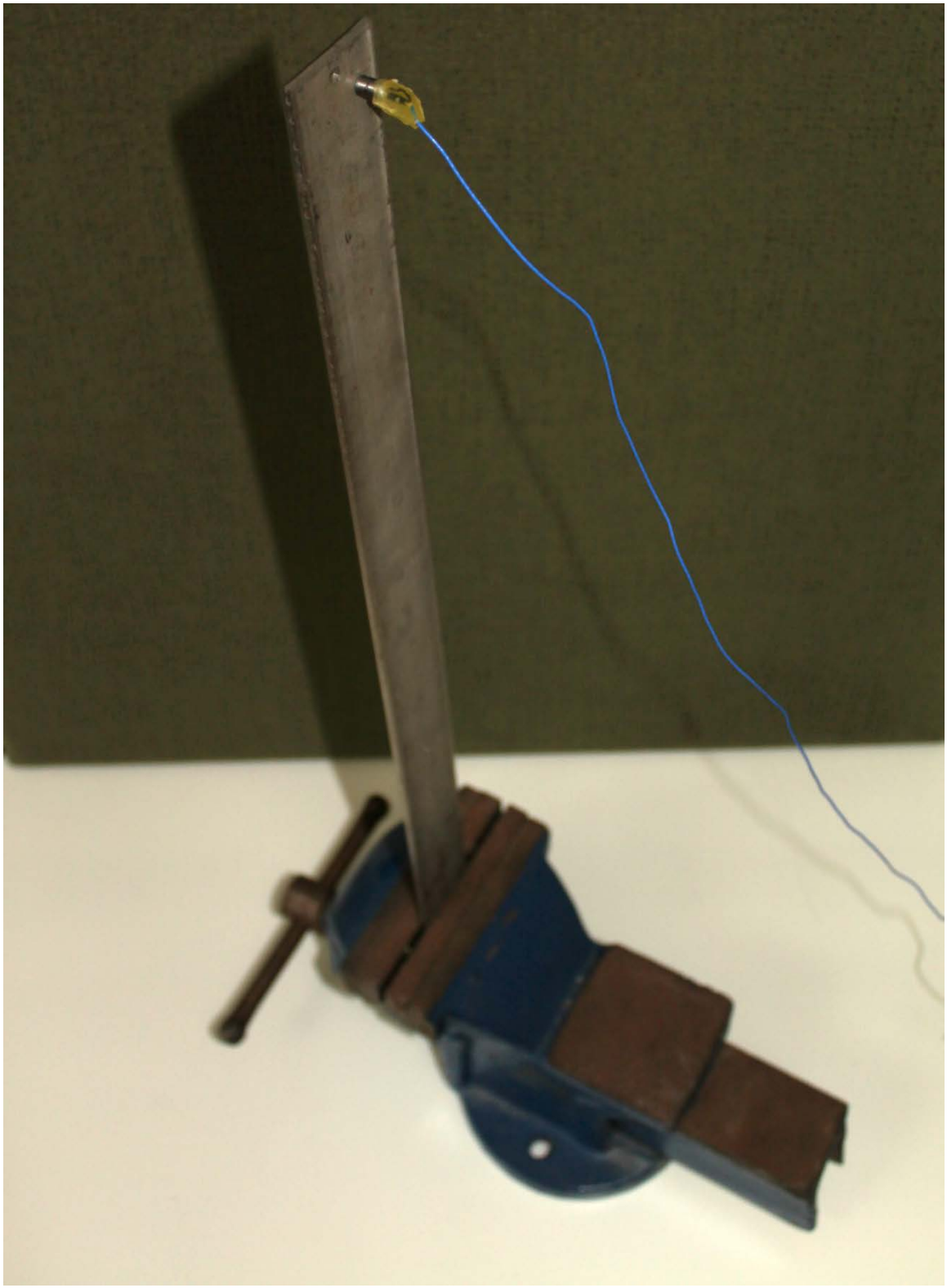

Figure 8.3. Testing beam.

8.2.3. Acquisition setup

The maximum sampling rate of the acquisition card is 1MHz; for this experiment the sampling frequency chosen is 50KHz. The acquisition is set to stop after 150000 scans, i.e. after 3 seconds. Both of these settings along with a graphic display of *DaqView* software are shown in Figure (8.3).

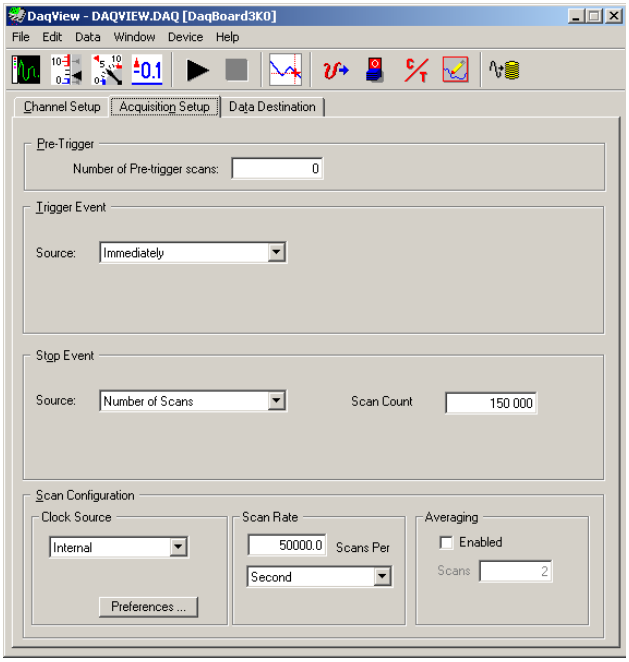

Figure 8.3. Acquisition setup window in DaqView software.

8.2.4. Acquisition Process

The process begins with a basic equipment check. The acquisition cards, the conditioner and the accelerometer must be calibrated; if data from the impact hammer are to be used, then the hammer must be calibrated as well.

The next step is to determine the exact position where to place the accelerometer, because it defines whether a natural frequency will be excited within the frequency span of interest or not (further discussion can be found in Chapter 12).

The same goes for the location of the impact force excitation on the test structure, which directly affects which vibration modes will be excited.

Table 8.1 shows the first eigenfrequencies of the vibrating beam. Note that the third vibration mode is the first torsional mode, and more than one accelerometer is needed in order to ensure proper measurements. In most cases, even if the vibration mode is excited, its amplitude will be very low compared to the other modes.

Table 8.1. Experimental natural frequencies of the cantilever beam.

MODE NUMBER	EXPERIMENTAL FREQUENCY (Hz)
1	10.33
2	67.00
3	-
4	185.00
5	274.30
6	376.00

8.2.5. Post processing experimental data

Following the measurement procedure, the collected data are being analyzed. Due to a number of unpredictable factors, like signal interferences from cables, harmonic distortions from the electronic devices, the human element, humidity and dirt, surface/mass of the transducers, temperature or resonances from the mechanical parts, etc., every signal acquires some noise that should be eliminated, or some unwanted frequencies that should be perceived.

There are several restoration routines, such as the removal of the offset DC component from a signal, general denoising, checking for signal clipping, removing of excessive background noise, and others.

For the above reasons, a Matlab® script (Appendix A) was developed, the results of which are shown in Figures (8.4) and (8.5).

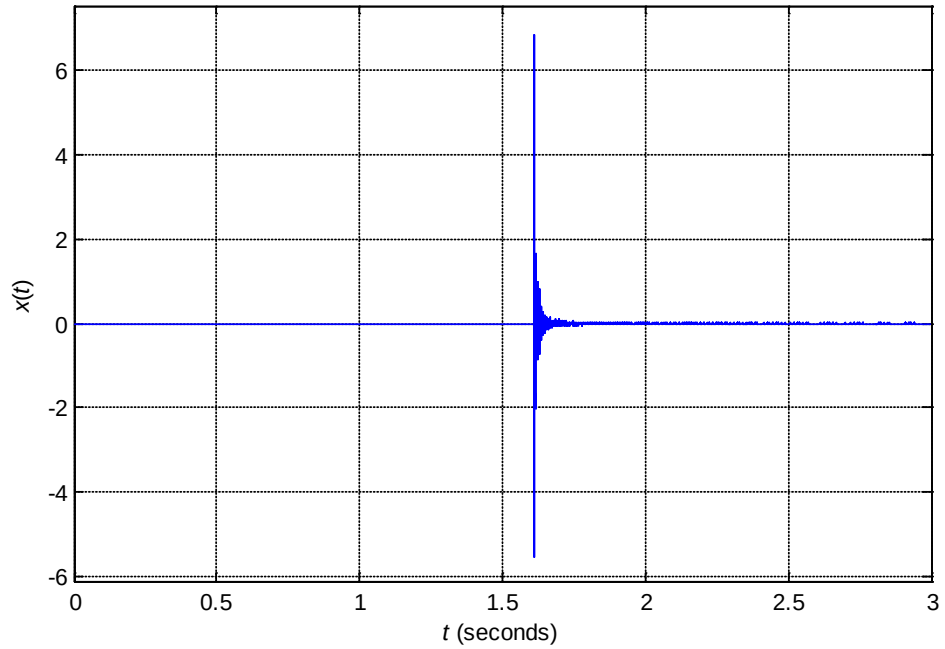

Figure 8.4. Response signal to the impact measured from the accelerometer.

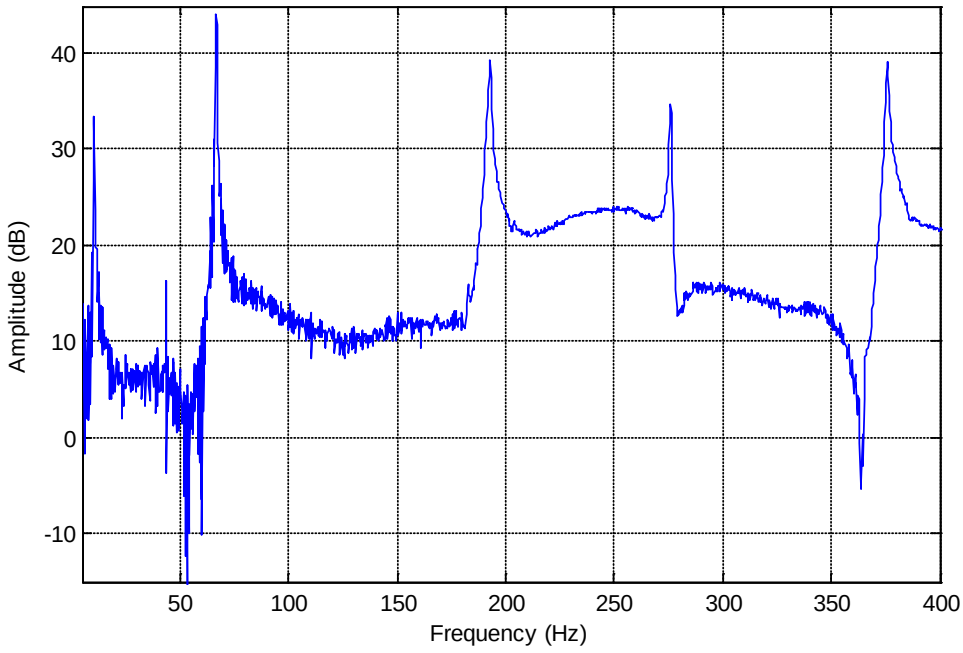

Figure 8.5. Frequency response of the cantilever beam in a range of 0 to 400 Hz.

8.2.6. Notes

During the measurements, some observations were made. The PCB conditioner appeared to present a harmonic distortion, when the preamplifier's gain was set to x10 or x100. Measurements were made with a x1 gain, which of course did not affect the procedure at all, since the signal's amplitude was by definition quite high, due to the impact.

Throughout the procedure, attention must be paid to the amplitude of the input signal, as, due to the impact, it is very easy to get clipped.

Examples

9. Vibrating string

9.1. Introduction

In the following example, the natural frequencies of a pre-tensioned string are computed using the 2D Truss interface. This is an example of *stress stiffening*. In fact, the transverse stiffness of truss elements is directly proportional to the tensile force.

Strings made of piano wire have an extremely high yield limit, thus enabling a wide range of pre-tension forces. The results are compared with the analytical solution.

9.2. Model Definition

9.2.1. Geometry

The finite element idealization consists of a single line, with length $L = 0.5\ \mathrm{m}$, created by the *Bézier Polygon* tool from the *Geometry* node.

The diameter of the wire is irrelevant to the solution of this particular problem, but it must still be given. The cross section area for $1.0\ \mathrm{mm}$ diameter is defined from the *cross section* node, and it is $A = 0.785\ \mathrm{mm}^2$.

9.2.2. Material

The following material properties are defined through the *materials* node:

i. Young's modulus, $E = 210\ \mathrm{GPa}$;
ii. Poisson's ratio, $\nu = 0.31$, and
iii. Mass density, $\varrho_L = 7850\ \mathrm{kg/m}^3$.

9.2.3. Constraints

Both ends of the wire are fixed, thus the two points that constitute the model are constrained as *pinned*.

9.2.4. Load

The wire is pre-tensioned to $T = 1520\ \mathrm{MPa}$; this *initial axial stress* must be given at *Initial Stress and Strain* of the *Linear Elastic Material* node.

9.2.5. Mesh

An *Edge* mesh is used (Fig. 9.1), with $0.05\ \mathrm{m}$ *Maximum element size*, which gives:

i. Number of vertex elements, 2;
ii. Number of boundary elements, 10.

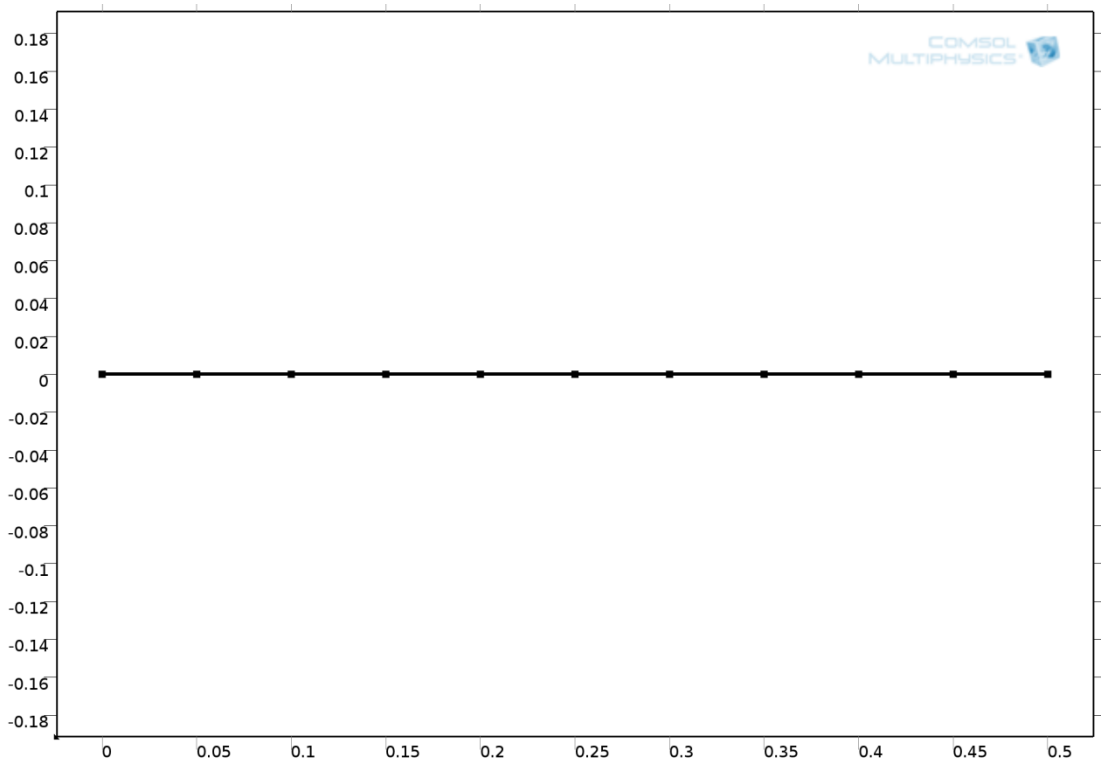

Figure 9.1. Edge mesh with 10 boundary elements.

9.2.6. Study

An eigenfrequency module is used for finding out the natural frequencies and their corresponding mode shape. The *Number of degrees of freedom solved for* was 42.

9.3. Results

The analytical solution for the natural frequencies of the vibrating string comes from Equation (3.14):

$$f_n = \frac{n}{2L}\sqrt{\frac{T}{\varrho_L}} \tag{9.1}$$

The pre-tensioning stress T in this example is tuned so that the first natural frequency will be Concert A; 440 Hz.

In Table (9.1) the computed results are compared with the results from Equation (9.1). The agreement is quite satisfying. The accuracy will decrease with increasing complexity of the mode shape, because the possibility for the relatively coarse mesh to describe such a shape is limited. The mode shapes for the first three modes are shown in Figure (9.2) through Figure (9.4).

Table 9.1. Comparison between analytical and computed natural frequencies.

MODE NUMBER	ANALYTICAL FREQUENCY (Hz)	COMSOL RESULT (Hz)
1	440.00	440.04
2	880.00	880.16
3	1320.00	1320.80
4	1760.00	1762.96
5	2200.00	2208.43

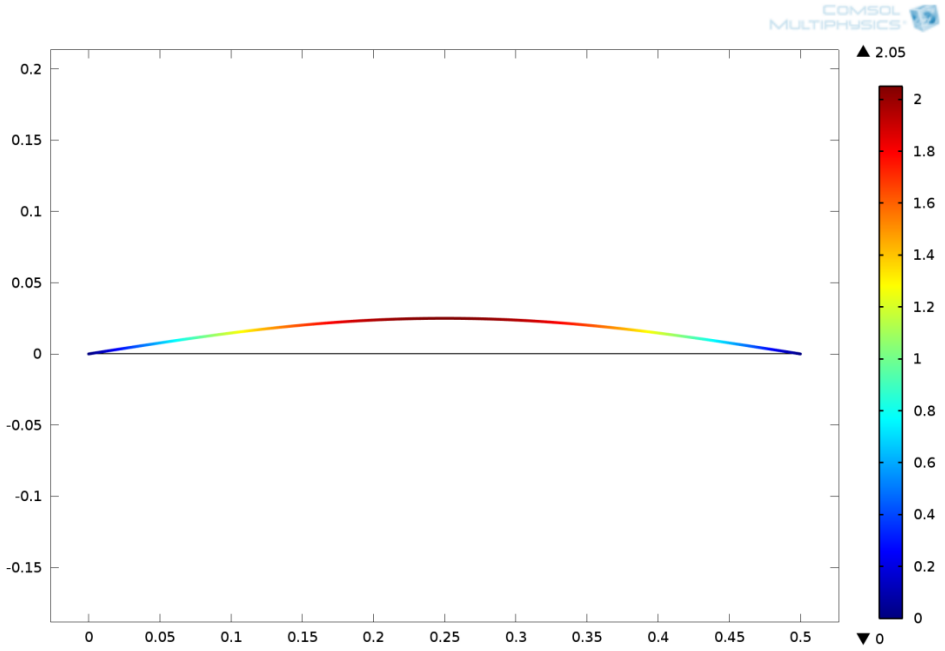

Figure 9.2. Mode shape of the 1st natural frequency of a fixed string.

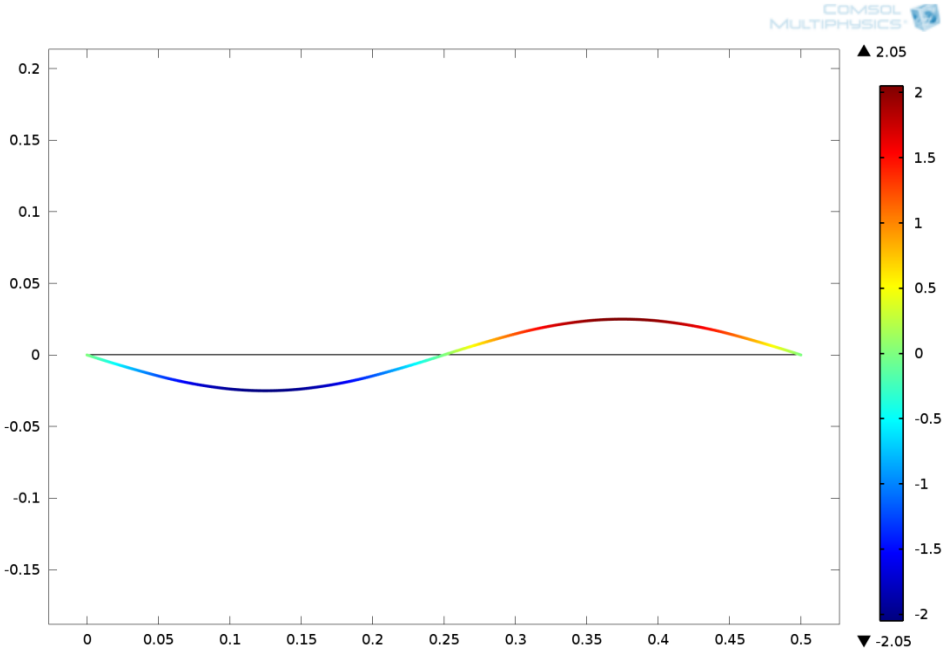

Figure 9.3. Mode shape of the 2nd natural frequency of a fixed string.

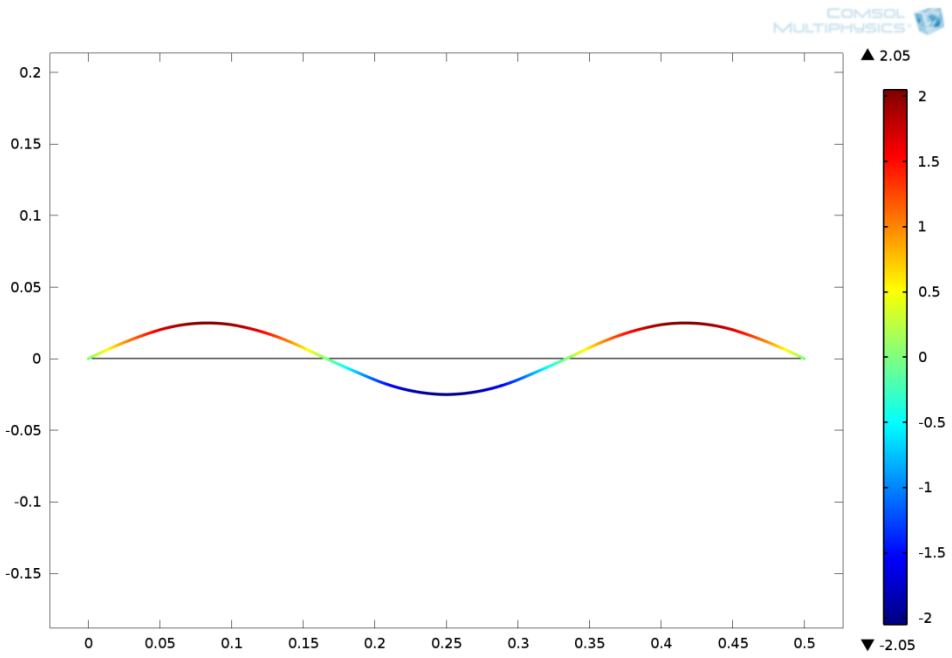

Figure 9.4. Mode shape of the 3rd natural frequency of a fixed string.

10. Nodal positions and mode shapes of a free beam

10.1. Introduction

In general, the nodal positions can be described as the positions along a vibrating system where the deflection is zero. In this example, two different Finite Element Method studies are being processed and described. The results are plotted and compared with theoretical ones.

10.2. Model Definition – Beam 2D Interface

10.2.1. Geometry

Like *Truss 2D* interface, in the previous chapter, the Finite Element idealization here also consists of a single line, with $1\,\mathrm{m}$ length, created by the *Bézier Polygon* tool from the *Geometry* node.

10.2.2. Material

Nodal positions do not depend upon material, but one material should be defined; from the *material library, Structural steel* is selected, with material properties:

i. Young's modulus, $E = 200\ \mathrm{GPa}$;
ii. Poisson's ratio, $\nu = 0.33$, and
iii. Mass density, $\varrho_L = 7870\ \mathrm{kg/m^3}$.

10.2.3. Constraints

No constraints are applied because the bar is free.

10.2.4. Load

In an eigenfrequency analysis, loads and forces are not taken into consideration.

10.2.5. Mesh

An *Edge* mesh is defined (Fig. 10.1), with 0.01 m *Maximum element size*, which yields:

i. Number of vertex elements, 2;
ii. Number of boundary elements, 100.

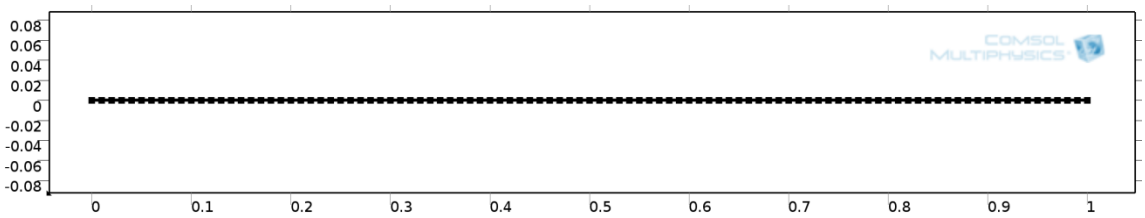

Figure 10.1. Edge mesh of 100 elements.

10.2.6. Study

An eigenfrequency module is used for finding out the natural frequencies and their corresponding mode shape. A *search for eigenfrequencies around* 20 Hz was performed for better accuracy and the *Number of degrees of freedom solved for* was 303.

10.3. Model Definition – Solid Mechanics 2D Interface

10.3.1. Geometry

The length of the bar is the most important feature regarding nodal positions. A rectangle with $a = 1$ m length and $b = 0.004$ m height is created from the *Geometry* node. Note that the height at the *Solid Mechanics 2D* interface represents the thickness. The actual thickness of the bar in the *Solid Mechanics* node is irrelevant for this model but it should still be defined; $d = 0.004$ m is given.

10.3.2. Material

The material selected is *Structural steel,* with the same material properties as above.

10.3.3. Constraints

Again, no constraints are applied because the bar is free.

10.3.4. Load

Loads are not needed in this case either.

10.3.5. Mesh

A *Free Triangular* mesh is defined (Fig. 10.2), with 0.005 m *Maximum element size*, which yields:

i. Number of vertex elements, 4;
ii. Number of boundary elements, 408;
iii. Number of elements, 428.

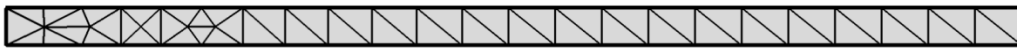

Figure 10.2. Partial view of a free triangular mesh in a two-dimensional interface.

10.3.6. Study

An eigenfrequency module is used. A *search for eigenfrequencies around* 20 Hz was performed for better accuracy and the *Number of degrees of freedom solved for* was 2530.

10.4. Results

Fletcher and Rossing [1998] give the nodal positions for the first four bending vibrational modes of a bar with free ends. Table (10.1) shows a comparison of the nodal points given, with the ones calculated by COMSOL. For this occasion a Matlab script (Appendix A) was developed in order to post process the exported COMSOL data.

Figure (10.3) shows the nodal points, along with the mode shapes as plotted for a 1m length beam with free ends.

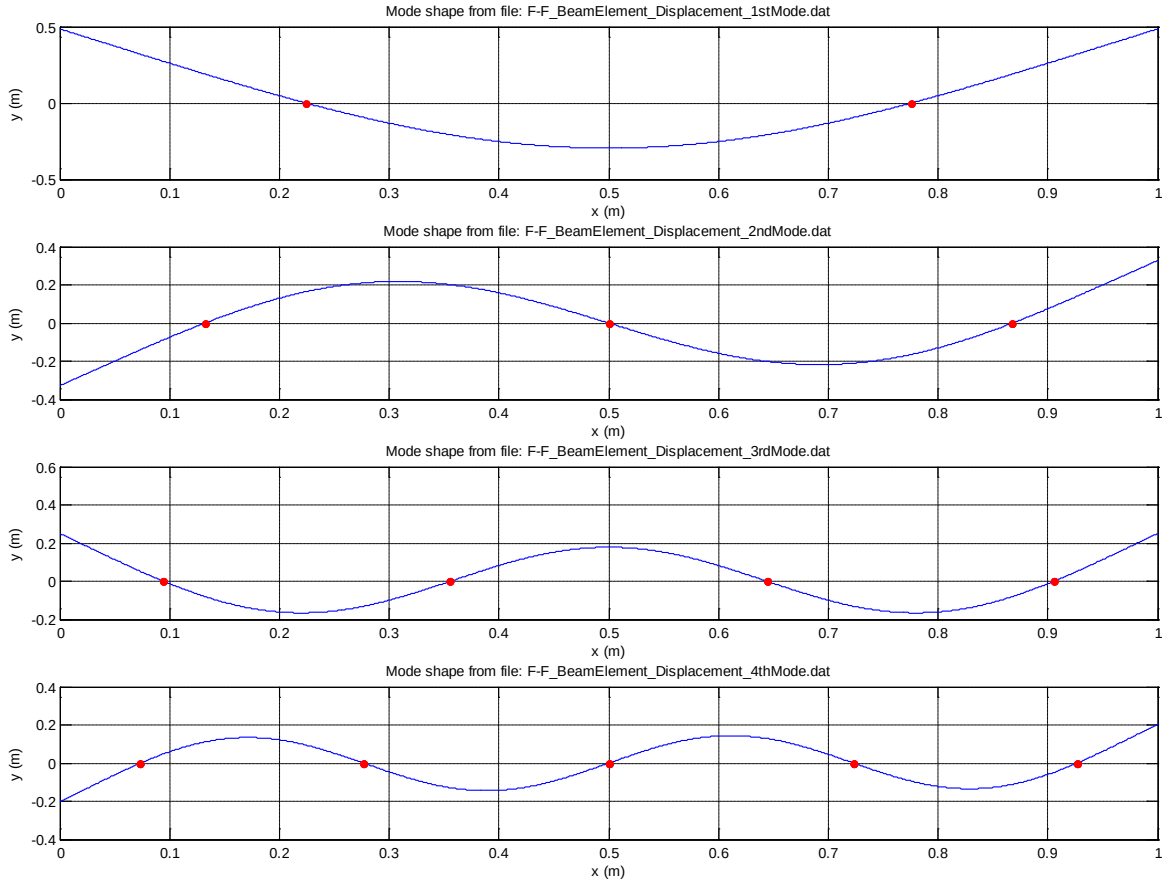

Figure 10.3. Shapes and nodal positions for the first four eigenfrequencies of a free beam with length 1m.

Table 10.1. Characteristics of transverse vibrations in a bar with free ends.

Mode	Nodal Positions (m) derived from analytical solution					Nodal Positions (m) derived from numerical solution – COMSOL Beam 2D interface					Nodal Positions (m) derived from numerical solution - COMSOL Solid Mechanics 2D interface				
1st	0.224	0.776				0.224160	0.775840				0.224160	0.775900			
2nd	0.132	0.500	0.868			0.132110	0.500000	0.867890			0.132110	0.500010	0.867890		
3rd	0.094	0.356	0.644	0.906		0.094443	0.355800	0.644200	0.905560		0.094452	0.355800	0.644200	0.905550	
4th	0.073	0.277	0.500	0.723	0.927	0.073453	0.276780	0.500000	0.723220	0.926550	0.073457	0.276780	0.500000	0.723220	0.926540

Geometry characteristics (m)		Beam Element		Solid Mechanics Element	
Length	1	Number of vertex elements	2	Number of vertex elements	4
Height	0.004	Number of boundary elements	100	Number of boundary elements	408
Thickness	0.004	Search for eigenfrequencies around (Hz)	20	Search for eigenfrequencies around (Hz)	20
		Number of degrees of freedom solved for	303	Number of degrees of freedom solved for	2530

11. Deformed cantilever beam

11.1. Introduction

In this section, a statics problem is introduced and explained. A cantilever beam is modeled in COMSOL using the *Solid 3D* interface, and the deformed beam's top surface length is calculated and compared to the beam's top surface length in equilibrium.

11.2. Model Definition

11.2.1. Geometry

A *block* with sides length = 1500 mm, depth = 100 mm and height = 10 mm is created from the *Geometry* node (Fig. (11.1)).

11.2.2. Definitions

In order to calculate the length along the top surface of the cantilever, an *integration* is added from the *definitions* node and one of the two *edges* running the upper side of the cantilever is selected (Fig. (11.1)).

11.2.3. Material

A *Structural steel* material is added from the *material library,* with material properties:

i. Young's modulus, $E = 200\ \mathrm{GPa}$;
ii. Poisson's ratio, $\nu = 0.33$, and
iii. Mass density, $\varrho_L = 7870\ \mathrm{kg/m^3}$.

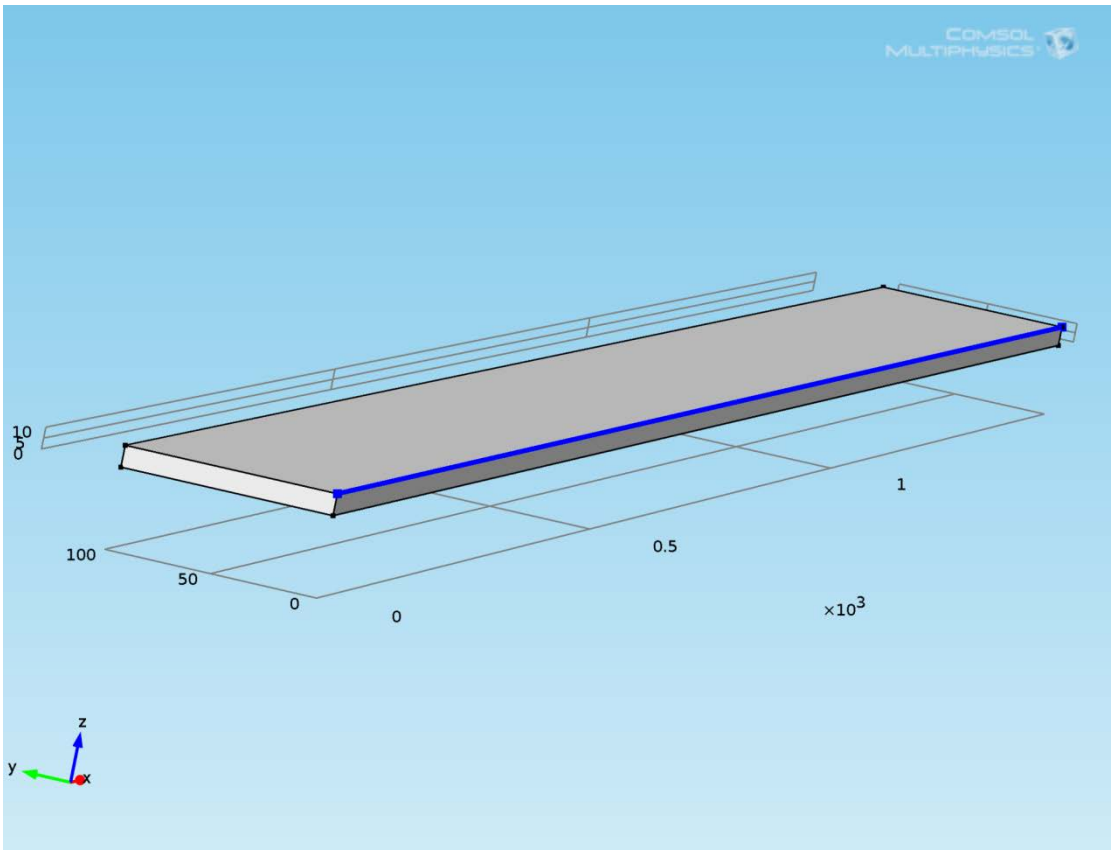

Figure 11.1. A bar modeled with an upper side edge selected.

11.2.4. Constraints

The beam is clamped at one end and free at the other, thus a *fixed constraint* boundary condition is added and *boundary 1* is selected.

11.2.5. Loads

The cantilever beam bends under its own weight; that could be effected by adding a *body load* in the z-direction. The force of this load should be of the type of mass times gravitational acceleration. In COMSOL this can be translated as solid.rho*g_const.

11.2.6. Mesh

A *Free Triangular* mesh is used (Fig. (11.2)), with 120 mm *Maximum element size*, which gives:

i. *Number of vertex elements*, 8;
ii. *Number of edge elements*, 388;
iii. *Number of boundary elements*, 2928;
iv. *Number of elements*, 3839.

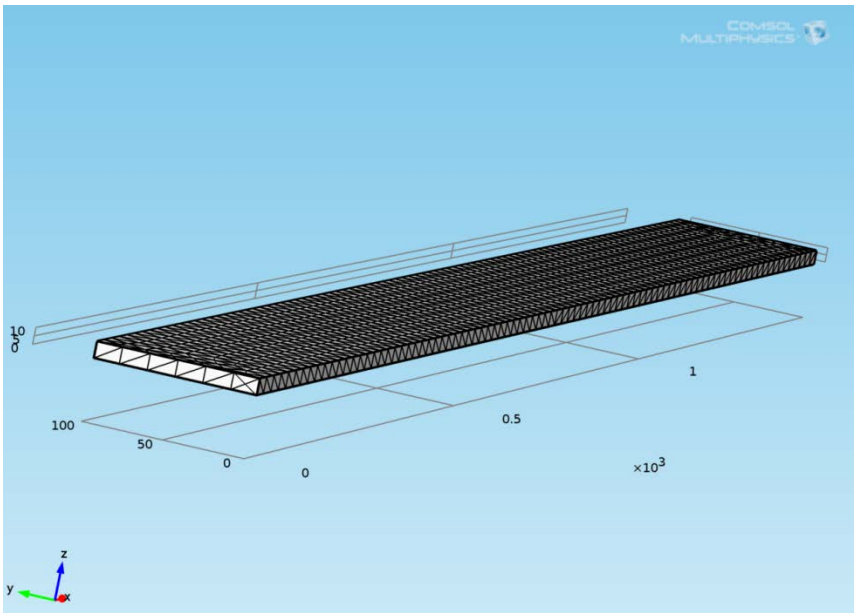

Figure 11.2. Free triangular mesh.

11.2.7. Study

A Stationary module is implemented for a static/steady state analysis, where deformations and forces are being calculated. In this study, loads and constraints are constant in time.

Note that in order to get a difference between the *Material* and the *Spatial* frame, *Geometric Nonlinearity* must be active for the study step (i.e. *Include geometric nonlinearity* node).

The *Number of degrees of freedom solved for* was 24726.

11.3. Post processing data

Based on the theory explained in Chapter 4, and since this cantilever is bending downwards, the top surface will be stretched and longer than its initial length, while the bottom will be shorter. In order to get the integration along the deformed beam, one should collect the results under *Global Evaluation* node, adding the integration *expression* used in *definition* section (in this case, as Figure (11.3) indicates, *top_surface_1* and *top_surface_2*).

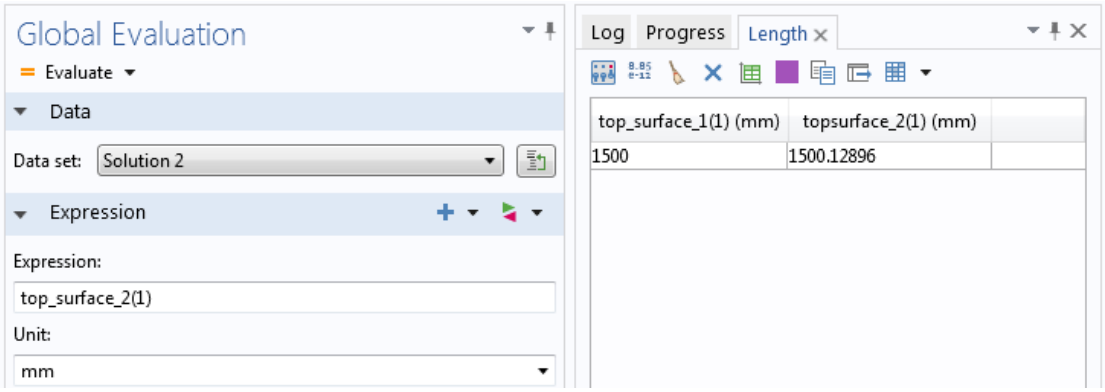

Figure 11.3. Settings under the Global Evaluation node for deriving the deformed beam's length.

11.4. Results

Table (11.1) shows the state of the upper side beam's length before and after deformation, and Figure (11.3) shows the stresses acting on the cantilever at a steady-state situation.

Table 11.1. Top surface beam's length before and after stationary analysis.

EQUILIBRIUM LENGTH (mm)	DEFORMED BEAM'S LENGTH (mm)
1500	1500.13

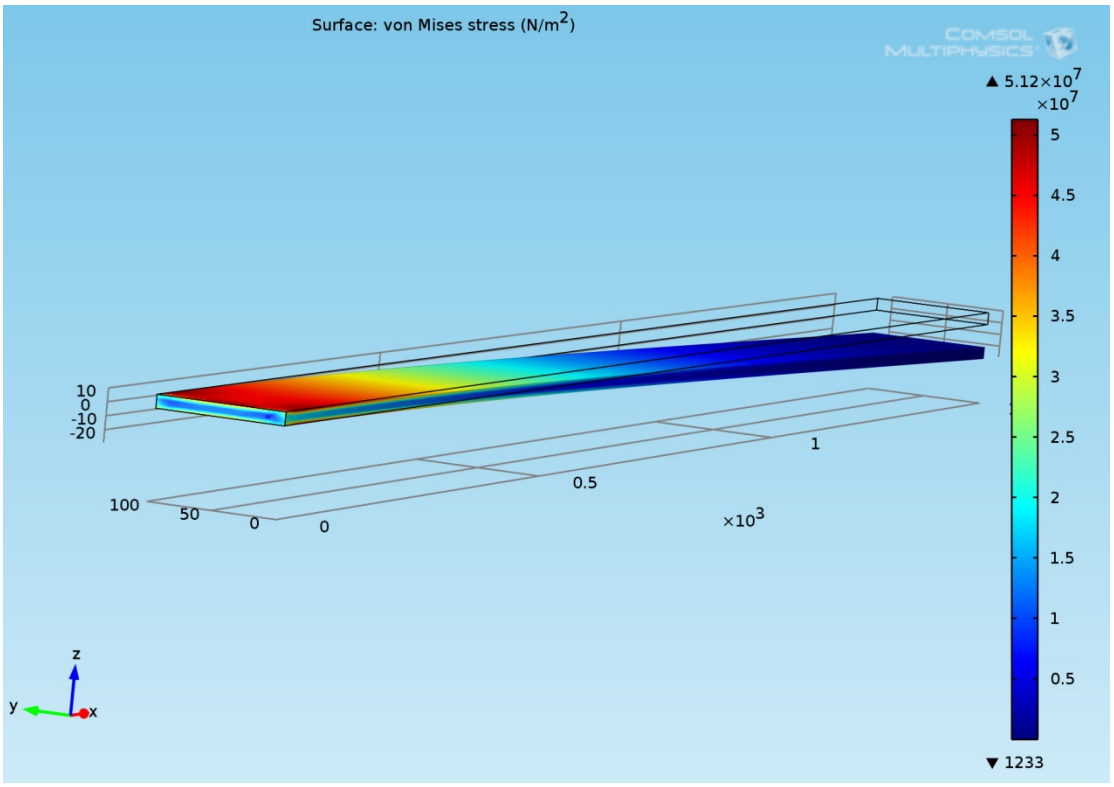

Figure 11.3. Stress forces on a deformed cantilever beam.

11.5. Further Notes

In *stationary* study steps, when the model obtains very large deformations, usually the geometrically nonlinear analysis has convergence problems. If so, the load must be increased gradually using a *continuation parameter* rather than applying the full load in one step.

12. Eigenfrequency Analysis of a Cantilever Beam

12.1. Introduction

In the present example, a steel beam with one end clamped and one free is modeled in two different COMSOL interfaces, and both results are compared with theoretical ones, as well as with experimental data from Chapter 8. Interestingly enough, the differences observed are not limited only to frequency deviation, but in fact focus on frequency existence and diversity of vibration modes.

12.2. Model Definition – Beam 2D Interface

12.2.1. Geometry

A single line with $0.5\ \mathrm{m}$ length is created by the *Bézier Polygon* tool from the *Geometry* node.

12.2.2. Material

In case of eigenfrequency, the material of the structure is extremely essential (see Chapter 2). From the *material library, Structural steel* is selected, with material properties:

i. Young's modulus, $E = 190\ \mathrm{GPa}$.
ii. Poisson's ratio, $\nu = 0.33$, and
iii. Mass density, $\varrho_L = 8000\ \mathrm{kg/m^3}$.

12.2.3. Constraints

The bar is clamped at one end and free at the other, therefore *Point 1* is selected to be *Fixed Constraint*.

12.2.4. Load

In an eigenfrequency analysis loads and forces are not taken into consideration.

12.2.5. Mesh

An *Edge* mesh is used (Fig. 12.1), with 0.025 m *Maximum element size*, and therefore results in:

i. Number of vertex elements, 2;
ii. Number of boundary elements, 20.

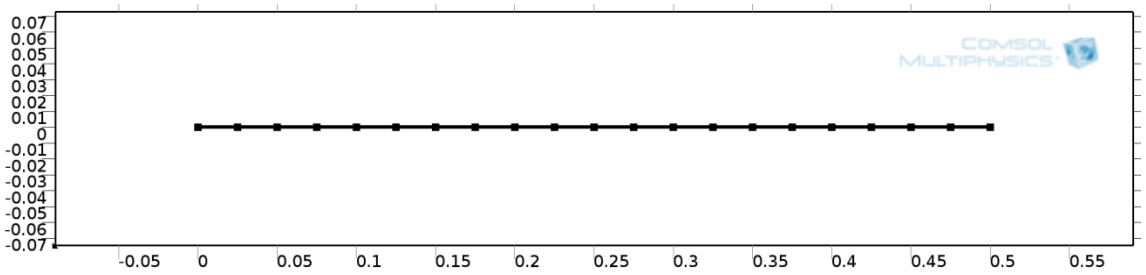

Figure 12.1. Edge mesh of 20 elements.

12.2.6. Study

An eigenfrequency module is used for finding out the natural frequencies and their corresponding mode shape. A *search for eigenfrequencies around* 10 Hz was performed for better accuracy and the *Number of degrees of freedom solved for* was 63.

12.3. Model Definition – Solid Mechanics 3D Interface

12.3.1. Geometry

A *Block* of Width = 0.5 m, Depth = 0.035 m and Height = 0.0035 m is created from the *Geometry* node.

12.3.2. Material

The material selected is *Structural steel,* with the same material properties as above.

12.3.3. Constraints

Again, the constraints are the same as in the previous interface.

12.3.4. Load

Loads are not needed in this case either.

12.3.5. Mesh

A *Free Tetrahedral* mesh is defined (Fig. 12.2), with 0.005 m *Maximum element size*, which yields:

iii. Number of vertex elements, 8;
iv. Number of edge elements, 616;
v. Number of boundary elements, 8114;
vi. Number of elements, 20592.

12.3.6. Study

An eigenfrequency module is used. A *search for eigenfrequencies around* 10 Hz was performed for better accuracy and the *Number of degrees of freedom solved for* was 107646.

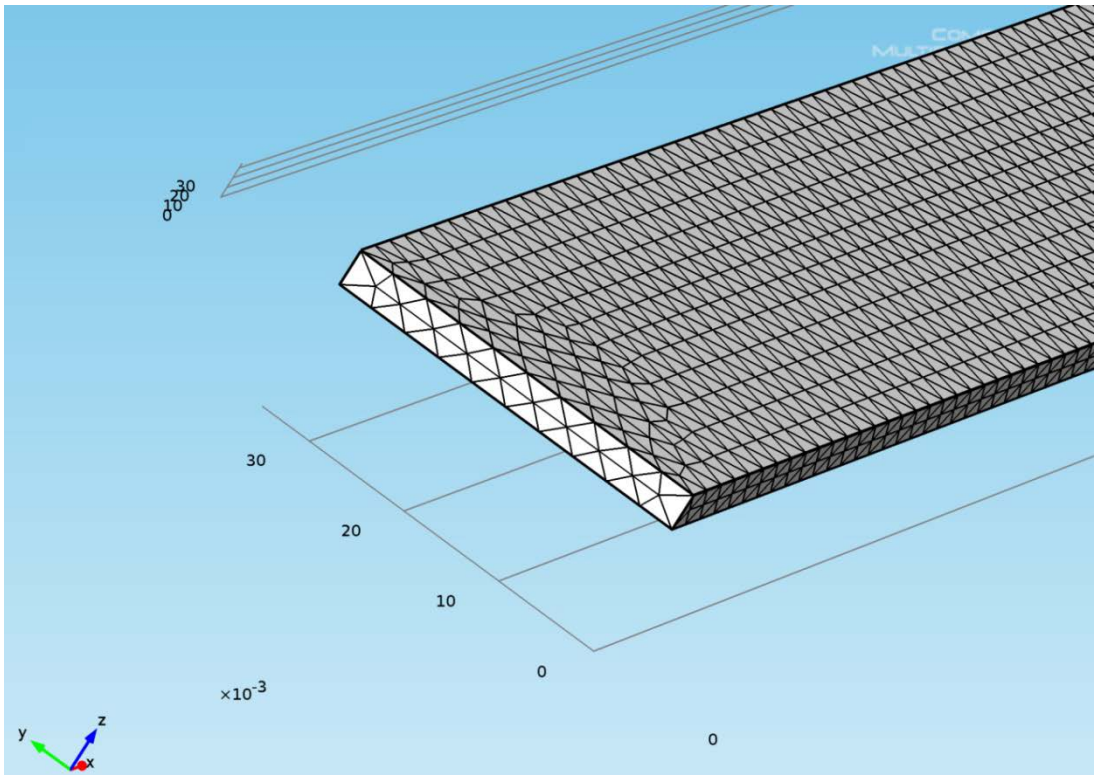

Figure 12.2. Partial view of a free tetrahedral mesh in a three-dimensional structure.

12.4. Results

Figure (12.3) depicts the first four mode shapes of a cantilever beam as calculated from *Beam 2D Interface*. Similarly, Figures (12.4) through (12.9) show the corresponding mode shapes in three dimensions. Finally, Table (12.1) presents a comparison between the FEM computations, the theoretical calculations and the experimentally derived values from the testing procedure of Chapter 8.

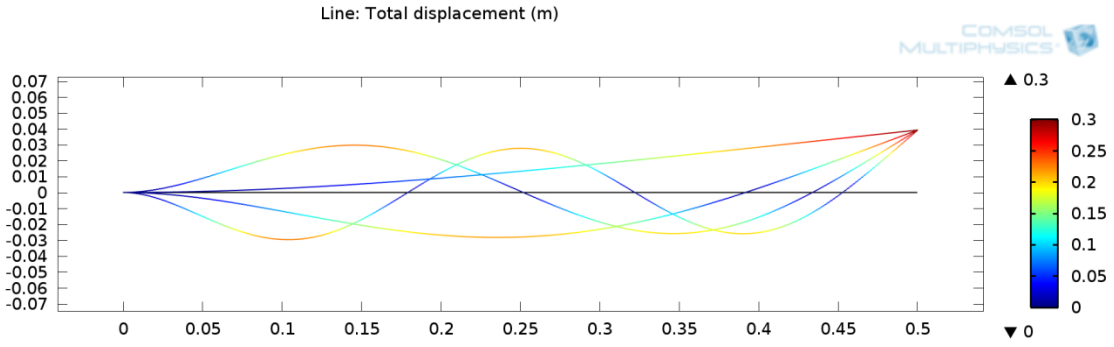

Figure 12.3. First four vibrating modes of a fixed-free beam.

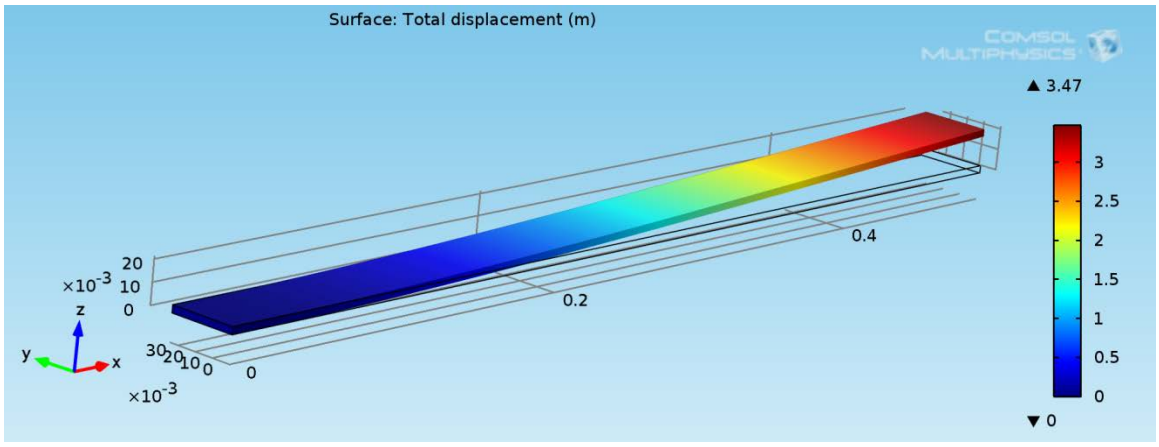

Figure 12.4. Mode shape of the first natural frequency found. 11.09 Hz .

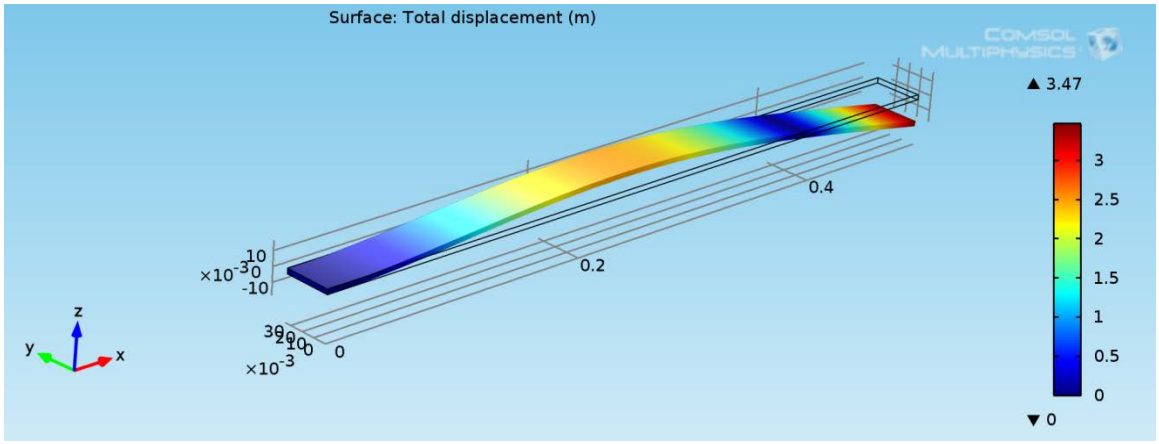

Figure 12.5. Mode shape of the second natural frequency found. 69.44 Hz .

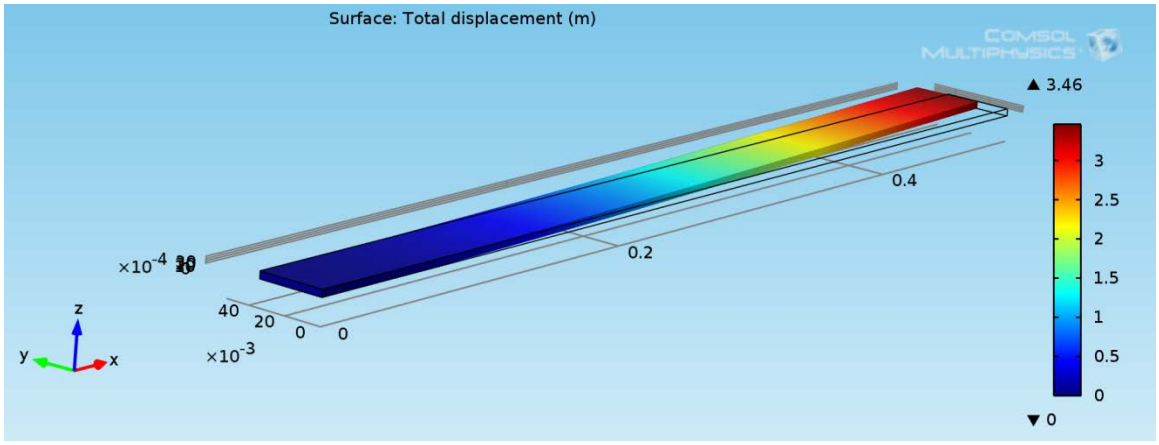

Figure 12.6. Mode shape of the third natural frequency found. 109.95 Hz .

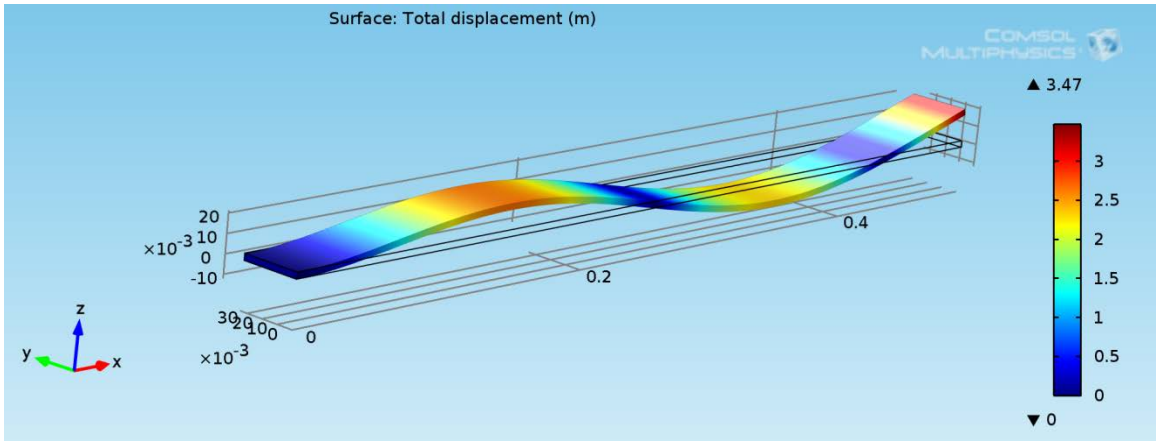

Figure 12.7. Mode shape of the fourth natural frequency found. 194.45 Hz .

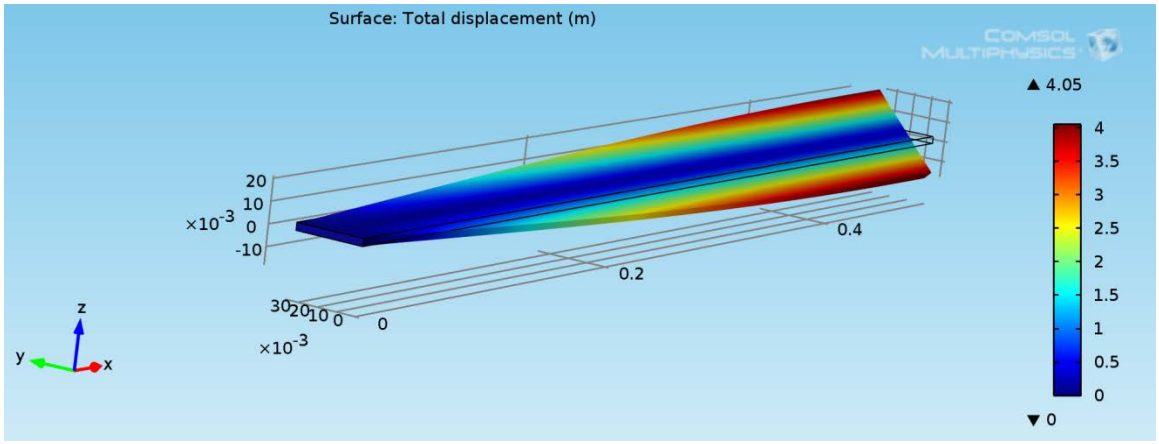

Figure 12.8. Mode shape of the fifth natural frequency found. 293.67 Hz .

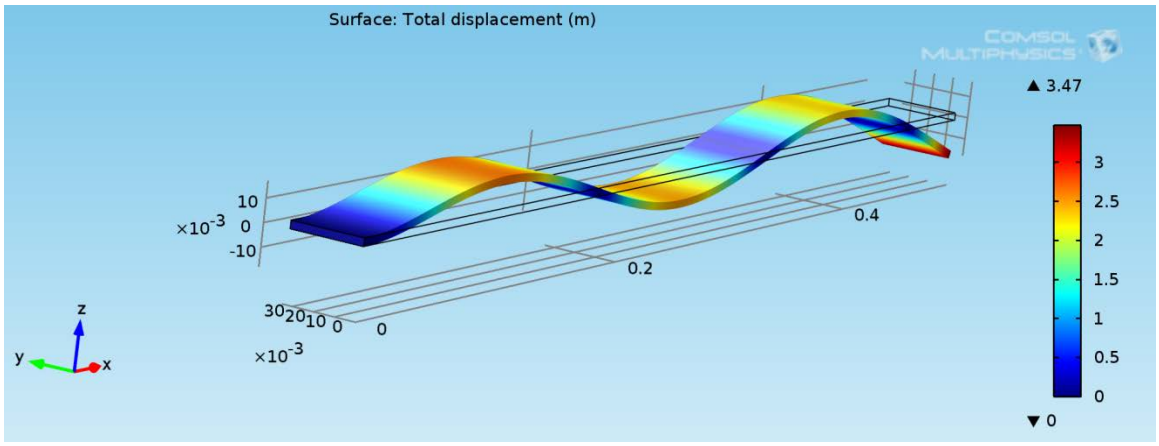

Figure 12.9. Mode shape of the sixth natural frequency found. 381.18 Hz .

Table 12.1. Frequency comparison for a beam of fixed-free boundary conditions.

TRANSVERSE MODES	TORSIONAL MODES	FREQUENCY RELATIONSHIP	ANALY-TICAL SOLUTION (Hz)	COMSOL 2D BEAM ELEMENT (Hz)	COMSOL 3D SOLID MECHANICS ELEMENT (Hz)	EXPERI-MENTAL (Hz)
1	-	f_1	11.03	11.02	11.08	10.33
2	-	$6.26f_1$	69.05	69.07	69.44	66.00
-	a	$9.92f_1$	-	-	109.95	-
3	-	$17.54f_1$	193.36	193.40	194.45	185.00
-	b	$26.49f_1$	-	-	293.67	274.30
4	-	$34.38f_1$	378.99	379.01	381.18	376.00

Note that as theory indicated (Chapter 4),

i. the frequencies are not harmonically related;

ii. the *Euler–Bernoulli* model gives good approximations for the low vibrating modes.

Moreover, another point to be made is that both analytical and COMSOL 2D solutions do not take into account the torsional modes. On the other hand, the three-dimensional element solves for both bending and rotational modes.

Further study of Table (12.1) shows that the torsional mode (Fig. (12.6)) is missing a value from the experimental data, and that is because the shape of the mode demanded a different set of impact hammer and accelerometer locations (see Section 8.2.4). On the contrary, and despite the fact that *b* vibration mode has also rotational behavior, the acquisition level was sufficient enough; this is explained in Figure (12.8) (compared with Fig. (12.6)).

13. Eigenfrequency Analysis of a free Plate – Nodal Patterns

13.1. Introduction

In the following example, the first vibrating modes for a free rectangular brass plate are calculated using the Finite Element Method, and their nodal patterns are presented along with Mary D. Waller's [1939] experimental results.

The nodal patterns are in fact the spatial coordinates where the displacement is zero. Those patterns consist of a number of lines; they are called *contour lines*, and an example of how they derive from COMSOL *Plate 2D* interface is given below.

13.2. Model Definition

13.2.1. Geometry

A rectangle with sides $a = 1$ m and $b = 0.5$ m is created from the *Geometry* node. These are arbitrary values chosen to confirm the $a / b = 2$ ratio.

The thickness of the plate is given $d = 0.01$ m in the *Plate* node.

13.2.2. Material

A *Copper* material is selected from the *material library,* with material properties:

i. Young's modulus, $E = 110$ GPa;
ii. Poisson's ratio, $\nu = 0.35$, and
iii. Mass density, $\varrho_L = 8700$ kg / m^3 .

13.2.3. Constraints

No constraints are applied because the plate is free.

13.2.4. Load

In an eigenfrequency analysis loads are not needed.

13.2.5. Mesh

A *Free Triangular* mesh is used (Fig. 13.1), with 0.02 m *Maximum element size*, which gives:

i. Number of vertex elements, 4;
ii. Number of boundary elements, 150;
iii. Number of elements, 3150.

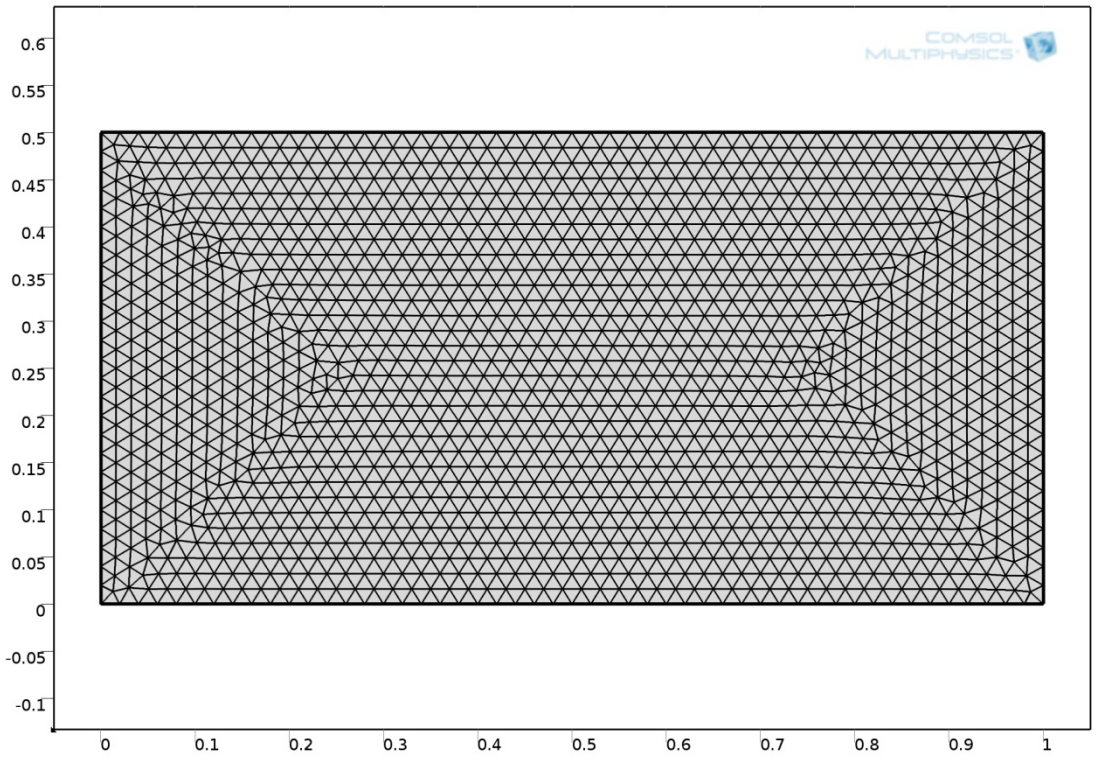

Figure 13.1. Free triangular mesh of 3150 elements.

13.2.6. Study

An eigenfrequency module is used for finding out the natural frequencies and their corresponding mode shape. The *Number of degrees of freedom solved for* was 38706.

13.3. Post processing COMSOL data

13.3.1. Exporting contour lines

At this stage, a standard post processing procedure is followed regarding plotting graphs. Through the *results* node, a *2D Plot Group* is added and then a *Contour* plot.

In general, contour line plots are a way of depicting levels, and, in this particular case, displacements. In order to achieve contours of equal displacement, a displacement *Level* or *Range* should be predefined; this setting is located at the *Contour* plot node (Fig (13.2)).

In Figure (13.3) a contour plot is shown, where a small level range around zero is set with an arbitrary quite small step - for better display; it is also the one used in the results section.

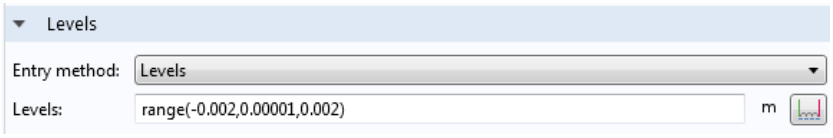

Figure 13.2. Levels subnode and Levels method.

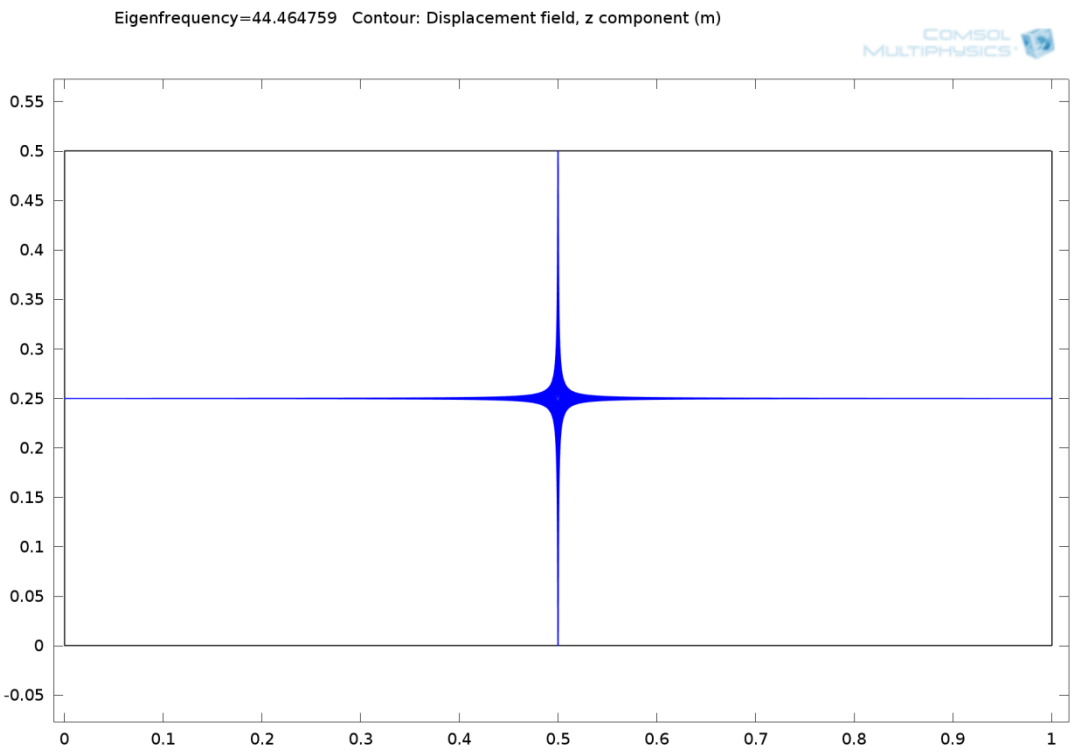

Figure 13.3. Contour Plot that consists of a specific range of Levels.

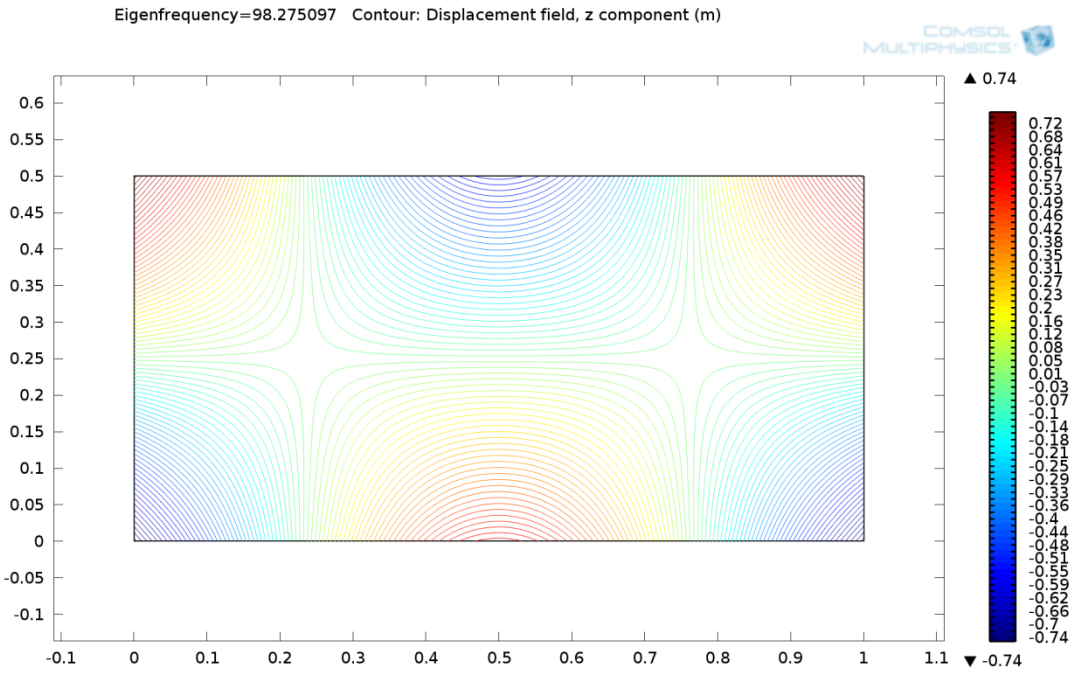

Figure 13.4. Contour Plot that consists of 80 contour Levels.

Figure (13.4) shows an additional way of using contour lines, the *number of levels* method.

13.4. Results

Figures (13.5) and (13.6) show the experimental and the calculated nodal patterns respectively, and figures (13.7) through (13.9) show single selected detailed mode shapes.

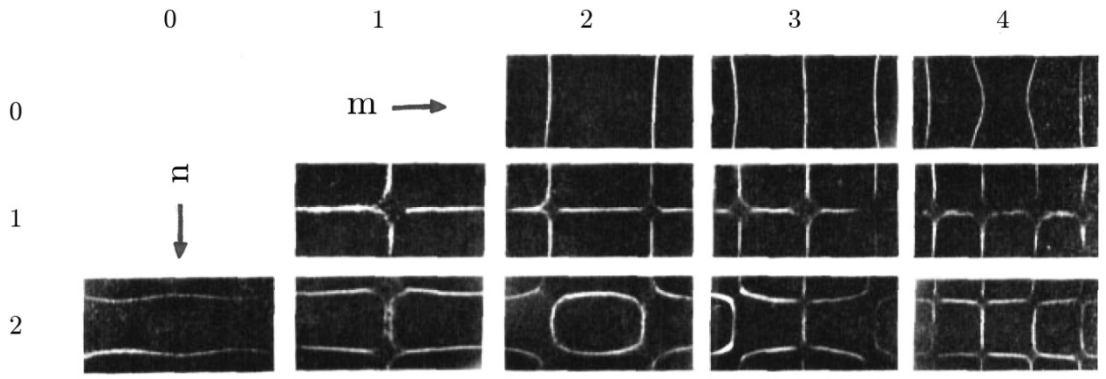

Figure 13.5. Experimentally observed nodal patterns for a completely free brass plate with a/b=2.

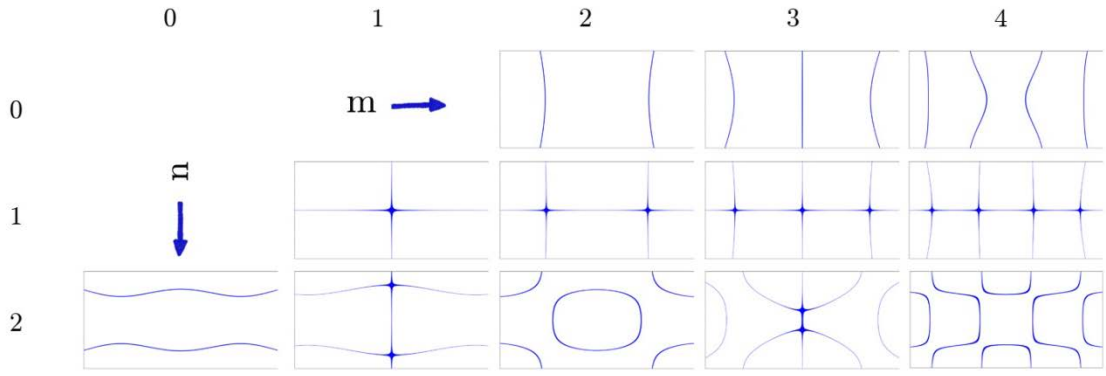

Figure 13.6. FEM calculated nodal patterns for a completely free brass plate with a/b=2.

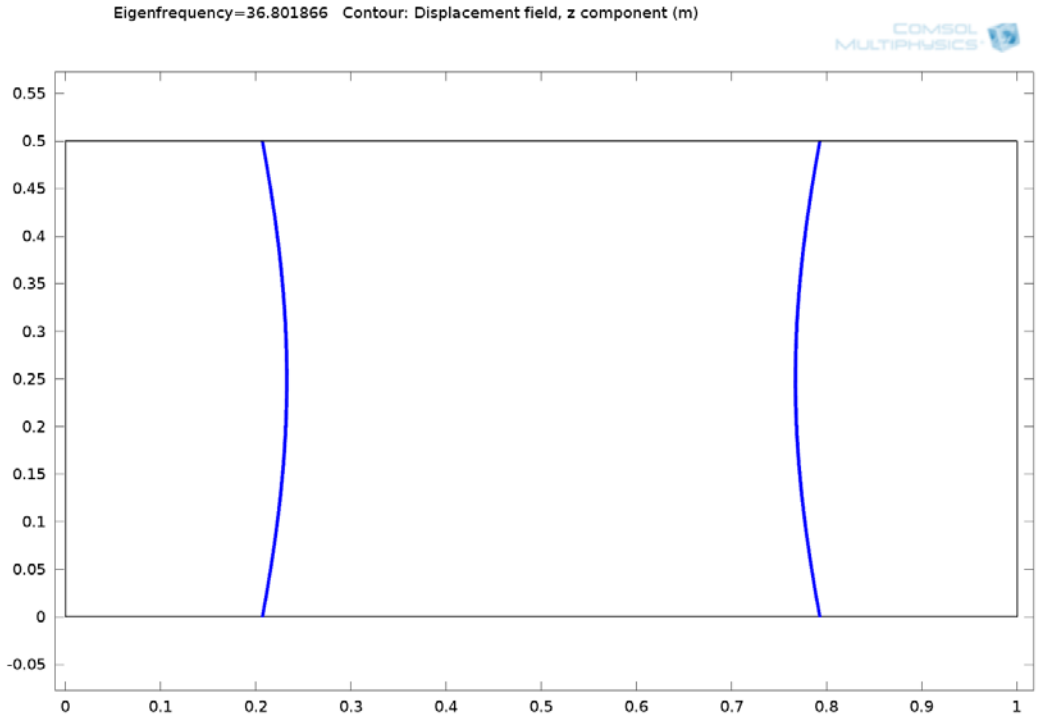

Figure 13.7. Mode shape of the 1st natural frequency of a completely free rectangular brass plate.

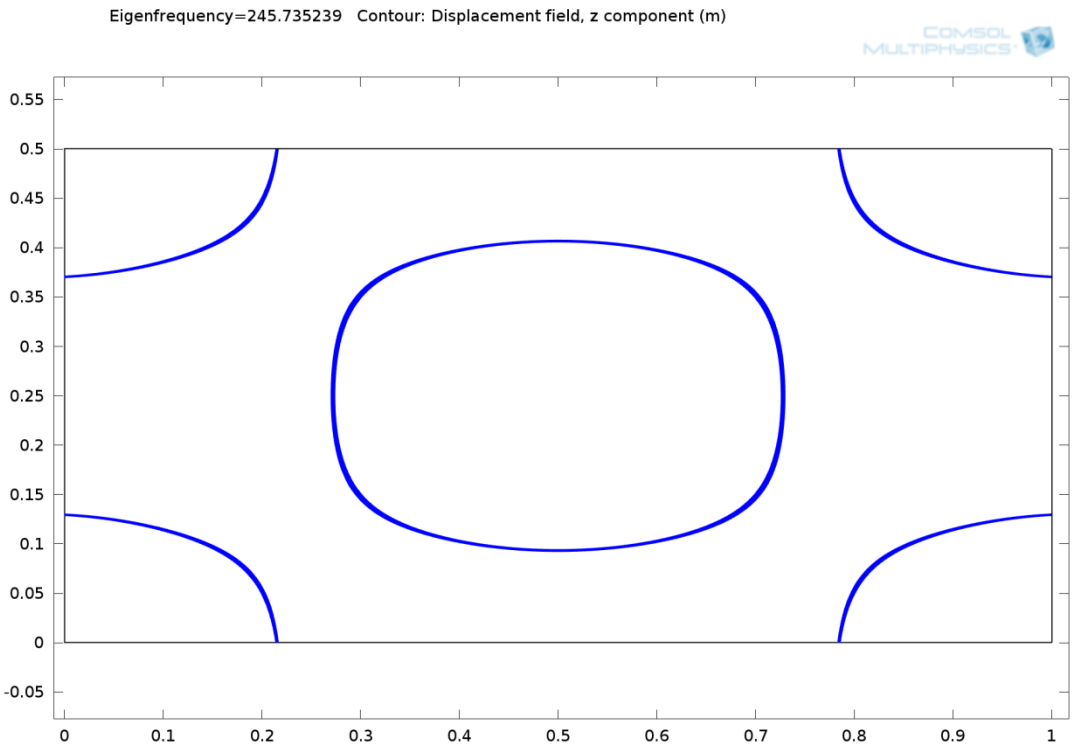

Figure 13.8. Mode shape of the 9^{th} natural frequency of a completely free rectangular brass plate.

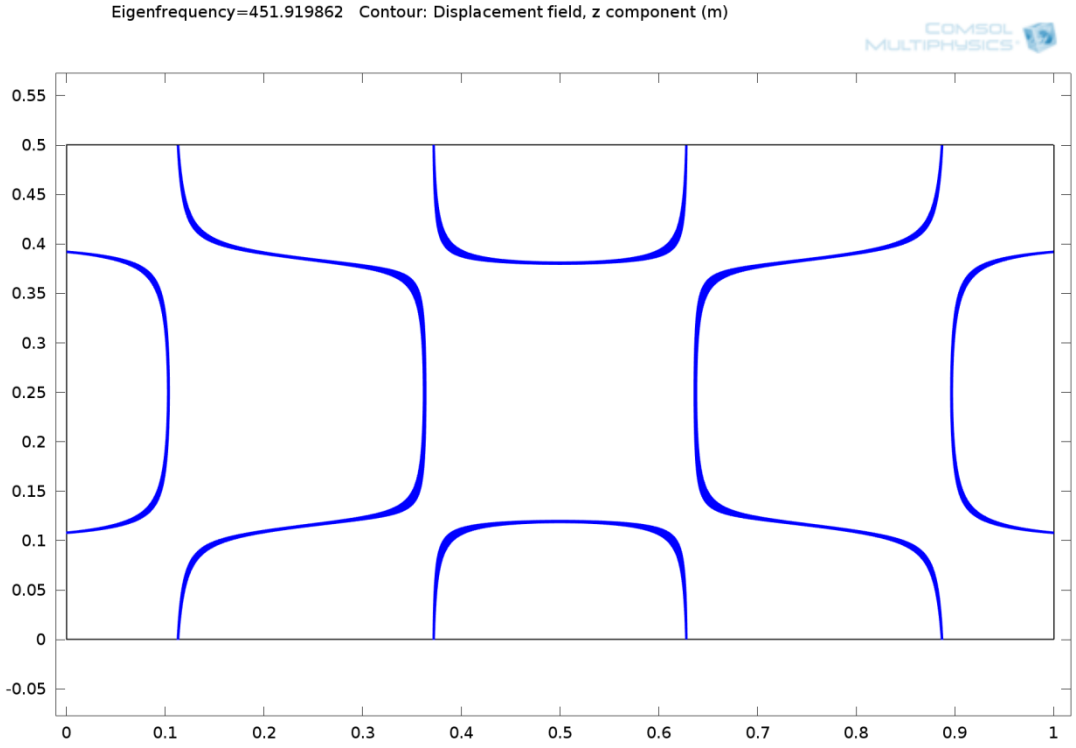

Figure 13.9. Mode shape of the 16^{th} natural frequency of a completely free rectangular brass plate.

14. Eigenfrequency Analysis of a Free Square Plate – Relative frequency comparison

14.1. Introduction

In this example, the first eigenfrequencies of a completely free square brass plate are calculated numerically via COMSOL, and their ratio of frequencies relative to the fundamental are compared with Waller's [1939] experimental results.

For the FEM evaluation, the *Plate 2D* interfaced is used.

14.2. Model Definition

14.2.1. Geometry

A *square* with sides 1 m is created from the *Geometry* node, although the dimensions are irrelevant to finding relative frequencies. The thickness of the plate is given d = 0.01 m in the *Plate* node.

14.2.2. Material

A *Copper* material is selected from the *material library,* with material properties:

i. Young's modulus, E=110 GPa ;
ii. Poisson's ratio was changed to ν=1/3 in order to match the experimental data, and
iii. Mass density, $\varrho_L = 8700\ \mathrm{kg/m^3}$.

14.2.3. Constraints

No constraints are applied because the plate is free.

14.2.4. Load

In an eigenfrequency analysis loads are not needed.

14.2.5. Mesh

A *Free Triangular* mesh is used (Fig. 14.1), with 0.02 m *Maximum element size*, which yields:

i. *Number of vertex elements*, 4;
ii. *Number of boundary elements*, 200;
iii. *Number of elements*, 6282.

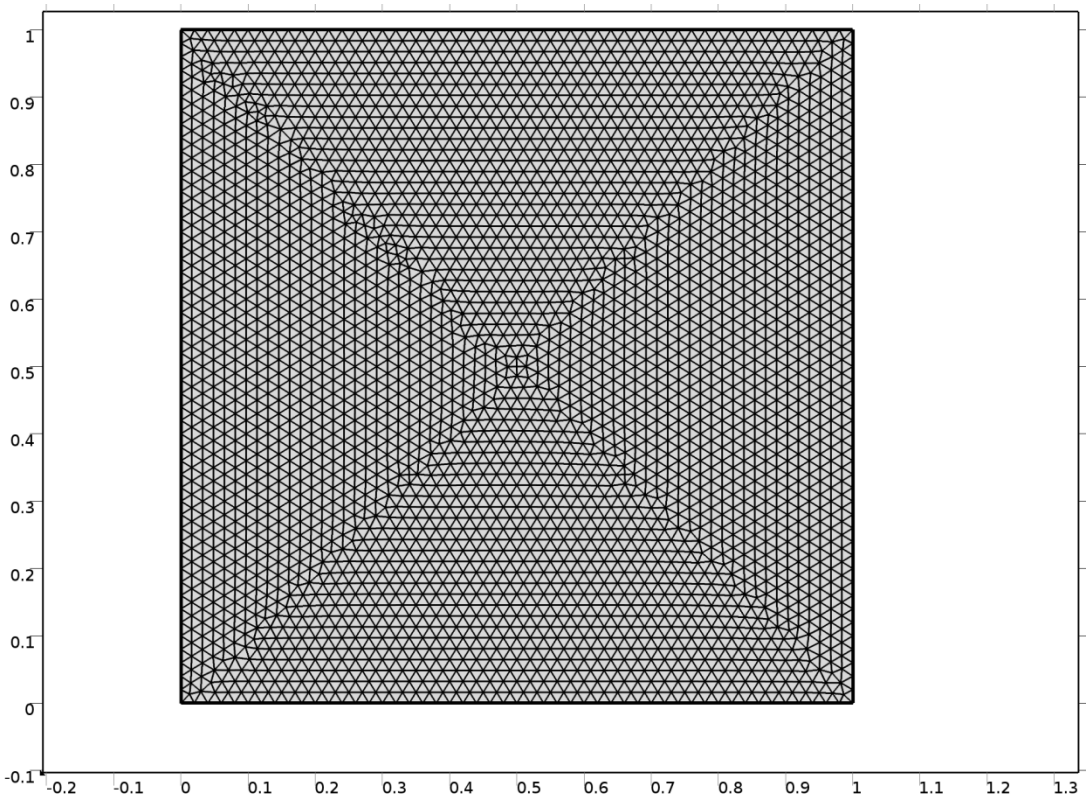

Figure 14.1. Free triangular mesh of 6282 elements.

14.2.6. Study

An eigenfrequency module is used for finding out the system's natural frequencies. The *Number of degrees of freedom solved for* was 76590.

14.3. Results

Waller [1939] obtained experimental frequencies for square brass plates ($\nu = 1/3$). The ratio of frequencies relative to the fundamental is given in Table 14.1 for various m/n ratios; the ones derived from COMSOL are shown in Table 14.2; the indicators m and n correspond to the number of nodal lines running parallel to the y and x axes, respectively.

Table 14.1. Experimentally determined relative frequencies for a completely free square brass plate.

m/n	**0**	**1**	**2**	**3**	**4**	**5**	**6**
0	-	-	1.52	5.10	9.14	15.80	23.00
1	-	1.00	2.71	5.30	10.30	15.80	23.90
2	1.94	2.71	4.81	8.52	12.40	19.00	26.40
3	5.10	6.00	8.52	11.80	16.60	22.60	30.00
4	9.90	10.30	13.20	16.60	21.50	28.70	35.50

Table 14.2. Numerically calculated relative frequencies for a completely free square brass plate.

m/n	**0**	**1**	**2**	**3**	**4**	**5**	**6**
0	-	-	1.46	4.64	8.85	15.00	22.14
1	-	1.00	2.60	5.17	9.92	15.34	23.11
2	1.86	2.60	4.76	7.89	12.10	18.26	25.25
3	4.64	5.85	7.89	11.44	16.14	21.83	29.43
4	9.31	9.92	12.69	16.14	21.01	27.20	34.40

15. Eigenfrequency Analysis of a Rectangular Plate for Multiple Boundary Conditions

15.1. Introduction

In this example, several models of the same rectangular plate with different boundary conditions are simulated in *2D Plate* interface, and each fundamental frequency is calculated. The results are plotted and compared with Janich's [1962] theoretical solutions.

15.2. Model Definition

15.2.1. Geometry

A *rectangular* with sides $a = 2\ m$ and $b = 1\ m$ is created with thickness $h = 0.001\ m$.

15.2.2. Material

The material chosen is *Aluminum,* with the following material characteristics:

i. Young's modulus, E=70 GPa;
ii. Poisson's ratio was changed to ν=0.25 in order to match the theoretical solutions, and
iii. Mass density, $\rho_L = 2700\ kg/m^3$.

15.2.3. Constraints

The constraints differ from model to model; the boundary conditions of each case are shown in Table (15.1).

15.2.4. Load

No loads are needed.

15.2.5. Mesh

A Free Triangular mesh is used (Fig. (15.1)), with 0.02 m *Maximum element size*, which yields:

i. *number of vertex elements*, 4;
ii. *number of boundary elements*, 300;
iii. *number of elements*, 12480.

15.2.6. Study

An eigenfrequency module is implemented to calculate the natural frequencies and their corresponding mode shape. A search for eigenfrequencies is employed to all studies for more accurate results.

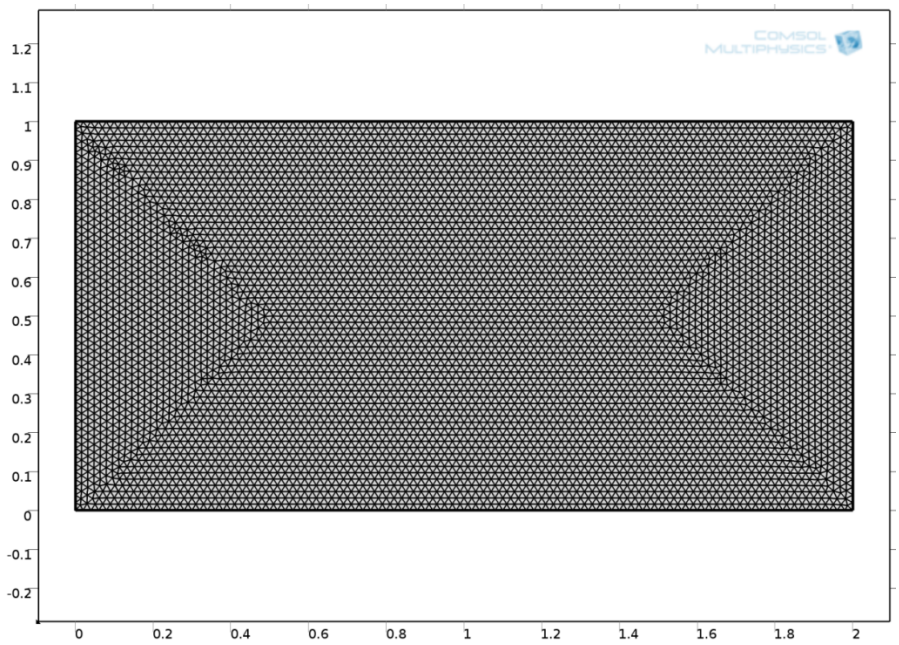

Figure 15.1. Free triangular mesh of 12480 elements.

15.3. Results

A comprehensive set of solutions for rectangular-shaped plates was given by Janich [1962], where fundamental frequencies were obtained for 18 combinations of boundary conditions. He employed the Rayleigh method, but used simple trigonometric functions which satisfied only the geometric boundary conditions. Leissa [1969] gives the natural frequencies for $\nu=0.25$ by

$$\omega^2 = \frac{\pi^4 D}{a^4 \varrho}\frac{K}{N} \tag{15.1}$$

Table (15.1) shows the N and K constants for different combinations, together with a comparison of the fundamental frequency values derived from the theoretical solution (Eq. (15.1)) and the numerical solution.

Figures (15.2) through (15.5) show the mode shapes of the 5 cases indicated in Table (15.1).

Table 15.1. - Frequency comparison for different boundary conditions of a rectangular plate.

BOUNDARY CONDITION	N	K	THEORETICAL	COMSOL
C-C-C-C	2.25	$12 + 8\left(\frac{a}{b}\right)^2 + 12\left(\frac{a}{b}\right)^4$	6.10542	5.93644
C-C-F-F	0.0514	$0.0071 + 0.024\left(\frac{a}{b}\right)^2 + 0.0071\left(\frac{a}{b}\right)^4$	1.22405	1.04510
C-F-F-F	0.2268	0.0313	0.22146	0.20921
SS-SS-SS-SS	0.25	$0.25 + 0.5\left(\frac{a}{b}\right)^2 + 0.25\left(\frac{a}{b}\right)^4$	2.98072	2.98041
SS-F-SS-F	0.5	0.5	0.59614	0.58147

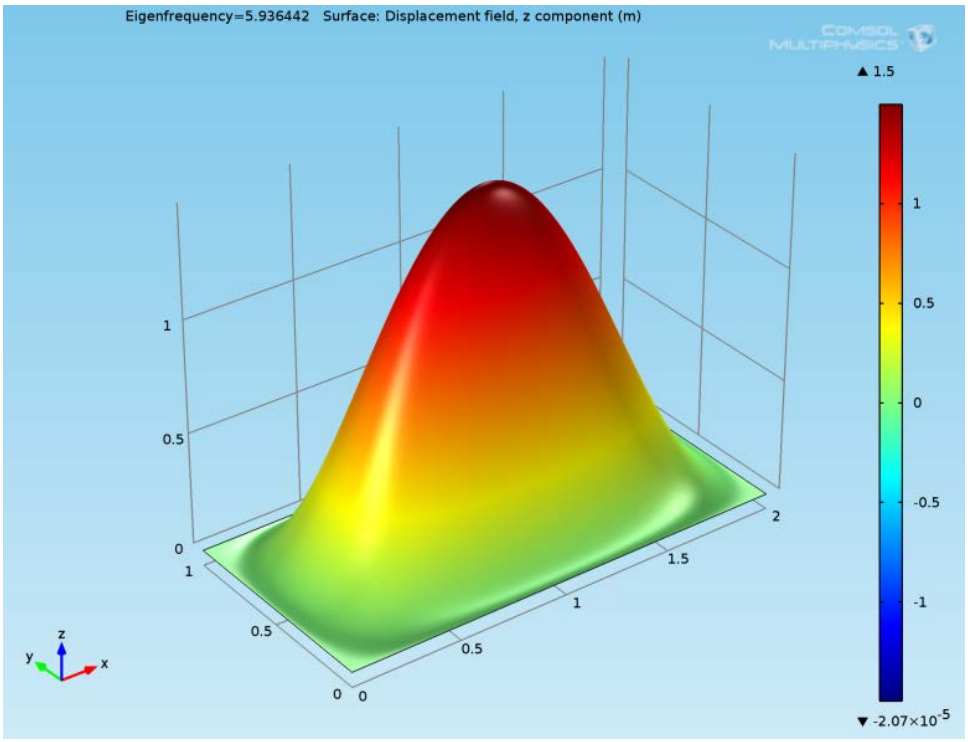

Figure 15.2. Eigenmode of a fully clamped rectangular plate.

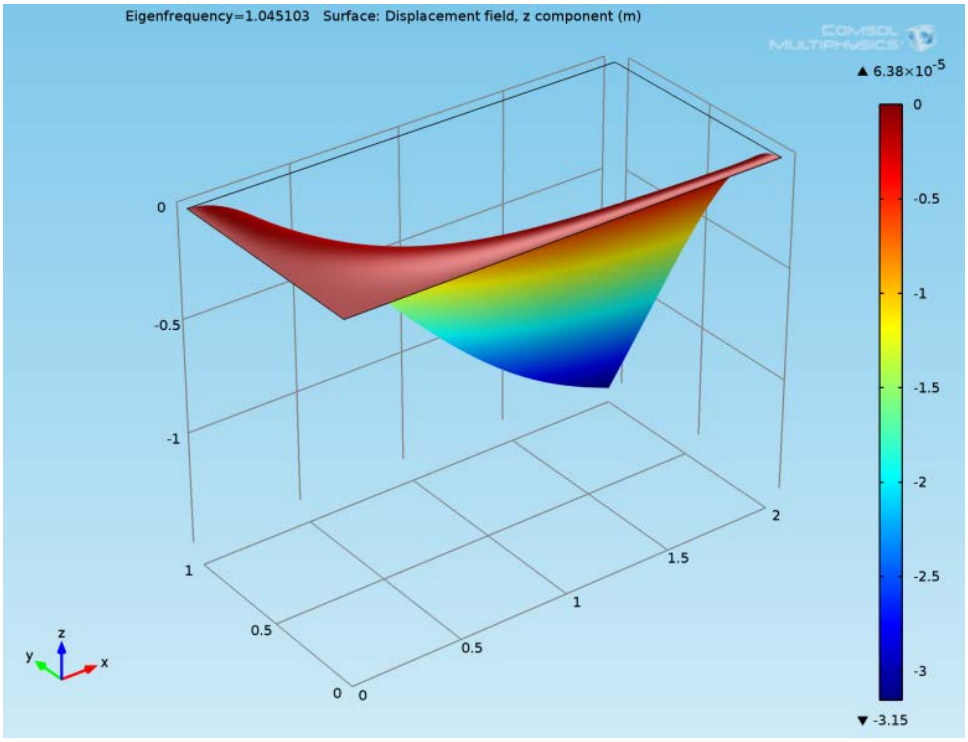

Figure 15.3. Eigenmode of a SS-SS-F-F rectangular plate.

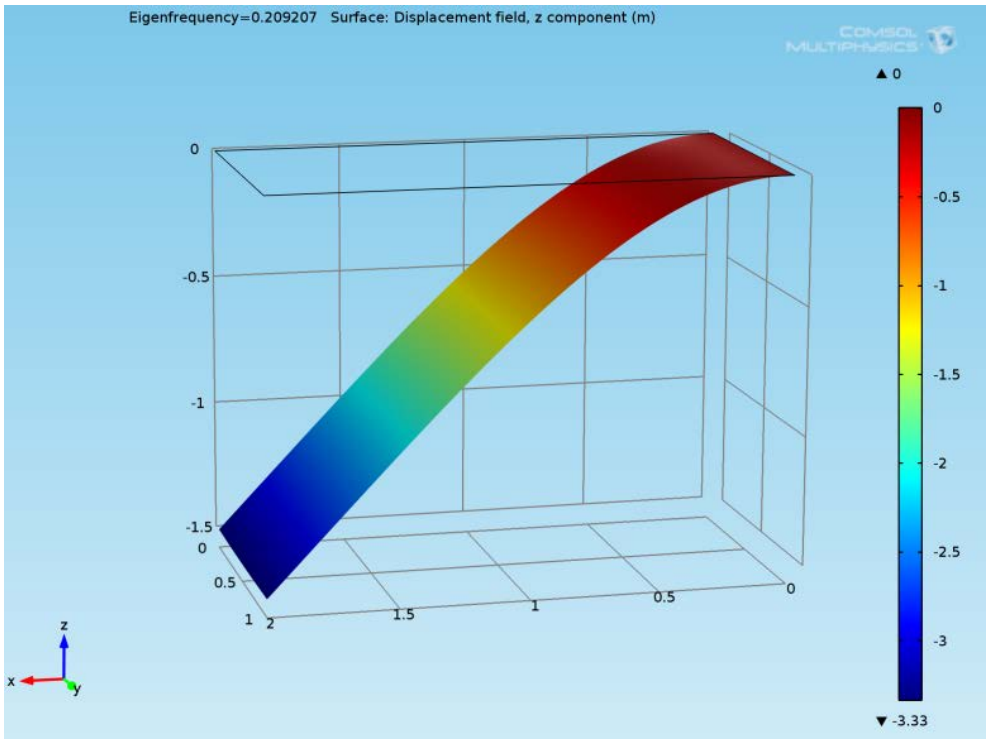

Figure 15.4. Eigenmode of a cantilever rectangular plate.

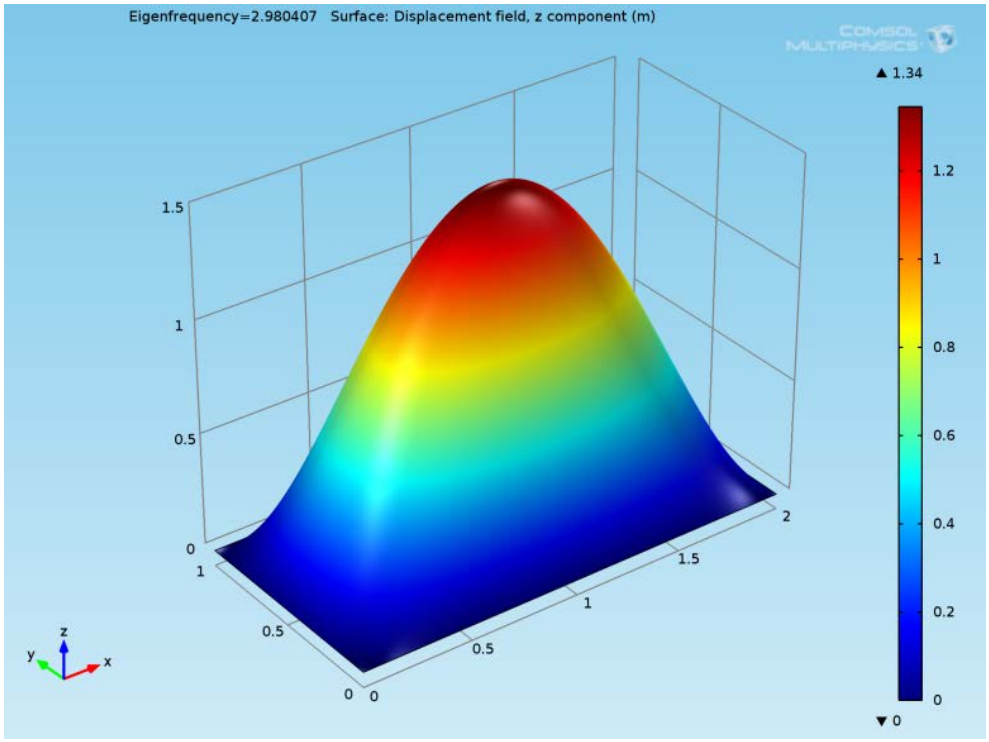

Figure 15.5. Eigenmode of a fully simple-supported rectangular plate.

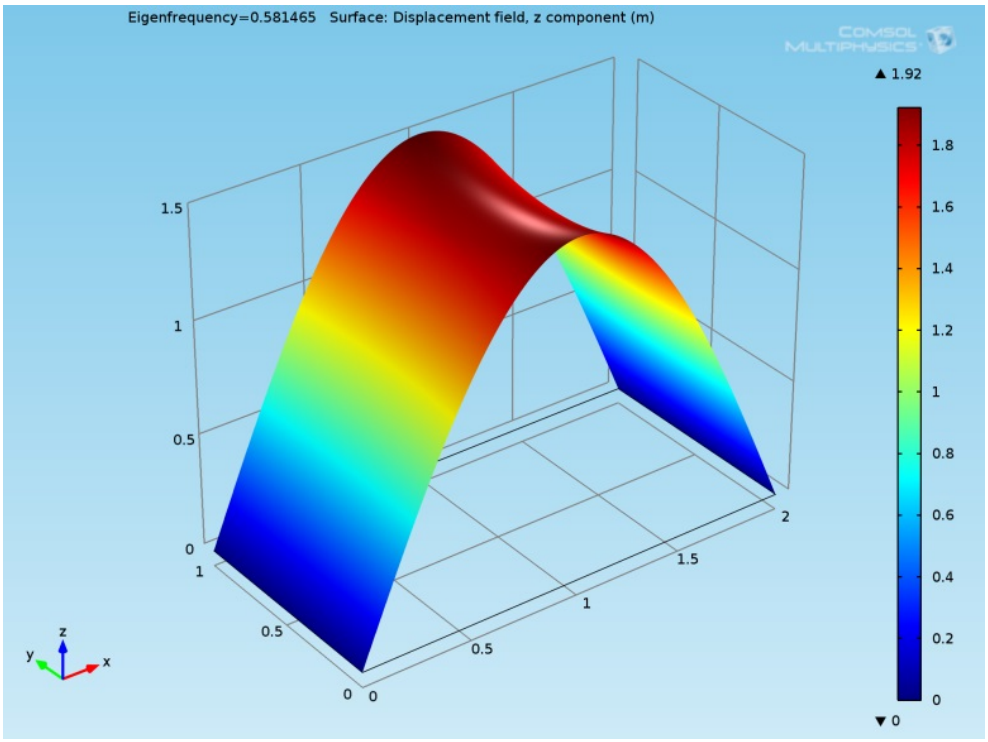

Figure 15.6. Eigenmode of a SS-F-SS-F rectangular plate.

16. Eigenfrequency Analysis of a Rectangular Cantilever Plate

16.1. Introduction

Martin [1956] devised a variational procedure similar to the Rayleigh-Ritz method and used it to compute the frequencies of a mild steel cantilever plate with dimensions $a = 0.13005\ m$, $b = 0.070104\ m$ and $h = 0.0013462\ m$.

In this example, a rectangular cantilever plate is modeled in *2D Plate* interface, and the natural frequencies are derived and compared with the theoretical ones, as well as with experimental data found by Grinsted [1952].

Furthermore, the corresponding mode shapes are plotted in both surface and contour graphs.

16.2. Model Definition

16.2.1. Geometry

A *rectangular* with sides $a = 0.13005\ m$, $b = 0.070104\ m$ and $h = 0.0013462\ m$ is created (Fig. (16.1)).

16.2.2. Material

A *Structural steel* material is selected from the *material library,* with material properties:

i. Young's modulus, $E=200\ GPa$;
ii. Poisson's ratio, $\nu=0.33$, and
iii. Mass density, $\varrho_L = 7850\ kg/m^3$.

16.2.3. Load

In an eigenfrequency analysis loads are not needed.

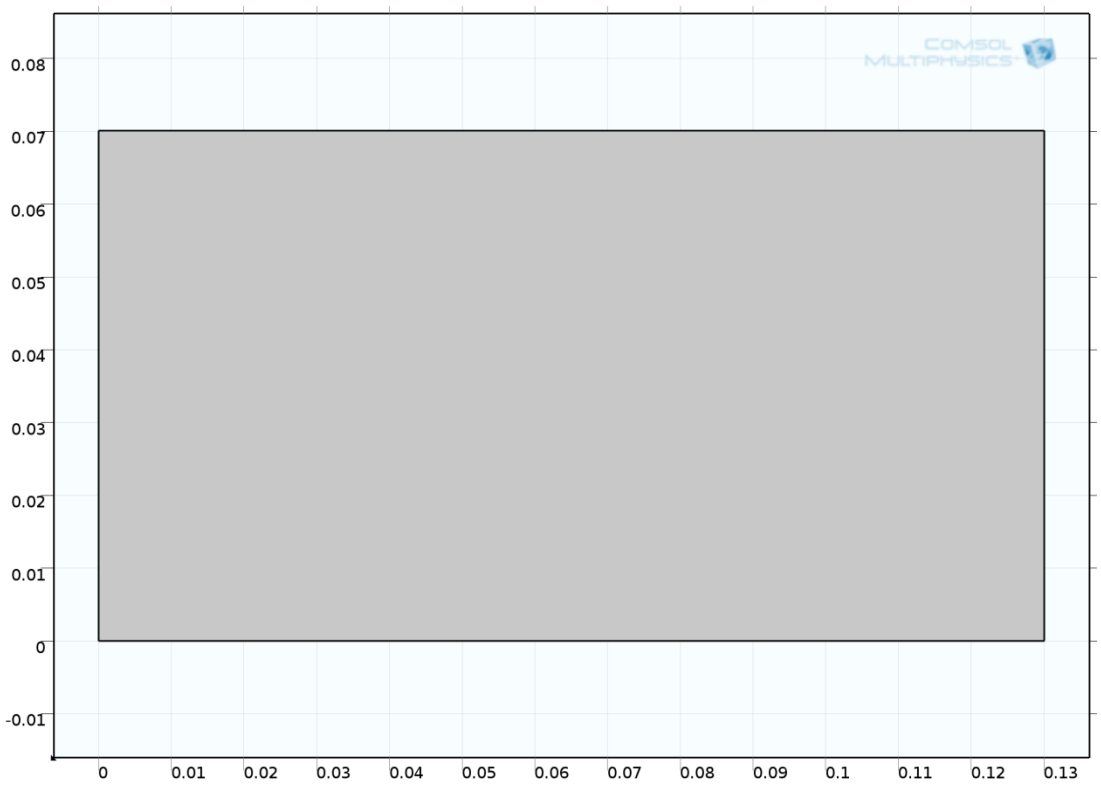

Figure 16.1. Two-dimensional model of a rectangular plate.

16.2.4. Constraints

A cantilever plate is the case of one side clamped and all the others free of constraints; a *Fixed Constraint* node is added and boundary *1* is selected from the *boundary selection* list.

16.2.5. Mesh

A Free Triangular mesh of 0.0026 m *Maximum element size* is used, which yields:

i. *Number of vertex elements*, 4;
ii. *Number of boundary elements*, 154;
iii. *Number of elements*, 3418.

16.2.6. Study

An *eigenfrequency* module is used for calculating the system's natural frequencies. The *desired number of eigenfrequencies* is set to 40; a *search for eigenfrequencies around* 67 Hz was performed for better accuracy and the *Number of degrees of freedom solved for* is 164190.

16.3. Results

Table (16.1) shows a frequency comparison between experimental, theoretical and analytical data. The percentage difference is also given. The indicators m and n correspond to the number of nodal lines running parallel to the $y-$ and $x-$axes, respectively.

Table 16.1. Frequency comparison for values m/n of a rectangular cantilever plate.

n	TYPE	m					
		0	**1**	**2**	**3**	**4**	**5**
0	Experimental	64.0	405.0	1120.0	2233.0	3736.0	5573.0
	Theoretical	69.5	436.0	1220.0	2390.0	3940.0	5900.0
	Theoretical % difference	8.59%	7.65%	8.93%	7.03%	5.46%	5.87%
	COMSOL	67.0	416.2	1164.2	2339.7	3836.1	5708.2
	Numerical % difference	4.62%	2.77%	3.95%	4.78%	2.68%	2.43%
1	Experimental	260.0	-------	1676.0	2804.0	4335.0	-------
	Theoretical	276.0	905.0	1743.0	2970.0	4530.0	-------
	Theoretical % difference	6.15%	-------	4.00%	5.92%	4.50%	-------
	COMSOL	265.0	871.7	1703.8	2853.7	4393.0	6275.2
	Numerical % difference	1.91%	-------	1.66%	1.77%	1.34%	-------
2	Experimental	1606.0	-------	3160.0	4428.0	6009.0	7859.0
	Theoretical	1610.0	2260.0	3280.0	4660.0	6350.0	8350.0
	Theoretical % difference	0.25%	-------	3.80%	5.24%	5.67%	6.25%
	COMSOL	1576.1	2157.1	3164.6	4461.3	6065.6	7970.5
	Numerical % difference	1.86%	-------	0.15%	0.75%	0.94%	1.42%
3	Experimental	4235.0	4773.0	5739.0	7069.0	-------	-------
	Theoretical	4250.0	4810.0	5950.0	7450.0	9200.0	11280.0
	Theoretical % difference	0.35%	0.78%	3.68%	5.39%	-------	-------
	COMSOL	4128.6	4733.6	5720.3	7089.2	8796.5	10794.2
	Numerical % difference	2.51%	0.82%	0.33%	0.29%	-------	-------

In order to provide a better understanding of the contour lines of a vibrating plate, Figures (16.2) through (16.6) show the first five mode shapes plotted in three-dimensional surface and two-dimensional contour graphs, simultaneously. The fundamental vibrating mode is shown in Figure (16.2); it is clear that it consists of zero nodal lines, since it represents the $0\,|\,0$ mode shape.

Note that only the mode shapes are of real importance, because the displacement values in any eigenfrequency study have no use and cannot be taken into account. The magnitude of displacements is relative and normalized by COMSOL. For use of amplitude values, a frequency domain study is required.

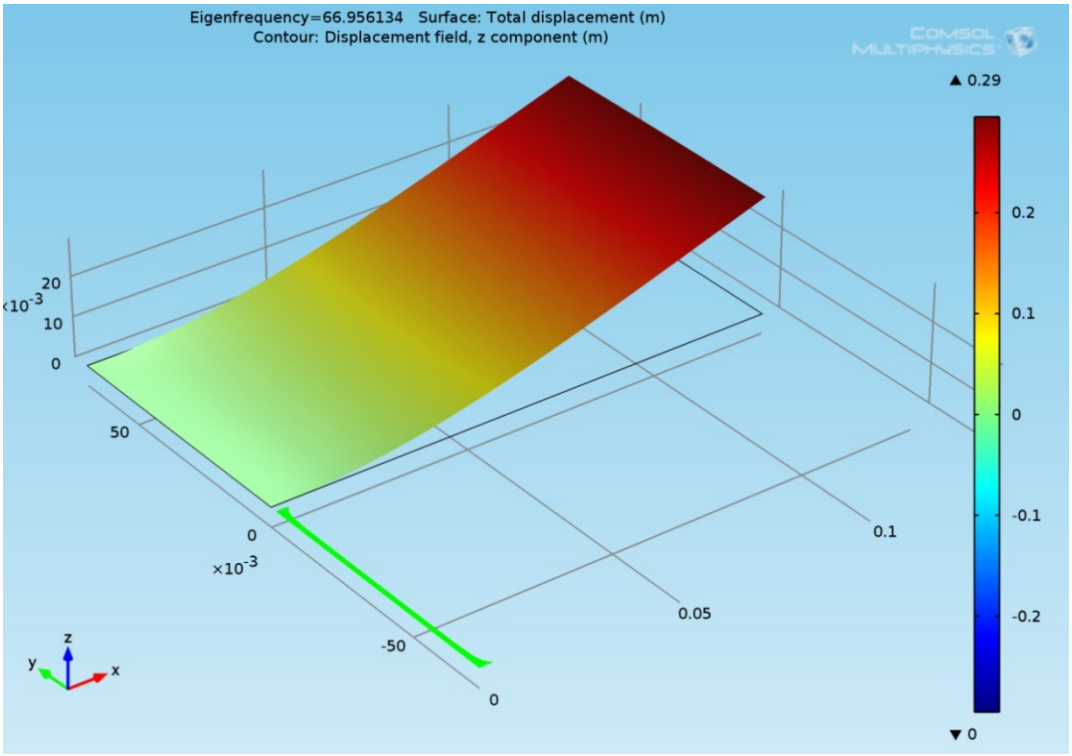

Figure 16.2. First vibrating mode of a cantilever plate.

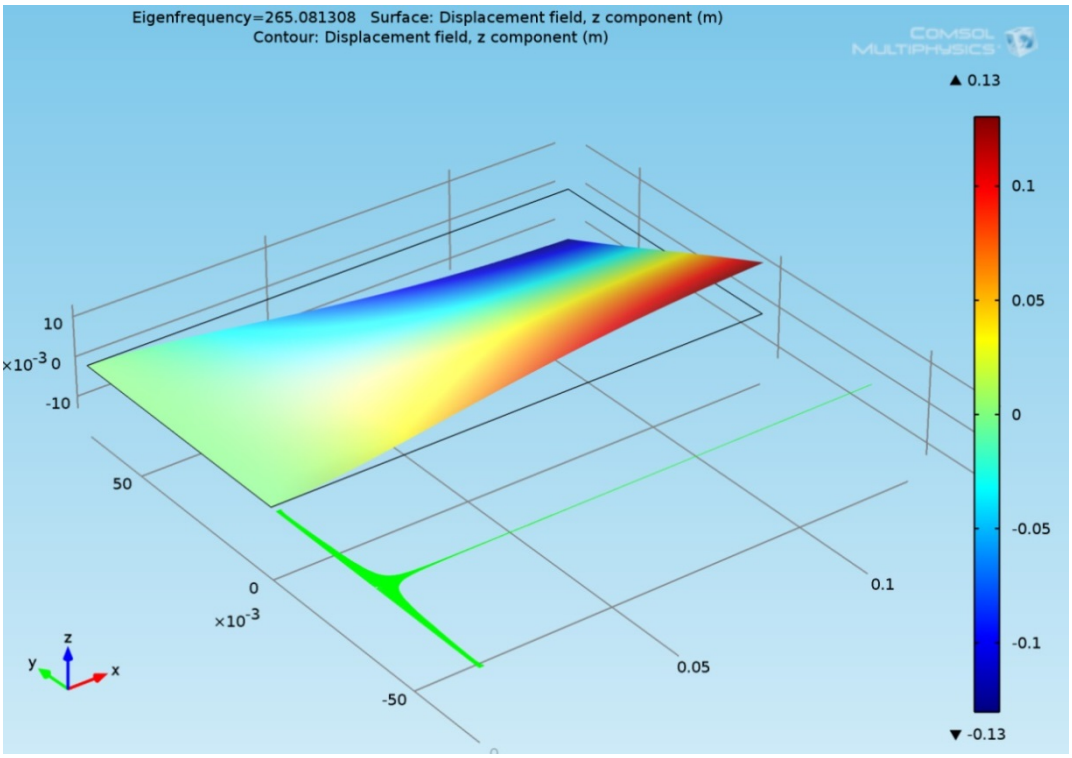

Figure 16.3. Mode 0/1 of a cantilever plate.

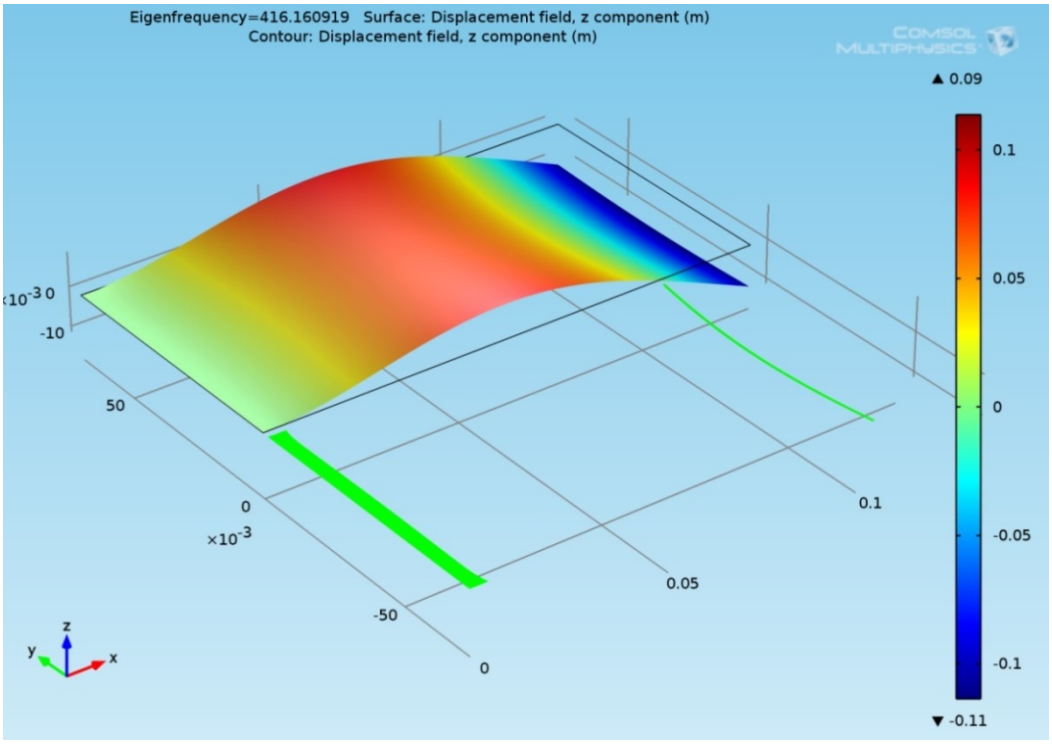

Figure 16.4. Mode 1/0 of a cantilever plate.

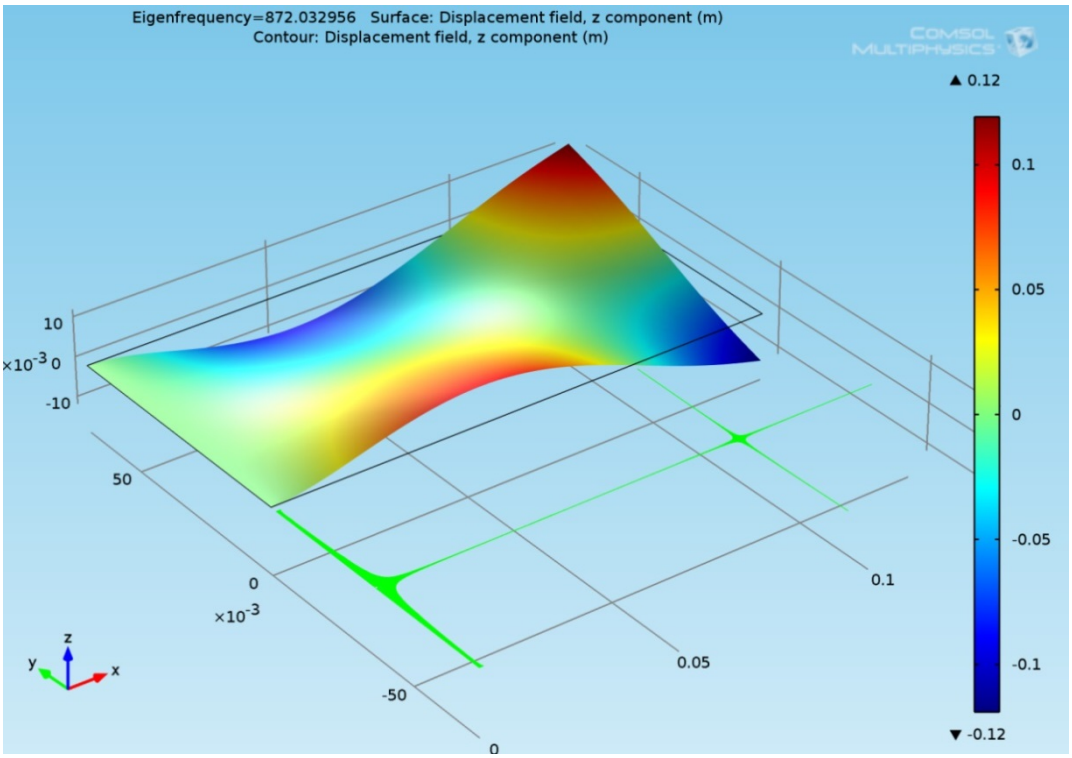

Figure 16.5. Mode 1/1 of a cantilever plate.

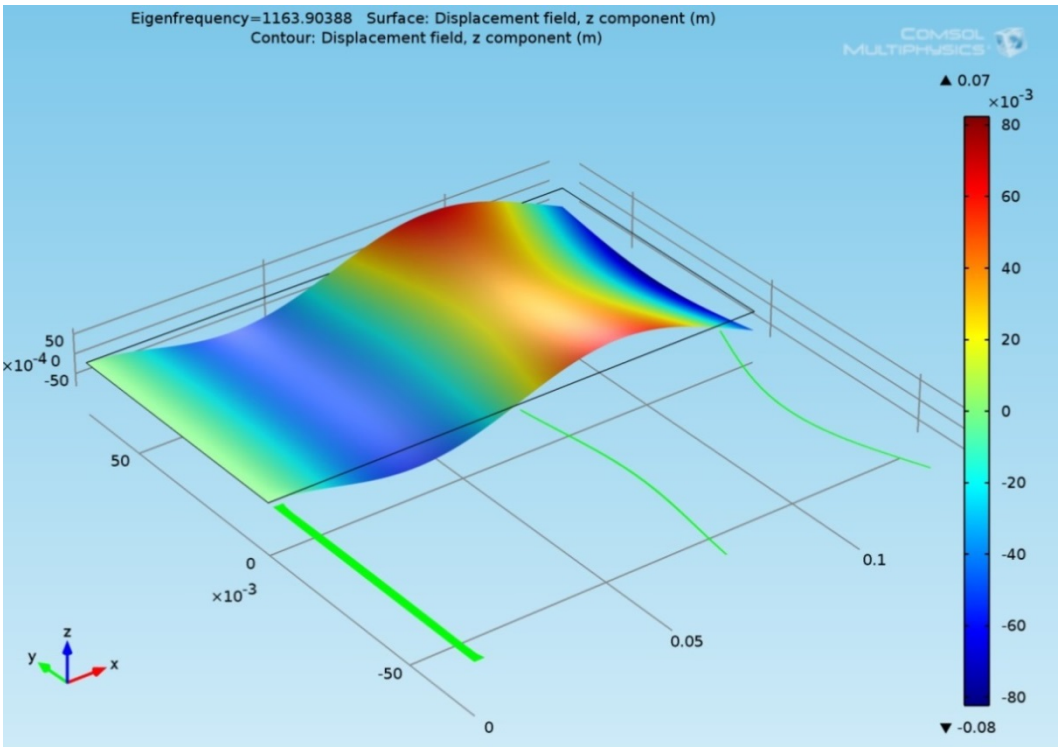

Figure 16.6. Mode 2/0 of a cantilever plate.

17. Concluding Remarks

17.1. With respect to the theoretical background

On an academic level, the first part of this thesis (Ch.1-7) has introduced the theory of vibrations and solids, before moving on to explore more specific vibrating systems, and has explained how to apply the finite element method in the study of different types of vibrating systems.

17.2. With respect to Comsol Multiphysics®

In the 8 modeled examples contained in this thesis, both statics and dynamics problems have been solved, using 5 different interfaces (2D plate, 2D & 3D Solid Mechanics, 2D Beam and 2D Truss interface) of the COMSOL Multiphysics® software.

A demonstration was given of how to model a problem from the start, how to compute and derive the eigenfrequencies and eigenmodes of the systems, how to create contour plots, and how to proceed with the post processing of the results within the software.

In this context, this thesis illustrated that the Finite Element Method is a useful tool for deriving numerical solutions. It has demonstrated how some examples of known problems can be simulated by use of the COMSOL Multiphysics® software. It has also shown that this method may be used in various applications, and mainly for educational purposes, in a highly efficient way.

17.3. Study limitations

The finite element method is not part of the curriculum of the Music Technology and Acoustics Department. In that respect, the time needed to study and research this particular field was a major limitation in itself. In addition, due to the lack of experimental equipment, the testing procedure had to be limited to specific specimens and boundary conditions. However, this obstacle did not impede the overall process, as the software was able to adapt to these requirements.

17.4. Areas for future research

The work presented in this thesis could be further developed in a number of ways. The next logical step would be to extend the modeled examples to areas that have not been addressed herein, such as frequency responses, time domain studies and prestressed analyses. Research could also be extended to include springs, masses, or even damping in the systems. Another course of action would be to model solids with different boundary conditions and complex geometries, or to model other types of systems, such as membranes. An additional suggestion for extending this thesis is to develop interactive models, such as structural mechanics and acoustics; this approach could find applications in a number of examples, including acoustic transmission loss, wave propagation, loudspeaker simulation, waves in tubes, eigenmodes of a room, etc.

Appendix A – Some MATLAB Scripts

```
%This program plots the first four modes for the three different boundary
%conditions of a string (fixed-fixed, free-free, fixed-free). The graphs
%are made in a way to depict fully the vibration of the string.

clc;
clear all;
close all;

L=1; % length of string
x=[0:0.001:L]; %resolution

for n=1:4
    y1=sin((n*pi*x)/L); %fixed-fixed mode shape
    figure (1)
    subplot(4,1,n)
    plot(x,y1, 'b', 'linewidth',2);hold on
        xlabel('Length of string (m)');ylabel('Amplitude (m)'); grid;
    if n==1
        title(['First four mode shapes of a fixed-fixed string']);
    end
%     plot(x,-y1,'b','linewidth',2);

    for m=-0.9:0.3:0.9
    plot(x,m*y1,'b:');
    end
    y2=sin(((n*pi-(1/2)*pi)*x)/L); %fixed-free mode shape
    figure (2)
    subplot(4,1,n)
    plot(x,y2, 'b', 'linewidth',2);hold on

%     plot(x,-y2, 'b', 'linewidth',2);
    xlabel('Length of string (m)');ylabel('Amplitude (m)'); grid;
        if n==1
        title(['First four mode shapes of a fixed-free string']);
    end
        for m=-0.9:0.3:0.9
    plot(x,m*y2,'b:');
    end
    y3=cos((n*pi*x)/L); %free-free mode shape
    figure (3)
    subplot(4,1,n)
    plot(x,y3, 'b', 'linewidth',2);hold on
```

```
%     plot(x,-y3, 'b', 'linewidth',2);
    xlabel('Length of string (m)');ylabel('Amplitude (m)'); grid;
        if n==1
        title(['First four mode shapes of a free-free string']);
    end
        for m=-0.9:0.3:0.9
    plot(x,m*y3,'b:');
    end
end
```

```
%This script file loads a proper .dat file extracted from DaqView
%software, that contains 4 columns, separated by tabs. The first column
%is the acquisition time, the second is the input signal's amplitude, the third
%is the output signal's time, and the fourth the output signal's amplitude.
%I only used the data of the output signal, although the code was initially
%made to analyze the impact hammer's data too.

%The DC offset component is being removed from both input and output
%signals, and then DFT is performed. The signals are plotted in both time
%and frequency domain.

clc;
clear all;
close all;

%Reading the experimental data
[fname,path] = uigetfile('*.*','Please select the *.dat file to be loaded:');
fprintf('%s %s\n','This is file: ',fname');
[x1,y1,x2,y2] = textread([path,fname],'%f %f %f %f','headerlines', 1);

%Sampling frequency of the measurment
fs=50000;

%defining the frequency domain
N = length(y1);
f=fs*(0:N-1)/N;

%defining the time domain
T=N/fs;
t=0:1/fs:T-1/fs;

%removing the DC offset of the input and output signals
y1 = y1 - mean(y1);
y2 = y2 - mean(y2);

%Plotting the input signal in the time domain
set(figure(1), 'Position', [10   540   620  400])%figure window size
plot(t, y1); axis([0 T -1.1*max(-y1) 1.1*max(y1)]);grid on
xlabel('\itt\rm (seconds)'); ylabel('\itx\rm(\itt\rm)')

%Plotting the output signal in the time domain
set(figure(2), 'Position', [645   540   625  400])%figure window size
```

```
plot(t, y2); axis([0 T 1.1*-max(y2) 1.1*max(y2)]);grid on
xlabel('\itt\rm (seconds)'); ylabel('\itx\rm(\itt\rm)')

Y1=fft(y1); %Performing the DFT of input signal
Y2=fft(y2); %Performing the DFT of output signal


%Plotting the input signal in the frequency domain
set(figure(3), 'Position', [10   50   620  400])%figure window size
plot(f,20*log10(abs(Y1)));grid on;
axis([5 400 -max(20*log10(abs(Y1))) max(20*log10(abs(Y1)))])
xlabel('Frequency (Hz)'); ylabel('Amplitude (dB)')

%Plotting the output signal in the frequency domain
set(figure(4), 'Position', [645   50   625  400])%figure window size
plot(f,20*log10(abs(Y2)));grid on;
% axis([5 400  -max(-real(Y2))  max(real(Y2))])
%axis([5 400  -min(20*log10(abs(Y2))) max(20*log10(abs(Y2)))])
axis([5 400 -max(20*log10(abs(Y2))) max(20*log10(abs(Y2)))])
xlabel('Frequency (Hz)'); ylabel('Amplitude (dB)')
```

```
% This is a program that loads all the proper *.dat files from a specific folder
% exported from COMSOL Beam element, which contains the x, y node
% coordinates (y always zero) and the corresponding displacement values
% (deformation y - in the 5th column). It also contains information that are
% not in need, such as colour (3rd column), deformation x (4th) and radius (6th).

% The program  finds the zero level nodes and plots the shape of the
% imported (bar) mode. Then it finds the nodal positions on the x-axis and
% plots them in red on the mode graph. It prints out the accurate estimation
% of the position of the nodes (for the corresponding imported data files).

clear all
clc
close all
format longg

disp(['Please make sure to import small number of files']);

cd('BeamElement2D'); %reads all the files
files = dir('*.dat');

for i=1:length(files)
[x,y] = textread([files(i).name],'%f %*d %*f %*f %f %*d','headerlines', 8); %stores the
data into variables
N=length(x);
if i==1
    disp(['The total number of nodes in this mesh is:      ',num2str(N)]);
    disp([' ']);
end
files(i).name=fix_under(files(i).name); %fixes the problematic titles on the Matlab plots

[x,j]=sort(x); % Sorting
y=y(j);

subplot(length(files),1,i) %plots the modeshapes
plot(x,y);title(['Mode shape from file: ',files(i).name]);hold on
xlabel('x (m)');ylabel('y (m)'); grid;

zc = 0;
xn=[];  % nodal values
for k=2:length(y),
   if y(k)/2*y(k-1) < 0,
```

```
      zc = zc+1;
      a=(y(k)-y(k-1))/(x(k)-x(k-1));
      xn=[xn,(a*x(k-1)-y(k-1))/a];
   end
end

disp(['The number of nodal points for the mode #', num2str(i), ' is:      ', num2str(zc)]);
disp(['The nodes are at:  ',num2str(xn)]);
disp([' ']);
disp([' ']);
czz=zeros(length(xn));

plot(xn,czz,'.r','MarkerSize',17); %plots the nodal points on the same graph with the
modeshapes
hold off
end
```

References

ACCELEROMETER 352B10: *Installation and operating manual*. PCB PIEZOTRONICS[INC.]

BENADE, ARTHUR H.: *Fundamental of Musical Acoustics*. Dover Publications, second revised edition, New York, 1990.

BHATTI, ASGHAR M.: *Advanced Topics in Finite Element Analysis of Structures*. John Wiley & Sons, New York & Canada, 2006.

CARROLL W. F.: *A Primer for Finite Elements in Elastic Structures*. John Wiley & Sons, 1999.

COMSOL Multiphysics®: *Introduction to Structural Mechanics Module*. Version 4.4, November 2013.

COMSOL Multiphysics®: *Introduction to Structural Mechanics Module*. Version 4.3a, October 2012.

COMSOL Multiphysics®: *Introduction to COMSOL Multiphysics®*. Version 4.3, January 2013.

COMSOL Multiphysics®: *Introduction to COMSOL Multiphysics®*. Version 4.4, November 2013.

COMSOL Multiphysics®: *Model Library Manual*. Version 4.4, November 2013.

COMSOL Multiphysics®: *Physics Builder Manual*. Version 4.4, November 2013.

COMSOL Multiphysics®: *Reference Guide*. Version 4.3b, November 2012.

COMSOL Multiphysics®: *Reference Manual*. Version 4.4, November 2013.

COMSOL Multiphysics®: *Release Notes*. Version 4.4, November 2013.

COMSOL Multiphysics®: *Structural Mechanics Module Model Library Manual*. Version 4.4, November 2013.

COMSOL Multiphysics®: *Structural Mechanics Module User's Guide*. Version 4.3a, October 2012.

COMSOL Multiphysics®: *Structural Mechanics Module User's Guide*. Version 4.4, November 2013.

COMSOL Multiphysics®: *Structural Mechanics Module Verification Models*. Version 4.4, November 2013.

COMSOL Multiphysics®: *Structural Mechanics Module Verification Models*. Version 4.3a, October 2013.

COMSOL Multiphysics® tutorial examples: *Baffled Membrane.* Solved with Version 4.3.

COMSOL Multiphysics® tutorial examples: *Vibrating string.* Solved with Version 4.4.

COMSOL Multiphysics®: *User's Guide*. Version 4.3b, November 2012.

CHAKRAVERTY, S.: *Vibration of Plates*. CRC Press, 2009.

DaqBoard/3000 Series: *User's manual*. IOtech$^{INC.}$ 2005.

DaqView & ViewXL: *User's guide*. P/N 457-0909 Rev. 8.3.

FISH, JACOB & BELYTSCKO, TED: *A First Course in Finite Elements*. John Wiley & Sons, Fourth Edition, 2007.

FLETCHER, NEVILLE H. & ROSSING, THOMAS D.: *The Physics of Musical Instruments*. Springer, Second Edition, New York, 1998.

FLETCHER, NEVILLE H. & ROSSING, THOMAS D.: *Principles of Vibration and Sound*. Springer, Second Edition, New York, 2010.

GENTA, G.: *Vibration Dynamics and Control*. Springer, 2009

GINSBERG, JERRY H.: *Mechanical and Structural Vibrations*. John Wiley & Sons, 2001.

GRINSTED, B.: *Nodal Pattern Analysis*. Proc. Inst. Mech. Eng., ser. A, vol. 166, 1952, pp. 309-326.

HARTMANN, F. & KATZ, C.: *Structural Analysis with Finite Elements*. Springer, Second Edition, Berlin, 2007.

HAYEK, S.I.: *Advanced mathematical methods in science and engineering*. CRC Press, Second Edition, 2011.

INMAN, DANIEL J.: *Engineering Vibration*. Pearson, Third Edition, New Jersey, 2008.

JANICH, R.: *Die näherungsweise Berechnung der Eigenfrequenzen von rechteckigen Platten bei verschiedenen Randbedingungen*. Die Bautechnik, vol. 3, Mar. 1962, pp. 93-99.

KINSLER, L. E., FREY, A.R., COPPENS, A.B. & SANDERS, J.V.: *Fundamentals of Acoustics*. John Wiley & Sons, Fourth Edition, 2008.

KRENK, S. & HØGSBERG, J.: *Statics and Mechanics of Structures*. Springer, 2013.

KRYSL, PETR.: *Thermal and Stress Analysis with the Finite Element Method.* Pressure Cooker Press, San Diego, 2010.

LEISSA, ARTHUR D.: *Vibration of Plates*. Ohio State University Columbus, Washington, 1969.

LEISSA, ARTHUR D. & QATU, MOHAMAD S.: *Vibrations of Continuous Systems*. McGraw-Hill, 2011.

LIEW, K.M., WANG, C.M., XIANG, Y. & KITIPORNCHAI, S.: *Vibration of Midlin Plates*. Elsevier, UK, 1998.

MARTIN, A. I.: *On the Vibration of a Cantilever Plate*. Quart. J. Mech. Appl. Math, vol. 9, pt.1, 1956, pp. 94-102.

McCONNELL, KENNETH G. & VAROTO, PAULO S.: *Vibration Testing: Theory and Practice*. John Wiley & Sons, Second Edition, New Jersey & Canada, 2008.

METROVITCH, L.: *Fundamentals of Vibrations*. McGraw-Hill, New York, 2001.

MORIN, D.: *Introduction to Classical Mechanics*. Cambridge University Press, 2008.

NORTON, M. & KARCZUB D.: *Fundamentals of Noise and Vibration Analysis for Engineers*. Cambridge University Press, Second Edition, 2003.

PETERSSON, CREMER H.: *Structure-Borne Sound*. Springer, Third Edition, 2005.

PETYT, M.: *Introduction to Finite Element Vibration Analysis*. Cambridge University Press, Second Edition, USA, 2010.

RAO, SINGIRESU: *The Finite Element Method in Engineering*. Elsevier Science & Technology Books, UK, fourth edition, 2004.

REDDY, J. N.: *An Introduction to the Finite Element Method*. McGraw-Hill, third edition, 2006.

ROBERTS, A.: *Statics and Dynamics*. Cambridge University Press, UK, 2003.

ROSSING, THOMAS D.: *Handbook of Acoustics*. Springer, 2007.

PREUMONT, A.: *Twelve Lectures on Structural Dynamics*. Springer, Brussels, 2013.

SILVA, CLARENCE W.: *Computer Techniques in Vibration*. CRC Press, 2007.

SHIN, K. & HAMMOND, J.: *Fundamentals of Signal Processing for sound and vibration engineers*. John Wiley & Sons, 2008.

SHINHA, ALOK.: *Vibration of Mechanical Systems.* Cambridge University Press, 2010.

THORBY D.: *Structural Dynamics and Vibration in Practice*. Butterworth-Heinemann, 2008.

VENTSEL, E. & KRAUTHAMMER, T.: *Thin Plates and Shells: Theory analysis and Applications*. Marcel Dekker, New York & Basel, USA, 2001.

WALLER, MARY D.: *Vibrations of Free Square Plates*. Proc. Phys. Soc. (London), vol. 51, Jan. 1939, pp. 831-844.

WU, T.W.: *Boundary Element Acoustics: Fundamentals and Computer code*. WIT Press, 2000.

ZIENKIEWICZ, O. C. & TAYLOR, R.L.: *The Finite Element Method: Volume 1 The Basis*. Butterworth-Heinemann, Fifth Edition, 2000.

ΓΚΟΤΣΗΣ, ΠΑΣΧΑΛΗΣ Κ.: *Πεπερασμένα στοιχεία*. Εκδόσεις Ζήτη, Τρίτη Έκδοση, Θεσσαλονίκη 2013.

ΚΑΤΣΙΚΑΔΕΛΗΣ, ΙΩΑΝΝΗΣ Ι.: *Συνοριακά στοιχεία στην επιστήμη του μηχανικού: Θεωρία και εφαρμογές*. Εκδόσεις Συμεών, Αθήνα 1999.

ΛΟΥΤΡΙΔΗΣ, ΣΠΥΡΟΣ Ι.: *Ηλεκτροακουστική & ηχητικές εγκαταστάσεις*. Εκδόσεις Ίων, 2009.

ΣΚΑΡΛΑΤΟΣ, Δ.: *Εφαρμοσμένη Ακουστική*. Εκδόσεις GOTSIS, Τρίτη Έκδοση, Πάτρα, 2008.

ΤΣΑΜΑΣΦΥΡΟΣ, Γ. & ΘΕΟΤΟΚΟΓΛΟΥ, Ε. Ε.: *Η Μέθοδος των Πεπερασμένων Στοιχείων Ι.* Εκδόσεις Συμμετρία, Αθήνα, 2005.